ARL TR 75-0205

ADA 015 040

PERFORMANCE CHARACTERISTICS OF EJECTOR DEVICES

ENERGY CONVERSION RESEARCH LABORATORY/ARL

JUNE 1975

DDC

SEP 22 1975

B

AEROSPACE RESFARCH LABORATORIES/LE
Building 450 — Area B
Wright-Patterson Air Force Base, Ohio 45433

AIR FORCE SYSTEMS COMMAND

United States Air Force

REPORT DOCUMENTATION PAGE		READ INSTRUCTIONS BEFORE COMPLETING FORM
1. REPORT NUMBER ARL-75-0205	2. GOVT ACCESSION NO.	3. RECIPIENT'S CATALOG NUMBER
4. TITLE *(and Subtitle)* PERFORMANCE CHARACTERISTICS OF EJECTOR DEVICES		5. TYPE OF REPORT & PERIOD COVERED Final Apr 73 – Jan 75
		6. PERFORMING ORG. REPORT NUMBER
7. AUTHOR(s) Siegfried H. Hasinger		8. CONTRACT OR GRANT NUMBER(s) In-House Research
9. PERFORMING ORGANIZATION NAME AND ADDRESS Energy Conversion Research Laboratory (LE) Aerospace Research Laboratories (AFSC) Wright-Patterson AFB, Ohio 45433		10. PROGRAM ELEMENT, PROJECT, TASK AREA & WORK UNIT NUMBERS 61102F 7116-02-08
11. CONTROLLING OFFICE NAME AND ADDRESS Aerospace Research Laboratories (AFSC) Bldg 450, Area B Wright-Patterson AFB, Ohio 45433		12. REPORT DATE JUNE 1975
		13. NUMBER OF PAGES 116
14. MONITORING AGENCY NAME & ADDRESS*(if different from Controlling Office)*		15. SECURITY CLASS. *(of this report)* Unclassified
		15a. DECLASSIFICATION/DOWNGRADING SCHEDULE

16. DISTRIBUTION STATEMENT *(of this Report)*

Approved for public release; distribution unlimited

17. DISTRIBUTION STATEMENT *(of the abstract entered in Block 20, if different from Report)*

18. SUPPLEMENTARY NOTES

19. KEY WORDS *(Continue on reverse side if necessary and identify by block number)*

Ejector Performance	Ejector Optimization	Fluid Momentum Exchange
Ejector Characteristic	Ejector Efficiency	
Heterogeneous Ejector	Ejector Pump	
Supersonic Ejector	Thrust Augmenter	

20. ABSTRACT *(Continue on reverse side if necessary and identify by block number)*

A comprehensive performance analysis of ejector devices, which accounts for compressibility, heterogeneous operating media, and incidental flow losses under the simplifying assumptions of one-dimensional flow conditions and complete mixing at the end of the mixing section, leads to quite lengthy relations, which in part can be solved only by iteration. This report aims at arranging these relations in a way that they can be readily handled on a programmable desk calculator. The purpose is to study ejector devices on a basis as general (cont'd)

DD FORM 1473 1 JAN 73   EDITION OF 1 NOV 65 IS OBSOLETE

20. Cont'd.

as possible without sacrifice in accuracy. Various mixing modes, at constant
area, at constant pressure, and at a defined pressure distribution are studied.
An investigation of the optimum ejector reveals that an essential factor for
the lay-out is the choice of the inlet Mach number ratio of the operating media.
For constant area mixing the optimum ratio falls within a range, where the
mixing mode has little influence on the performance. Thus the performance of
constant pressure mixing, which is in general superior to that of constant area
mixing, can be approached by constant area mixing if the inlet Mach number ratio
is optimized. This is very important for supersonic ejectors since they do not
allow the realization of constant pressure mixing due to the inherent presence
of supersonic shocks during mixing.

PREFACE

This is the final report on in-house research carried out under Project No. 7116-02-08 at the Energy Conversion Research Laboratory from April 1973 to January 1975. A previous report on in-house research under this project is ARL 73-0149, AD 772 675, entitled "Simplified Lay-out of Supersonic, Heterogeneous Ejectors" by Siegfried H. Hasinger.

Contract research performed by TRW Systems Group, Redondo Beach, CA. under this project is covered by ARL 75-0015, entitled "Feasibility Study of High Energy Ejector Systems".

I would like to thank Mrs. Rose Garfield for her careful typing of this report.

TABLE OF CONTENTS

TABLE OF CONTENTS (CONT'D)

LIST OF ILLUSTRATIONS

SECTION I

INTRODUCTION

Ejector devices are distinguished by their simple mechanical construction derived from a simple working principle which consists in transferring momentum from one fluid to another by fluid shear in a mixing process. This apparent simplicity, however, does not extend to the performance analysis of these devices. A sufficient comprehensive analysis which accounts for compressibility, conservation of energy, and also heterogeneous operating media results in lengthy relations which in part can be solved only by iteration. Ejector layout requirements can differ drastically with the type of application, making an extensive individual treatment for each application necessary. Since a great variety of operating conditions are of technical interest, a large number of variables have to be dealt with in a general analysis.

Due to the analytical complexities ejector performance calculations usually either employ extended simplifications or are directed toward specific applications (Refs. 1 to 6). As a consequence general trends in the behavior of ejectors and also the optimization of their performance remain in an unclarified state. The present analysis attempts to bring the system of relations governing the ejector performance into a form which facilitates numerical evaluations and allows explicit illustrations of results while maintaining a minimum of simplifying assumptions. The final performance relations are still rather lengthy, but they can be readily managed on a programmable desk calculator. Though the specific ejector devices considered, which are the common ejector pump and the "thrust augmenter", require still a considerable amount of individual treatment, new unifying trends become apparent in the present treatment.

A special effort is devoted to the study of the loss mechanism in an ejector. This study provides a way for the systematic optimization of the ejector performance and clarifies the role of the mixing modes in this process. Three modes of mixing are considered in the ejector performance calculations: at constant area, at constant pressure, and at a defined pressure rise. Mixing is always assumed to be completed at the end of the mixing section, and no detailed considerations of the mixing process, including those for the mixing length, enter the analysis.

The flow is treated as one-dimensional, a basic assumption which previous ejector treatments have found to be a fairly realistic one. Conservation of energy, a condition which is in general not very influential for the ejector behavior (Ref. 5), is fully observed in the present analysis. Otherwise, compressibility and heterogeneous properties of the operating media are accounted for. Diffuser and wall friction losses enter the analysis in parametric form. Some consideration is given to the influence of incomplete mixing.

The principle result of the analysis consists in the presentation of the performance behavior of ejector devices in comparatively simple graphs and in providing a process to arrive at optimum ejector geometries. As an additional result the present analysis allows a reinterpretation of the simplified ejector analysis presented in Ref. 5, extending greatly its general validity.

Under the conditions assumed for the present analysis the ejector performance, i.e., the pressure ratio and the mass ratio of the ejector, can be presented as an explicit function of the ejector inlet conditions. For the reversed case where the inlet conditions must be derived for a given ejector performance, no algebraic solution of the ejector equations is possible and iteration methods must be applied for a solution. In the following the basic ejector equations are first derived for the direct case which allows a straightforward solution. Whenever advantageous for the representation of the characteristic ejector behavior the reversed case is applied and the necessary iteration process developed.

SECTION II

THE BASIC EJECTOR EQUATIONS

1. GENERAL CONSIDERATIONS

In the following the various modes of mixing are analyzed and compared
with each other in their performance as a matter of free choice of the
mixing mode. Also a free choice is given to the ratios of the inlet Mach-
numbers and the inlet areas for the primary and secondary operating media.
The ejector loss considerations in Section IV will show that quite specific
choices must be made for these three design parameters to arrive at an
optimum ejector performance.

2. CONSTANT AREA MIXING

a. Ejector Flow Scheme

Figure 1 shows the ejector flow scheme for constant area mixing.
Three essential cross sections enter the analysis with the following
specifications:

(1) At the entrance to the mixing section the driver-gas and the
driven gas which are referred to as primary and secondary medium, respectively,
enter with the Mach numbers M_p and M_s. The static pressure for each medium
is assumed to be the same at this cross section.

For supersonic inlet conditions this assumption implies that the flow
enters the mixing section through a properly expanded supersonic nozzle.
The assumption reflects desirable conditions for an ejector device, but
restricts the analysis to design point conditions, i.e., ideal inlet nozzles.
The restriction is not severe. If we compare the momentum of a gas expanded
through a correct supersonic nozzle and through the same nozzle with the
expanded part cut off, we find the difference to be negligible for low super-
sonic velocities up to, say, Mach number 1.2. At Mach number 2 the momentum
loss is about 5%. At Mach number infinity the loss is still only 30% at
$\gamma = 1.4$. The comparatively small losses at these extreme off design condi-
tions indicate that the performance of an ejector is not very sensitive to
incorrect nozzle designs, provided the nozzle is underexpanded. For an
overexpanded nozzle, i.e. if the Mach number is lower than the nozzle is
designed for, the overexpanded part of the nozzle acts as a flow blockage
and interferes with the mixing process.

(2) At the end of the mixing section both media are assumed to be
completely mixed. In case of supersonic inlet conditions it is assumed that
due to a normal or pseudo-shock the exit Mach number is always subsonic.

(3) At the exit of the diffuser, conditions vary significantly with
each ejector application. For the ejector pump a maximum of static pressure
should, in general, be obtained. Therefore, the specific assumption is in
this case that the exit velocity from the diffuser is low, and the static
and total pressure at the diffuser exit are for practical purposes the same.

For the thrust augmenter, there is an optimum pressure rise in the diffuser for best performance. To find these optimum conditions, the diffuser area ratio will be treated as an independent variable.

b. Derivation of the Basic Equations

(1) Mass Ratio

The ratio between primary and secondary mass flow is an important design magnitude for any ejector device. With the continuity law,

$$m = V \cdot \rho \cdot A \tag{1}$$

velocity of sound,

$$a = \sqrt{\gamma \cdot R \cdot T} \tag{2}$$

the equation of state,

$$\rho = \frac{p}{R \cdot T} \tag{3}$$

and the temperature change during adiabatic expansion,

$$\frac{(T)_0}{T} = 1 + \frac{\gamma - 1}{2} M^2 \tag{4}$$

the mass ratio can be expressed in terms of essential ejector data:

$$\frac{m_p}{m_s} = \frac{A_p}{A_s} \frac{M_p}{M_s} \sqrt{\frac{\gamma_p \, R_s \, (T_s)_0 \, [2 + (\gamma_p - 1) M_p^2]}{\gamma_s \, R_p \, (T_p)_0 \, [2 + (\gamma_s - 1) M_s^2]}} \tag{5}$$

This relation is independent of the mixing conditions and therefore applies to all cases of mixing treated in this analysis.

(2) Pressure Rise During Mixing

The pressure rise during mixing cannot be immediately determined. However, from conservation of momentum, its dependency from ejector operating conditions can be narrowed down:

$$m_p \cdot V_p + m_s \cdot V_s - (m_p + m_s) V_{Ex} = (A_p + A_s)(p_{Ex} - p_s + \Delta p_W) \tag{6}$$

Δp_W accounts for the pressure loss due to wall friction. This term will be examined later in Section II, paragraph 1.b (5). Dividing Eq. 6 by the area term gives

4

$$\frac{m_p \cdot v_p}{A_p\left(1+\frac{A_s}{A_p}\right)} + \frac{m_s \cdot v_s}{A_s\left(1+\frac{A_p}{A_s}\right)} - \frac{m_p + m_s}{A_p + A_s} \; v_{Ex} = p_{Ex} - p_s + \Delta p_w \tag{7}$$

Considering

$$\frac{v \cdot m}{A} = p \cdot \gamma \cdot M^2 \tag{8}$$

we obtain, when dividing also by p_s,

$$\frac{\gamma_p \cdot M_p^2}{1+\frac{A_s}{A_p}} + \frac{\gamma_s \cdot M_s^2}{1+\frac{A_p}{A_s}} + 1 - \frac{\Delta p_w}{p_s} = \frac{p_{Ex}}{p_s}\left(\gamma_{Ex} M_{Ex}^2 + 1\right) \equiv B_A \tag{9}$$

For the complete determination of p_{Ex}/p_s from this equation, the exit Mach number M_{Ex} and also γ_{Ex} must be known. In abbreviated form the pressure rise during mixing can be expressed by

$$\frac{p_{Ex}}{p_s} = \frac{B_A}{\left(\gamma_{Ex} M_{Ex}^2 + 1\right)} \tag{10}$$

B_A is in general given by the ejector design. M_{Ex} and γ_{Ex} will be determined next.

(3)   Exit Mach Number M_{Ex}

Determining M_{Ex} requires the solution of the thermodynamic mixing relations for the ejector operating media. From continuity one has

$$v_{Ex} = \frac{m_{Ex}}{A_{Ex} \cdot \rho_{Ex}} \tag{11}$$

Using Eqs (2) and (3) and normalizing the equation with the flow condition of the secondary medium before mixing, we can write

5

$$\frac{M_{EX}}{M_S} = \frac{m_{EX} \cdot A_S \cdot p_S}{m_S \cdot A_{EX} \cdot p_{EX}} \sqrt{\frac{\gamma_S \cdot R_{EX} \cdot T_{EX}}{\gamma_{EX} \cdot R_S \cdot T_S}} \qquad (12)$$

The following mixing relations can be applied to evaluate Eq (12):

Mass

$$\frac{m_{EX}}{m_S} = \frac{m_p + m_S}{m_S} = \frac{m_p}{m_S} + 1 \qquad (13)$$

Cross section area

$$\frac{A_{EX}}{A_S} = \frac{A_p + A_S}{A_S} = \frac{A_p}{A_S} + 1 \qquad (14)$$

Gas constant

$$\frac{R_{EX}}{R_S} = \frac{1}{R_S}\left(\frac{m_S}{m_{EX}} R_S + \frac{m_p}{m_{EX}} R_p\right) \qquad (15)$$

$$= \frac{m_S}{m_p + m_S} + \frac{m_p}{m_p + m_S} \frac{R_p}{R_S} \qquad (15a)$$

Ratio of specific heats

$$\frac{\gamma_{EX}}{\gamma_S} = \frac{\beta}{\gamma_S}\left(\frac{m_S}{m_{EX}}\gamma_S + \frac{m_p}{m_{EX}}\gamma_p\right) \qquad (16)$$

$$= \beta\left(\frac{m_S}{m_p + m_S} + \frac{m_p}{m_p + m_S}\frac{\gamma_p}{\gamma_S}\right) \qquad (16a)$$

6

The factor β has been added in this relation to allow an independent change of the gas properties of the mixed gases beyond those resulting from the perfect gas mixing laws. By a proper choice of this factor gas imperfections as they are associated with dissociation and condensation can to some degree be accounted for. An example for its use is given in Reference 5. In this analysis only perfect gas conditions are considered and this factor is taken as unity.

Relations (15a) and (16a) combined give

$$\frac{\gamma_S \cdot R_{EX}}{\gamma_{EX} \cdot R_S} = \frac{1 + \frac{m_P}{m_S}\frac{R_P}{R_S}}{\beta\left(1 + \frac{m_P}{m_S}\frac{\gamma_P}{\gamma_S}\right)} \tag{17}$$

Total temperature

$$\frac{(T_{Ex})_0}{(T_S)_0} = \frac{1}{(T_S)_0} \cdot \frac{c_{p-p} \cdot m_P \cdot (T_P)_0 + c_{p-s} \, m_S \, (T_S)_0}{c_{p-p} \, m_P + c_{p-s} \, m_S} \tag{18}$$

$$= \frac{\frac{c_{p-p} \, m_P \, (T_P)_0}{c_{p-s} \, m_S (T_S)_0} + 1}{\frac{c_{p-p} \, m_P}{c_{p-s} \, m_S} + 1} \tag{18a}$$

For a perfect gas c_p is a unique function of γ and R. The specific heat c_p is, however, carried in the following as an independent variable to account for gas imperfections (see remark to Eq (16)).

We write also

$$\frac{T_{Ex}}{T_S} = \frac{(T_{Ex})_0}{(T_S)_0} \cdot \frac{T_{Ex}}{(T_{Ex})_0} \cdot \frac{(T_S)_0}{T_S} \tag{19}$$

Introducing the mixing relations into Eq (12), we obtain

$$\frac{M_{EX}}{M_S} = \frac{\left(1 + \frac{m_P}{m_S}\right)}{\left(1 + \frac{A_P}{A_S}\right)} \frac{p_S}{p_{EX}} \cdot \sqrt{\frac{\left(1 + \frac{m_P R_P}{m_S R_S}\right)}{\beta \left(1 + \frac{m_P}{m_S} \frac{\gamma_P}{\gamma_S}\right)} \frac{\left(\frac{C_{P\cdot P}}{C_{P\cdot S}} \frac{m_P}{m_S} \frac{(T_P)_0}{(T_S)_0} + 1\right)}{\left(\frac{C_{P\cdot P}}{C_{P\cdot S}} \frac{m_P}{m_S} + 1\right)} \frac{(T_S)_0}{T_S} \frac{T_{EX}}{(T_{EX})_0}} \qquad (20)$$

To evaluate this equation further we substitute for p_S/p_{Ex} and $T_{Ex}/(T_{Ex})_0$ by means of Eqs (10) and (4) respectively and bring all terms which depend on M_{Ex} and γ_{Ex} to the left side. We obtain

$$\frac{M_{Ex}\left(1 + \frac{\gamma_{Ex}-1}{2} M_{Ex}^2\right)^{\frac{1}{2}}}{1 + \gamma_{Ex} M_{Ex}^2} = \frac{M_S}{B_A} \frac{\left(\frac{m_P}{m_S} + 1\right)}{\left(\frac{A_P}{A_S} + 1\right)} \sqrt{\frac{\left(1 + \frac{m_P \cdot R_P}{m_S \cdot R_S}\right)}{\beta \left(1 + \frac{m_P \cdot \gamma_P}{m_S \cdot \gamma_S}\right)} \frac{\left(\frac{C_{P\cdot P}}{C_{P\cdot S}} \frac{m_P (T_P)_0}{m_S (T_S)_0} + 1\right)}{\left(\frac{C_{P\cdot P}}{C_{P\cdot S}} \frac{m_P}{m_S} + 1\right)} \frac{(T_S)_0}{T_S}} \equiv E_A \qquad (21)$$

The right side of Eq (21), abbreviated by E_A, contains only ejector design data or derivatives of them. Equation (21) can be readily solved for M_{Ex}:

$$M_{Ex}^2 = \frac{1 - \left[\begin{smallmatrix}+\\(-)\end{smallmatrix}\right]\sqrt{1 - 2\gamma_{Ex} E_A^2 \left(1 + \frac{1}{\gamma_{Ex}}\right) + 2\gamma_{Ex} E_A^2}}{2\gamma_{Ex}^2 E_A^2 - \gamma_{Ex} + 1} \qquad (22)$$

Only the positive root in this relation, which yields the subsonic flow conditions, applies in the present case of constant area mixing.

With M_{Ex} known, Eq (10) can be solved for the pressure ratio p_{Ex}/p_S across the mixing process. Also the layout of the flow diffuser following the mixing section can now be completed. A discussion on E_A as a meaningful ejector parameter is given in the following.

8

(4) Flow Density Parameter E_A

Equation (21) can be given a useful interpretation. With the help of already cited relations the left side of this equation can be written

$$\frac{M_{Ex}\left(1+\frac{\gamma_{Ex}-1}{2}M_{Ex}^2\right)^{\frac{1}{2}}}{1+\gamma_{Ex}M_{Ex}^2} = M_{Ex}\sqrt{\frac{(T_{Ex})_0}{T_{Ex}}}\,\frac{p_{Ex}}{p_S}\,\frac{1}{B_A} \qquad (23)$$

or

$$\approx V_{Ex}\cdot\rho_{Ex}\sqrt{\frac{(T_{Ex})_0\,R_{Ex}}{\gamma_{Ex}}}\,\frac{1}{p_S\,B_A} \qquad (23a)$$

The expression $\sqrt{(T_{Ex})_0\,R_{Ex}/\gamma_{Ex}}\,/B_A$ also occurs on the right side of Eq (21) as can be proven by means of Eqs (10), (17), and (18a). Dividing both sides of Eq (21) with this expression, we obtain

$$V_{Ex}\cdot\rho_{Ex}\frac{1}{p_S} = M_S\frac{\left(1+\frac{m_p}{m_s}\right)}{\left(1+\frac{A_p}{A_S}\right)}\sqrt{\frac{\gamma_S}{R_S\,T_S}} \qquad (24)$$

or

$$V_{Ex}\cdot\rho_{Ex}\cdot\frac{1}{p_S} \approx V_S\cdot\rho_S\cdot\frac{1}{p_S}\,\frac{(m_p+m_s)}{m_s}\,\frac{A_S}{(A_p+A_S)} \qquad (25)$$

If we multiply both sides by p_s, we obtain the original continuity condition for deriving Eq (21), but written in a somewhat different form,

$$V_{Ex}\cdot\rho_{Ex} = V_S\cdot\rho_S\frac{(m_p+m_s)}{m_s}\,\frac{A_S}{(A_p+A_S)} \qquad (26)$$

The product $v_{Ex}\cdot\rho_{Ex}$ remaining on the left side is the flow density, i.e., the mass flow per unit area at the mixing section exit. Thus E_A is the flow density at the mixing section exit made dimensionless by the expression $\sqrt{(T_{Ex})_0\,R_{Ex}/\gamma_{Ex}}\,/p_s$ and extended by the dimensionless magnitude B_A. In this form the flow density can be solely expressed either in terms of exit conditions (left side of Eq (21) or in terms of inlet conditions (right side of Eq (21)) and equated as in Eq (21). The particular meaning of this equation for the ejector analysis is the following:

9

The left side gives a dimensionless flow density E_A expressed in terms of the flow Mach number. Figure 2 gives a plot of the relation $E_A = f(M_{Ex})$. As expected, the flow density is highest at $M_{Ex} = 1$. In the upper part of the curve a subsonic and a supersonic Mach number satisfy the relation, representing the condition for a normal shock or a pseudo-shock in a constant area duct. From Eq (22) follows that E_A becomes a maximum if the root is zero or

$$E_{A\text{-}max} = \sqrt{\frac{1}{2(\gamma_{Ex}+1)}}$$
(27)

M_{Ex} becomes infinite if the denominator of Eq (21) becomes zero or

$$\left(E_A\right)_{M=\infty} = \frac{1}{\gamma_{Ex}}\sqrt{\frac{\gamma_{Ex}-1}{2}}$$
(28)

The right side of Eq (21) is a complex expression made up of design data which can be chosen arbitrarily. However, only such combinations of design data which result in an E_A equal to or smaller than $E_{A\text{-}max}$ can be realized in a constant area duct. Certain combinations of design data which lead to an exit Mach number of one, i.e., to choking, are possible. Equation (21) is too complex to allow recognition of trends for choking. However, on physical grounds it can be stated that any increase in the heterogeneity of the operating media brings any ejector with subsonic exit Mach number closer to choking since the mixing losses associated with heterogeneous operating conditions have the effect of an internal heat addition during mixing, leading to an increase of the exit Mach number. Examples in Section III will show this trend.

If the primary and secondary flow are identical, their common Mach number corresponds to that upstream of a normal shock. This condition is useful in the interpretation of ejector characteristics discussed in Section III. Equation (21) properly modified, appears again with the other mixing modes treated in this analysis.

(5) Pressure Loss Due to Wall Friction

The pressure loss Δp_W, accounting in Eq (6) for wall friction, depends on the specific design of the mixing chamber, as for instance on the position of the primary and secondary flow with respect to the wall. It depends also on the mixing process itself as far as it influences the velocity distribution along the wall. In particular, it will be different with the type of mixing. Above all it depends on the mixing length, which by itself depends strongly on the number of primary nozzles provided. An explicit determination of Δp_W is not possible under the given conditions. A parametric approach based on a simple pipe friction analogy is therefore used.

10

As with pipe friction the pressure drop due to wall friction is referred to a significant dynamic pressure of the flow system. The analysis allows the determination of the dynamic pressure at three locations of the mixing section: at the inlet of the primary and secondary flow and at the exit. In the analysis all three dynamic pressures are used as reference pressures. Which pressure to choose in an evaluation depends on the design and the operating conditions of an ejector device. For subsonic flow, as typical for thrust augmentation, the secondary flow inlet is the best reference point, since the secondary flow is an essentially constant velocity flow predominantly in touch with the wall. For supersonic flows with shocks occurring during mixing, the mixing section exit may be preferrable as reference. For constant pressure mixing, where the velocity on the wall generally increases along the mixing section, the exit becomes particularly significant as reference location.

(a) Δp_W Referred to M_s^2 and M_p^2

Analogous to the pressure loss in a pipe, we can write for the pressure drop in the mixing section

$$\Delta p_W = c_f \cdot \rho_s \cdot \frac{v_s^2}{2} \cdot \frac{l}{d} \tag{29}$$

Considering

$$\rho_s \cdot v_s^2 = p_s \cdot \gamma_s \cdot M_s^2 \tag{30}$$

we can write for $(\Delta p / p_s)_W$ in Eq (9)

$$\frac{\Delta p_W}{p_s} = c_f \frac{l}{2d} \cdot \gamma_s \cdot M_s^2 \tag{31}$$

The mixing chamber geometry given by $l/(2d)$ appears now in explicit form. The pipe friction coefficient is a well known function of the pipe flow Reynolds number.

The case of referring the wall friction losses to the dynamic pressure at the primary flow inlet instead of at the secondary flow inlet is obtained from above derivations by simply switching indices for the primary and secondary flows.

(b) Wall Friction Losses Referred to M_{Ex}^2

In this case the derivations are much more involved. If we write the analog to Eq (31)

$$\frac{\Delta p_W}{p_{Ex}} = c_f \cdot \gamma_{Ex} \cdot M_{Ex}^2 \frac{l}{2d} \tag{32}$$

and introduce this relation into Eq (9), we obtain

$$\frac{\gamma_p \cdot M_p^2}{1 + \frac{A_s}{A_p}} + \frac{\gamma_s \cdot M_s^2}{1 + \frac{A_p}{A_s}} = \frac{p_{Ex}}{p_s} \left[M_{Ex}^2 \gamma_{Ex} \left(c_f \frac{l}{2d} + 1 \right) + 1 \right] \equiv B_{\lambda - W} \tag{9a}$$

11

and

$$\frac{p_{EX}}{p_S} = \frac{B_{A-W}}{M_{EX}^2 \gamma_{EX} \left(c_f \frac{L}{2d} + 1\right) + 1} \tag{10a}$$

Then the flow density parameter becomes

$$E_{A-W} = \frac{M_{EX}\left(1 + \frac{\gamma_{EX}-1}{2} M_{EX}^2\right)^{\frac{1}{2}}}{1 + \gamma_{EX} M_{EX}^2 \left(c_f \frac{L}{2d} + 1\right)} \tag{21a}$$

and the solution for M_{EX}^2 is

$$M_{EX}^2 = \frac{1 - \left[\sqrt{1 - \frac{\alpha}{c}\left(2c + \frac{1}{\gamma_{EX}} - 1\right)} + \alpha\right]}{c \cdot \alpha \cdot \gamma_{EX} - \gamma_{EX} + 1} \tag{22a}$$

where

$$\alpha = 2\gamma_{EX} E_{A-W}^2 c$$

$$c = 1 + c_f \frac{L}{2d}$$

The flow density parameter E_{A-W} accounts for an external pressure force acting on the flow, such as wall friction. It reaches a maximum at a M_{EX} smaller than one. This is a consequence of the basic assumption, as expressed by Eq (32), that the impulse loss due to wall friction increases with M_{EX}^2. For $c = 1.0$ all relations revert to those originally derived in paragraph (3) of this section.

3. CONSTANT PRESSURE MIXING

a. Basic Flow Schemes

For constant pressure mixing it is assumed that no shocks occur during mixing. Thus the flow can be subsonic as well as supersonic at the mixing section exit. Two flow schemes result. At subsonic exit velocity (Figure 3a) a subsonic flow diffuser follows immediately the mixing section. For a supersonic exit velocity (Fig. 3b) a shock diffuser is placed between the mixing section and subsonic diffuser.

To maintain constant pressure during mixing, the flow cross section must in general be reduced toward the mixing section exit. The area change along the mixing section is a function of the state of mixing. For the purpose of the analysis the state of mixing is specified only for the

12

mixing section exit, i.e. mixing is completed. This assumption is sufficient for the analysis. The contour of the mixing section remains undetermined.

b. Derivation of Basic Equations

The derivation of the relations for constant pressure mixing follows in principal the same pattern which applies to constant area mixing. Equations (1) to (5) remain unchanged. Since for constant pressure mixing $p_{Ex} = p_p = p_s$, no net pressure forces act on the flow. Expressing for the moment the wall friction forces summarily by F_f, one obtains for the basic Eq (6)

$$m_p \cdot v_p + m_s \cdot v_s - \left(m_p + m_s\right) v_{EX} = F_f \tag{6a}$$

Introducing Eq (8) and dividing the equation by $A_p + A_s$ and by the pressure term, considering $p_{Ex} = p_p = p_s$, we obtain

$$\frac{\gamma_p M_p^2}{1 + \frac{A_s}{A_p}} + \frac{\gamma_s \cdot M_s^2}{1 + \frac{A_p}{A_s}} - \frac{\gamma_{EX} M_{EX}^2 A_{EX}}{A_p + A_s} = \frac{F_f}{\left(A_F + A_s\right) p_{EX}} \tag{9b}$$

The wall friction forces are again expressed in parametric form. Pressure losses due to wall friction occur for constant pressure mixing predominantly at the mixing section exit since the flow velocity along the wall is here in general the highest. The proper dynamic pressure to be used for reference in expressing the wall losses is therefore the one at this location. To arrive at a simple formulation for the wall friction term in the ejector equations the pressure loss in the conical mixing section is expressed in terms of an equivalent cylindrical section with A_{Ex} as cross section area. The length to diameter ratio l/d of this equivalent section must be chosen such that its pressure loss is the same as that of the actually conical one. A crude approximation for this procedure is to take the median length to diameter ratio of the actual conical mixing section. With above equivalence assumption we can write for the wall friction force

$$F_f = \left(c_f \frac{l}{2d}\right) \cdot p_{EX} \cdot \gamma_{EX} \cdot M_{EX}^2 \cdot A_{EX} \tag{33}$$

The expression in parenthesis appears again as the wall friction parameter in the analysis.

With Eq (33) the ejector equation for constant pressure mixing becomes

$$\left[\frac{\gamma_p M_p^2}{1 + \frac{A_s}{A_p}} + \frac{\gamma_s M_s^2}{1 + \frac{A_p}{A_s}}\right] \frac{1}{1 + c_f \frac{l}{2d}} - \gamma_{EX} M_{EX}^2 \frac{A_{EX}}{A_p + A_s} \equiv B_p \tag{9c}$$

13

For determining the mixing section exit Mach number M_{Ex}, Eq (12) applies again. All mixing relations except Eq (14) remain the same. The area ratio A_{Ex}/A_s must now be derived from Eq (9b) and is written in the form

$$\frac{A_s}{A_{Ex}} = \frac{\gamma_{Ex} \cdot M_{Ex}^2}{B_p \left(1 + \frac{A_p}{A_s}\right)} \tag{34}$$

Equation (20) becomes then, upon considering $p_{Ex} = p_s$, bringing again all the terms which depend on M_{Ex} to the left side, and also utilizing Eq (4),

$$\frac{\left(1 + \frac{\gamma_{Ex}-1}{2} M_{Ex}^2\right)^{\frac{1}{2}}}{\gamma_{Ex} \cdot M_{Ex}} = \frac{M_s}{B_p} \frac{\left(1 + \frac{m_p}{m_s}\right)}{\left(1 + \frac{A_p}{A_s}\right)} \sqrt{\frac{\left(1 + \frac{m_p \cdot R_p}{m_s \cdot R_s}\right)\left(\frac{c_{p \cdot p}\, m_p (T_p)_0}{c_{p \cdot s}\, m_s (T_s)_0} + 1\right)\left(T_s\right)_0}{\beta\left(1 + \frac{m_p \cdot \gamma_p}{m_s \cdot \gamma_s}\right)\left(\frac{c_{p \cdot p}\, m_p}{c_{p \cdot s}\, m_s} + 1\right) T_s}} \equiv E_p \tag{21b}$$

The right side of Eq (21b) is again given by initial ejector data. Equation (21b) can be readily solved for M_{Ex}^2:

$$M_{Ex}^2 = \frac{1}{\left(\gamma_{Ex} E_p\right)^2 - \frac{\gamma_{Ex}-1}{2}} \tag{22b}$$

The mixing section exit conditions are now completely determined. The mixing section contraction ratio becomes with Eq (9c)

$$\frac{A_{Ex}}{A_p + A_s} = t = \frac{B_p}{\gamma_{Ex} M_{Ex}^2} \tag{35}$$

4. MIXING AT A DEFINED PRESSURE DISTRIBUTION

If in a conical mixing section as necessary for constant pressure mixing (Figure 3) the pressure actually rises during mixing, wall forces acting in the direction of the flow appear, and an accounting for these forces in the ejector equations becomes necessary. If A_w is the wall area projection in the direction of the flow and p_w is the local pressure in the mixing section the resulting wall pressure force acting on the flow is

$$\Delta F_w = \int_{A_{Ex}}^{A_p + A_s} (p_w - p_s)\, dA_w \tag{36}$$

14

For the purpose of the analysis this relation is expressed in a form which allows a simple parametric presentation

$$\Delta F_W = \left(A_p + A_s - A_{Ex}\right) \frac{p_{Ex} - p_s}{2} \cdot i \tag{37}$$

i.e. we assume that the median pressure difference between inlet and exit of the mixing section acts uniformly on the flow throughout the mixing section, modified by the factor i so that the resulting force ΔF_W acting on the walls in flow direction becomes equal to the integrated value. If the pressure rises proportionally with the cross section, the factor i is one. If there is no pressure rise along the entire mixing section, the factor i is zero. If the pressure in the mixing section would rise to its final value immediately at the inlet and stay constant throughout the mixing section, the value of i would be 2. Further implications of the factor i are discussed at the end of this section.

Due to the pressure rise during mixing the pressure force

$$\Delta F_p = A_{Ex} \cdot p_{Ex} - A_{Ex} \cdot p_s \tag{38}$$

acts also on the flow. The total pressure force acting on the flow is then

$$\Delta F_{W+p} = \left(A_p + A_s - A_{Ex}\right) \frac{p_{Ex} - p_s}{2} \cdot i + A_{Ex}\left(p_{Ex} - p_s\right) \tag{39}$$

Using the abbreviation

$$t = \frac{A_{Ex}}{A_p + A_s} \tag{40}$$

one can transform Eq (39) into

$$\Delta F_{W+p} = \left(p_{Ex} - p_s\right) \cdot t \cdot \left(A_p + A_s\right)\left(\frac{i}{2t} + 1 - \frac{i}{2}\right) \tag{39a}$$

With the abbreviation

$$\tau = \frac{i}{2t} + 1 - \frac{i}{2} \tag{41}$$

we obtain

$$\Delta F_{W+p} = t\left(A_p + A_s\right)p_s \cdot \tau\left(\frac{p_{Ex}}{p_s} - 1\right) \tag{39b}$$

15

The basic momentum equation for the ejector process with inclusion of the pressure forces is

$$m_p V_p + m_S V_S - \left(m_p + m_S\right) V_{EX} = \Delta F_{W \cdot p} + A_{EX} \cdot \Delta p_W \tag{6b}$$

Introducing Eq (39b) into this relation and using previous transformations, we obtain

$$\frac{\gamma_p^2 \cdot M_p^2}{1 + \frac{A_S}{A_p}} + \frac{\gamma_S^2 \cdot M_S^2}{1 + \frac{A_p}{A_S}} - \frac{p_{EX}}{p_S} \gamma_{EX} M_{EX}^2 \cdot t = t \cdot \tau \left(\frac{p_{EX}}{p_S} - 1\right) + \frac{p_{EX}}{p_S} \frac{c_f L}{2d} \gamma_{EX}^2 M_{EX}^2 \cdot t \tag{9d}$$

or, somewhat rearranged,

$$\frac{\gamma_p^2 M_p^2}{t\left(1 + \frac{A_S}{A_p}\right)} + \frac{\gamma_S^2 M_S^2}{t\left(1 + \frac{A_p}{A_S}\right)} + \tau = \frac{p_{EX}}{p_S}\left[\gamma_{EX} M_{EX}^2\left(c_f \frac{L}{2d} + 1\right) + \tau\right] \equiv B_\tau \tag{9e}$$

This equation yields p_{EX}/p_S for insertion into the continuity equation in accordance with the procedure applied for the other mixing modes, resulting in the following relation for the flow density parameter:

$$\frac{M_{EX}\left(1 + \frac{\gamma_{EX} - 1}{2} M_{EX}^2\right)^{\frac{1}{2}}}{\gamma_{EX} M_{EX}^2\left(c_f \frac{L}{2d} + 1\right) + \tau} = \frac{M_S}{B_\tau} \frac{\left(\frac{m_p}{m_S} + 1\right)}{\left(\frac{A_p}{A_S} + 1\right)} \sqrt{\frac{\left(1 + \frac{m_p}{m_S}\frac{R_p}{R_S}\right)\left(\frac{c_{p \cdot p}}{c_{p \cdot S}}\frac{m_p}{m_S}\frac{(T_p)_0}{(T_S)_0} + 1\right)}{\beta\left(1 + \frac{m_p}{m_S}\frac{\gamma_p}{\gamma_S}\right)\left(\frac{c_{p \cdot p}}{c_{p \cdot S}}\frac{m_p}{m_S} + 1\right)}} \frac{(T_S)_0}{T_S} \tag{21c}$$

$$\equiv E_\tau$$

For $\tau = 1$, which occurs if either $i = 0$ or $t = 1$, E_τ becomes equal to E_A given by Eq (21). This is obvious for the condition $t = 1$, since it represents constant area mixing and no wall forces can appear for any pressure rise. For the condition $i = 0$ the equality of E_τ and E_A means that the flow density in the exit is independent of t. Zero pressure rise, i.e., $i \to 0$, is not a readily obtainable condition. For supersonic conditions it is difficult to avoid a pressure rise during mixing since shocks are liable to occur.

For conditions with pressure rise in the mixing section it is essential to note that the flow density decreases with increasing τ. This is shown in

16

Figure 4, where E_τ is plotted over M_{Ex}. The curve with $\tau = 1$ is identical with the curve shown in Figure 2. Curves with higher τ - values lie below this top curve.

Equation (21c) can be solved for the exit Mach number with the result

$$M_{EX}^2 = \frac{1 - \left[\pm\sqrt{1 - \frac{\alpha\tau^2}{c}\left(2\frac{c}{\tau} + \frac{1}{\gamma_{EX}} - 1\right)} + \alpha\tau\right]}{c \cdot \alpha \cdot \gamma_{EX} - \gamma_{EX} + 1} \qquad (22c)$$

$$c = \left(c_f \frac{l}{2d} + 1\right)$$

$$\alpha = 2\gamma_{EX} E_\tau^2 \cdot c$$

Equation (9e) then yields the pressure rise p_{Ex}/p_s during mixing. Together with the pressure recovery obtained from M_{Ex} in the subsonic diffuser the overall pressure ratio $(p_{Ex})_o/p_s$ of the ejector can be determined.

By the nature of its definition the factor i can account for any kind of pressure distribution along the mixing section. The practical difficulty is that the pressure distribution is in general not known. Theoretical evaluations are too complex and experimentation in this area seems to be lacking. For special cases, however, the pressure distributions can be readily derived. Values of i determined from these cases, together with the obvious ones cited in connection with the definition of the factor i above, can serve as a measure for estimating i values for practical cases. The following special case is very instructive: The primary and secondary flow entering a mixing section with a reducing cross section area are supersonic and equal; i.e., mixing is reduced to zero. For ideal flow conditions, i.e., no supersonic shocks, the flow becomes sonic at the mixing section exit if sufficient area reduction is provided. This case is simply that of the reversed flow in a supersonic expansion nozzle. With the help of common flow tables and some simple plotting the following i-values, where M is the common Mach number of the entering flows can be determined:

M =	2	3	4
i =	0.49	0.23	0.08

17

The characteristic pressure distribution in this case is that of a slow pressure rise in the beginning and a steep rise toward the exit, more pronounced with increasing entrance Mach number.

If the above considered entrance Mach number is the result of mixing two flows with different Mach numbers under constant pressure, the initial rise in a mixing section, which accommodates such process, will be zero, causing above i-values to become even smaller. In real cases supersonic shocks occur during the mixing process; i.e., a pressure rise occurs right from the beginning. Due to the shocks, which occur particularly during the compression phase, the exit pressure is much lower than in the ideal case. Thus, a pressure distribution where the pressure rises strongly first to taper off toward the end of the mixing section results. Such a pressure distribution is characterized by i-factors larger than one, as is readily seen from its definition. The essential point to make here is that in ejector cases where the mixing section exit number is sonic i-values must be invariably above one, approaching possibly values not too far from two.

Of special interest is also the supersonic ejector case where the area reduction of the mixing section is not sufficient to reach sonic conditions at the exit. In this case the exit velocity is supersonic and shock compression occurs in the supersonic diffuser (Fig. 3b). Analytically this process is equal to a normal shock occurring at the mixing section exit. The pressure distribution is in this case such that the pressure rises first more or less steadily, jumps, however, suddenly at the exit to its final value due to the normal shock assumed at this location. The pressure distribution resembles in its shape somewhat that of the ideal case and results in i-values below one; however, with the essential difference that the exit Mach number is below one, the more so the higher the Mach number before the shock at the exit, which also means the lower the resulting i-value.

Above considerations show that the as such desirable condition of a low i-value together with a sonic mixing section exit velocity can never occur in the real case. This has important consequences for the optimization of the ejector performance, as will be shown in Section IV.

SECTION III

PERFORMANCE CHARACTERISTICS

1. EJECTOR PUMP

   a. Constant Area Mixing

      (1) "Ejector Pressure Ratio"

      For an ejector pump maximum pressure recovery in the diffuser is a typical requirement. This implies that the static pressure and the total pressure are very nearly equal at the diffuser outlet. For adiabatic compression in the diffuser, the static pressure ratio across the diffuser, upon using the polytropic diffuser efficiency to account for flow losses becomes

$$\frac{(p_{Ex})_0}{p_{Ex}} = \left(1 + \frac{\gamma_{Ex}-1}{2}M_{Ex}^2\right)^{\eta_{pol}\frac{\gamma_{Ex}}{\gamma_{Ex}-1}} \tag{42}$$

(See Section III, 3 for the definition of the polytropic efficiency.) The polytropic efficiency has the advantage, as compared with other commonly used efficiency definitions, that it is least influenced by the diffuser flow conditions, in particular by the diffuser inlet Mach number (Ref. 6). For the overall "ejector pressure ratio", i.e., the total pressure at the diffuser exit over the static pressure at the mixing section inlet, we obtain with Eq (10)

$$\frac{(p_{Ex})_0}{p_S} = \frac{B_A}{(\gamma_{Ex}M_{Ex}^2+1)} \cdot \left(1 + \frac{\gamma_{Ex}-1}{2}M_{Ex}^2\right)^{\eta_{pol}\frac{\gamma_{Ex}}{\gamma_{Ex}-1}} \tag{43}$$

In this equation B_A is determined from Eq (9) and M_{Ex} from Eq (22), using Eq (21) to find E_A and Eq (5) to find m_p/m_s. Thus a direct though lengthy process is obtained to determine the ejector pressure ratio from the ejector inlet conditions. For calculating the wall friction term in Eq (9) a value for the product of length to diameter ratio of the mixing section times the friction coefficient must be chosen and the wall friction term be determined with Eq 31 or 32, depending on the desired reference Mach number.

      (2) Presentation of Results

      With the help of Eq (43) any desired plot between magnitudes of the ejector problem can be made by utilizing graphical cross plotting. This is, however, in general a cumbersome procedure. In Ref. 1 it has been shown

19

and it will be explained later in this report, that a particular useful plot
to demonstrate the performance of an ejector pump is one in which the
secondary inlet Mach number is plotted against the primary inlet Mach number
in two sets of curves, one with the mass ratio and the other with the ejector
pressure ratio as parameter. The first set is directly given by Eq (5); the
other one derives from Eq (43) and requires iteration for an analytical
solution. Such a solution is preferrable since it allows to plot the ejector
performance curves directly on an automatic plotter. The necessary relations
for the plotting process are derived in the following.

For the curves with the mass ratio as parameter, Eq (5) can be solved
for the secondary Mach number:

$$M_S^2 = \frac{\sqrt{1 + N(\gamma_S - 1)} - 1}{\gamma_S - 1} \tag{44}$$

with the abbreviation

$$N = \left[\frac{A_p \, m_S}{A_S \, m_p}\right]^2 \frac{\gamma_p \, R_S}{\gamma_S \, R_p} \frac{(T_S)_0}{(T_p)_0} M_p^2 \left[2 + (\gamma_p - 1) M_p^2\right] \tag{45}$$

Equation (44) can be readily plotted in a $M_p - M_S$ diagram with m_p/m_S as
parameter. Magnitudes assumed to be given for such a plot are the inlet-area
ratio and the thermodynamic properties of the operating media in the form of
their ratios.

To obtain the second set of curves with the ejector pressure ratio
$(p_{Ex})_0/p_S$ as parameter an iterative solution, as indicated above, is required.
The following procedure, first applied in Ref. 5, leads to a fast convergence.
Equation (43) can be written in the form

$$B_A = f \cdot \frac{(p_{Ex})_0}{p_S} \tag{46}$$

20

where the factor f stands for

$$f = \frac{\left(\gamma_{EX} M_{EX}^2 + 1\right)}{\left(1 + \frac{\gamma_{EX}-1}{2} M_{EX}^2\right)^{\eta_{pol} \frac{\gamma_{EX}}{\gamma_{EX}-1}}} \qquad (47)$$

As shown in Ref. 5 the factor f varies for $\eta_{poly} = 1$ at the most from 1.0 to about 1.26 (depending also slightly on γ_{Ex}) for M_{Ex} changing from 0 to 1.0. By choosing for f an intermediate value, for instance 1.2, an approximate B_A can be determined with Eq (46) and an approximate value for M_{Ex} with Eqs (21) and (22). This approximate value is then used to obtain an improved f value. The process is repeated until the approximated and the last calculated f value coincide. In the calculations carried out for the following examples, high accuracy was in general obtained within about three iteration cycles. Calculation time on the Hewlett-Packard Calculator 9100B with Extended Memory 9101A, used for all numerical evaluations in this report, was about 3 sec for one curve point.

The number of cycles necessary for conversion begins to increase sharply if M_{Ex} approaches one. However, in general M_{Ex} values of up to, say, 0.98 are reached without difficulties. If in the plotting process the dependent variable approaches values which are small in comparison to those of the independent variable, the iteration process does not converge. A simple change in coordinates overcomes this problem.

The above described evaluation has been used to determine the typical performance of the ejector pump with constant area mixing. The results are shown in Figures 5 and 6, and discussed in the next paragraph.

(3) Discussion of the Characteristic Ejector Behavior

The solid curves in Fig 5 represent particularly simple ejector conditions. The inlet area ratio is one and the primary and secondary medium have the same thermodynamic properties, including equal total inlet temperature. Diffuser and wall friction losses are assumed zero. For this idealized "homogeneous" ejector layout the shape of the curves for constant ejector pressure ratio $(p_{Ex})_o/p_s$ become very nearly circular, the more so the higher the pressure ratio. (Details about the basic curve shape will be discussed in Section III.2.) As expected, the curves are symmetric to the line $M_p = M_s$. Along this line the operating media become identical in all details, and pressure ratios along this line pertain to the case of a single flow through a constant area duct where mixing is absent and only supersonic shocks occur. Along this line pressure ratios and Mach numbers are related to each other by the isentropic compression relations in the subsonic region and by normal shock relations in the supersonic region with subsonic isentropic compression added to obtain total pressure recovery. At the coordinate axis, where either M_s or M_p is zero, again the case of a single flow medium is represented; however, in this case it is subject

21

to a sudden expansion to twice its original flow cross section.

For comparison with this kind of basic performance curves a number of heterogeneous operating and external flow loss conditions are entered in Fig. 5. Table I identifies these various operating conditions. No. 2 in this table represents purely heterogeneous operating conditions for which the inlet total temperature ratio for the operating media is 4. Fig. 5 shows that such a temperature ratio has a comparatively small influence on the ejector pressure ratio in contrast to its great influence on the mass ratio of the operating media, which will be dealt with later. A new phenomenon appears, however. Due to the addition of thermodynamic mixing losses to the shock losses, the mixing section exit Mach number can become sonic in a wide region around the point $M_s = M_p = 1$. For the idealized homogeneous ejector this is the only point where the mixing section exit Mach number can become one, i.e., no choking will occur. The region of choking for the heterogeneous case is indicated in Fig. 5.

External flow losses have a somewhat different type of influence on the ejector performance than the mixing losses. The influence is comparatively small at high ejector pressure ratios, but quite substantial at lower pressure ratios. This is true for both, the diffuser losses and the wall friction losses, but is more pronounced for the latter ones (compare No. 3 and 4 operating conditions). The wall friction losses assumed here correspond to those of a mixing section with an ℓ/d of about 6. The choice of the reference dynamic pressure for the wall friction losses (see Sec. II-1-b (5)) is of little influence here if the comparison is made near the $M_p = M_s$ line, where all reference dynamic pressures become nearly the same or even identical, as is the case for the homogeneous ejector.

Heterogeneous conditions combined with external flow losses are covered by the No. 6 operating conditions. They represent an example of a practical heterogeneous ejector for nearly equal inlet total temperatures.

In general all operating points for heterogeneous media and with external flow losses are located to the right of the basic performance curves (solid lines); i.e., higher driver Mach numbers than those applying to the basic ejector are required in all these cases to obtain a given ejector pressure ratio. However, the solid lines in Fig. 5 present not necessarily the upper limit of performance. For the case in which the ratio of the specific heats is larger for the primary medium than for the secondary medium (case No. 5) the performance is better than for the homogeneous case, and the operating points fall to the left of the solid curves in Fig. 5. This can be readily explained. In accordance with Eq (9) a higher specific heat ratio gives a higher flow momentum at a given Mach number, or a given flow momentum is obtained with a lower flow Mach number.

For the performance curves in Fig. 6 all operating conditions remain the same as used in Fig. 5 with the only exception that the inlet area ratio A_p/A_s is now changed from 1.0 to 0.2. The performance curves are now drastically changed. The previously circular shape is changed to an elliptic one, however, in such a way that all points along the line $M_p = M_s$ have been

22

preserved. The position of the operating points for heterogeneous and external flow loss conditions relative to the solid base line remains about the same as in Fig. 5. If the reciprocal values of the magnitudes in Table I are taken as operating conditions, the complete set of curves and points is mirrored on the line $M_p = M_s$ with the operating points along this symmetry line remaining unchanged. Thus for an inlet area ratio of 5 the performance can be obtained from Fig. 5 by switching coordinates.

From the examples given above it becomes clear that the external flow losses have the dominant influence over that of the heterogeneous operating conditions. As we will see in the next paragraph, the reverse is true for the effects on the ejector mass ratio.

(4) Ejector Mass Ratio

Figures 7 and 8 give the ejector mass ratios as determined with the help of Eq (44) for the idealized homogeneous ejector together with the pressure ratio curves shown already in Figs. 5 and 6. The mass ratio curves away from the line $M_p = M_s$ are slightly bent. This is due to the influence of compressibility. The effects of heterogeneous operating conditions on the mass ratio for a given ejector pressure ratio are much too large to be shown properly in Figures 7 and 8. They can, however, be readily recognized from Eq (5), from which the mass ratio curves are derived. This equation shows that the mass ratio m_p/m_s is directly proportional to the inlet area ratio and to the square root of the product of the thermodynamic property ratios

$$\left[\gamma_p \cdot R_s \cdot (T_s)_0 \right] \Big/ \left[\gamma_s \cdot R_p \cdot (T_p)_0 \right]$$

The specific heat ratio appears a second time in the expressions in brackets, increasing the overall influence of the specific heat ratio.

The external flow losses do not directly enter the relation for the mass ratio. However, due to the change in Mach number caused by the external flow losses at a given ejector pressure ratio, as evident from Figs. 5 and 6, a slight change in mass ratio occurs with a change in the flow losses.

(5) Total Ejector Pressure Ratio

In many practical cases the plenum pressure of the secondary medium is a given constant. Then the total ejector pressure ratio $(p_{Ex})_0 / (p_s)_0$ becomes an important design parameter. By replacing the ejector pressure ratio in the pertinent equations by

$$\frac{(p_{Ex})_0}{p_s} \cong \frac{(p_{Ex})_0}{(p_s)_0} \frac{(p_s)_0}{p_s}$$

where $(p_s)_0/p_s$ is a function of M_s and γ_s, the total ejector pressure ratio can be readily introduced as parameter for making the $M_p - M_s$ plots.

Figures 9 and 10 give the total pressure ratio curves together with the mass ratio curves for the inlet area ratios 1.0 and 0.2, respectively. In both figures one recognizes that a mass ratio curve can intersect a given pressure ratio curve twice, indicating that the ejector operation can be optimized for a minimum mass ratio by choosing the proper secondary inlet Mach number. The curves also show that the primary Mach number can be considerably reduced by choosing a lower secondary Mach number at the expense of requiring a higher mass ratio. A complete performance optimization must also allow a change in inlet area ratio and mixing mode. Such complete optimization of the ejector operation is given in Section IV.

b. Constant Pressure Mixing.

(1) "Ejector Pressure Ratio"

For constant pressure mixing the "ejector pressure ratio" $(p_{Ex})_0/p_s$ derives from the recompression of the mixing section exit flow; i.e., it is a function of the mixing section exit Mach number M_{Ex} as obtained from Eq (22b).

If M_{Ex} is subsonic, the ejector pressure ratio is determined by the relation for adiabatic compression

$$\frac{(P_{Ex})_0}{P_s} = \left[1 + \frac{\gamma_{Ex}-1}{2} M_{Ex}^2 \right]^{\frac{\eta_{pol}\, \gamma_{Ex}}{\gamma_{Ex}-1}} \tag{48}$$

with the polytropic diffuser efficiency η_{pol} accounting for diffuser flow losses.

If M_{Ex} is supersonic, a realistic assumption is that the flow is first converted to subsonic flow in a pseudo ‑ ‑k diffuser with a pressure ratio accross the shock system equal to that ͺ a normal shock,

$$\frac{(P_{Ex})_{shock}}{P_s} = \frac{2\gamma_{Ex} M_{Ex}^2 - (\gamma_{Ex}-1)}{\gamma_{Ex}+1} \tag{49}$$

The subsequent subsonic diffusion takes place again according to Eq (48) with the Mach number being that down stream of the normal shock, given by the relation

$$\left(M_{Ex}^2 \right)_{after\, shock} = \frac{(\gamma_{Ex}-1) M_{Ex}^2 + 2}{2\gamma_{Ex} \cdot M_{Ex}^2 - (\gamma_{Ex}-1)} \tag{50}$$

24

The "ejector pressure ratio" becomes then

$$\frac{(P_{Ex})_0}{P_S} = \frac{(P_{Ex})_{shock}}{P_S}\left[1 + \frac{\gamma_{Ex}-1}{2}(M_{Ex}^2)_{shock}\right]^{\frac{\eta_{pol}\gamma_{Ex}}{\gamma_{Ex}-1}} \tag{51}$$

or

$$\frac{(P_{Ex})_0}{P_S} = \frac{2\gamma_{Ex}M_{Ex}^2 - (\gamma_{Ex}-1)}{\gamma_{Ex}+1}\left[1 + \frac{\gamma_{Ex}-1}{2}\frac{(\gamma_{Ex}-1)M_{Ex}^2+2}{2\gamma_{Ex}M_{Ex}^2-(\gamma_{Ex}-1)}\right]^{\frac{\eta_{pol}\gamma_{Ex}}{\gamma_{Ex}-1}} \tag{51a}$$

(2) Mixing Section Contraction

With the inlet Mach numbers M_p and M_s of the operating media given, the following sequence of equations, (5) (9b) (21b) (16a) (22b) (35) and (51a) yields directly the ejector pressure ratio and the mixing section contraction ratio. A useful plot of the results is that given in Fig. 11. In this figure the ejector pressure ratio is plotted over the mixing section contraction ratio with three independent parameters, primary inlet Mach number M_p, inlet area ratio A_p/A_s, and mass ratio m_p/m_s. The secondary Mach number M_s is in this case a constant. Diffuser and wall friction losses are assumed zero. Figure 11a shows the same plot with the properties of the operating media changed. In this plot the strong degradation of the performance due to diffuser and wall friction losses is also shown. Figure 12 shows another version of the plot where the inlet area ratio is a constant and the secondary inlet Mach number appears as curve parameter. Figures 11 and 12 show that constant pressure mixing requires considerable contraction ratios for small inlet area ratios and small secondary Mach number, respectively. Figure 12 shows that the contraction can change over to an expanding mixing section for high secondary Mach numbers in connection with heterogeneous operating media. Further implications of the mixing section contraction are discussed in Section III.2.

(3) Comparison with Constant Area Mixing.

For the constant area mixing case a useful presentation of the ejector performance consisted in plotting primary against secondary inlet Mach number with the ejector pressure ratio's serving as curve parameter. The same type of plot can be made for constant pressure mixing; an iterative solution for the applicable equation is now required. It was found convenient to use the mixing section contraction ratio as iteration criterion. The process starts with solving Eq (48) (subsonic case) or Eq (51a) (supersonic case) for the exit Mach number with a crude

estimate of γ_{Ex} (it is sufficient to take $\gamma_{Ex} = \gamma_s$ or γ_p). Equation (48) yields

$$M_{Ex}^2 = \frac{2}{\gamma_{Ex}-1}\left[\left(\frac{(p_{Ex})_0}{p_s}\right)^{\frac{\gamma_{Ex}-1}{\eta_{pol}\,\gamma_{Ex}}} - 1\right] \tag{52}$$

Equation (51a), which applies for supersonic M_{Ex}, cannot be algebraically solved. However, it is of the form

$$y = \left[1 + x\right]^n$$

and can be represented by the series

$$y = 1 + (n),x + (n_2)\,x^2 \cdots \cdots$$

Breaking off with the quadratic term, one can obtain an algetraic solution for M_{Ex}^2 with an accuracy of around 99%. The solution is rather lengthy:

$$M_{Ex}^2 = \frac{b + \sqrt{b^2 - 4ac}}{2a} \tag{53}$$

where

$$\alpha = \eta_{pol}\,\gamma_{Ex}\left(\gamma_{Ex}-1\right)\left[\gamma_{Ex} + \frac{\gamma_{Ex}-1}{8}\left(\eta_{pol}\,\gamma_{Ex} - \left[\gamma_{Ex}-1\right]\right)\right] + 4\gamma_{Ex}^2 \tag{53a}$$

$$-b = \eta_{pol}\,\gamma_{Ex}\left[2\gamma_{Ex} + \frac{\gamma_{Ex}-1}{2}\left(\eta_{pol}\,\gamma_{Ex} - 2\left[\gamma_{Ex}-1\right]\right)\right] - 2\gamma_{Ex}\left[\left(\gamma_{Ex}+1\right)\frac{(p_{Ex})_0}{p_s} + 2\left(\gamma_{Ex}-1\right)\right] \tag{53b}$$

$$c = \left(\gamma_{Ex}-1\right)\left[\frac{(p_{Ex})_0}{p_s}\left(\gamma_{Ex}+1\right) + \left(\gamma_{Ex}-1\right) - \eta_{pol}\,\gamma_{Ex}\left(1-\frac{1}{2}\left[\frac{\eta_{pol}\,\gamma_{Ex}}{\gamma_{Ex}-1} - 1\right]\right)\right] \tag{53c}$$

With M_{Ex} known a preliminary solution for M_p can be obtained from Eq (9b) by taking (t) in this equation as unity for a first step:

$$M_p^2 = \frac{A_s}{A_p\cdot\gamma_p}\left[\gamma_{Ex}\,M_{Ex}^2\cdot t\left(1 + \frac{A_p}{A_s}\right)\left(1 + c_f\frac{l}{2d}\right) - \gamma_s\,M_s^2\right] \tag{54}$$

26

Next, Eqs (5) and (16a) can be solved for a first approximation, and finally t is obtained from Eq (21b) with the result

$$t = \frac{M_S}{M_{EX}\left(1+\frac{\gamma_{EX}-1}{2}M_{EX}^2\right)^{\frac{1}{2}}\left(\frac{A_P}{A_S}+1\right)}\frac{\left(\frac{m_P}{m_S}+1\right)\sqrt{\left(1+\frac{m_P R_P}{m_S R_S}\right)\left(\frac{c_{P-P}}{c_{P-S}}\frac{m_P (T_P)_0}{m_S (T_S)_0}+1\right)(T_S)_0}}{\beta\left(1+\frac{m_P \gamma_P}{m_S \gamma_S}\right)\left(\frac{c_{P-P}}{c_{P-S}}\frac{m_P}{m_S}+1\right)T_S} \qquad (55)$$

The sequence of above equations is repeatedly solved until

$$t_n = t_{n-1}$$

In general about five iteration cycles are required. With the Hewlett-Packard calculator 9100B with Extended Memory 9101A calculation time is in general 5 to 10 sec for a curve point. In certain regions Eq (22b) becomes unmanageable. This difficulty can be overcome by switching coordinates. Since these regions are of little practical interest they are left blank in the following graphs.

Figure 13 presents a plot for constant pressure mixing with the same set of operating conditions used in Fig. 5 for constant area mixing. From the latter plot portions of the solid lines are replotted in Fig. 13 for comparison. The most conspicuous change against the previous performance curves is that the ellipses have become smaller, and for lower secondary inlet Mach number the required primary inlet Mach number became much lower than before; i.e., the ejector performance became much better. As expected, the operating points along the line $M_p = M_s$ remain the same for the homogeneous case (solid line). For the heterogeneous case the performance curves for both modes of mixing cross each other, and above a certain secondary inlet Mach number constant pressure mixing is no longer superior. A most significant feature of the plot is that in contrast to constant area mixing heterogeneous operating conditions and external flow losses have now a much larger influence on the performance curves.

In comparing the performance for the two mixing modes it must be considered that constant area mixing constitutes a very realistic case, whereas constant pressure mixing cannot be readily realized due to impact phenomena, particularly for supersonic flows.

(4) Ejector Mass Ratio and Total Ejector Pressure Ratio

Ejector Mass Ratio. As stated in connection with the derivation of Eq (5) the same mass ratio relations apply to all mixing modes. In Fig. 14 the ejector pressure ratio curves for constant pressure mixing are combined with the mass ratio curves previously determined for constant area mixing. For comparison, part of the pressure ratio curves for constant area mixing are also entered in the figure. The curves show that, for obtaining a

certain ejector pressure ratio at a given secondary inlet Mach number, constant pressure mixing requires a somewhat smaller mass ratio than constant area mixing with the primary Mach number appreciably reduced, as discussed before.

Ejector Total Pressure Ratio. Figure 15 shows the ejector performance for constant pressure mixing with the total ejector pressure ratio used as parameter. The basic shape of these curves is similar to that found for constant area mixing. Again there is a minimum mass ratio for a given total pressure ratio. As a comparison with Figure 9 shows, constant pressure mixing requires a smaller Mach number to accomplish a certain total pressure ratio at a given secondary Mach number than constant area mixing does, particularly for small secondary Mach numbers, as already evident from Fig. 13.

c. Mixing at a Defined Pressure Distribution

For plotting an ejector characteristic with M_p and M_s as coordinates and $(p_{Ex})_o/p_s$ as parameter, as done for the other mixing cases, the applicable equations must be solved by iteration. The same iteration method can be applied here as for constant area mixing (Section III.1.a). The right side of Eq (9e) can be written in analogy to Eq (46),

$$B_\tau = \frac{(p_{Ex})_0}{p_S} \frac{p_{Ex}}{(p_{Ex})_0} \left[\gamma_{Ex} M_{Ex}^2 \left(C_f \frac{L}{2d} + 1 \right) + \tau \right] \tag{56}$$

or

$$B_\tau = \frac{(p_{Ex})_0}{p_S} \frac{\left[\gamma_{Ex} M_{Ex}^2 \left(C_f \frac{L}{2d} + 1 \right) + \tau \right]}{\left[1 + \frac{\gamma_{Ex} - 1}{2} M_{Ex}^2 \right]^{\frac{\eta_{pol} \gamma_{Ex}}{\gamma_{Ex} - 1}}} = \frac{(p_{Ex})_0}{p_S} \cdot f_\tau \tag{57}$$

The factor f_τ is again used as the iteration criterion. For the first step in the iteration it can be taken to be unity. A preliminary M_p can then be determined from Eq (9e). Next, the mass ratio m_p/m_s is found from Eq (5). Also, E_τ can be determined from Eq (21c). Then Eq (16a) is solved and M_{Ex} is obtained from Eq (22c). Finally, a refined value for f_τ can be determined with Eq (57) to repeat the above process for solving for an improved f_τ. The iteration is completed if after n cycles

$$(f_\tau)_n = (f_\tau)_{n-1}$$

As with the previous iterations the conversion requires in general only a few cycles.

Figure 16 gives an example for an ejector characteristic determined with the above iteration process. The design conditions for the ejector are

indicated on the figure. The contemplated ejector has a mixing section exit to inlet area ratio t = 0.3. The value i = 0.6 has been chosen in accordance with some preliminary experimental data from an ejector of similar lay-out. This choice of i is still subject to discussions. More experimental substantiation is required to make this value typical for the present case (see discussion at the end of this paragraph and in Section II.4). Also, the diffuser efficiency of 0.6 in the present example had been chosen to match an available experimental point at pressure ratio $(p_{Ex})_o / (p_s)_o = 6$.

In determining the present operating characteristic a second iteration process was superimposed on the above explained one to adapt at each point the inlet area ratio A_p/A_s to the primary Mach number in such a way that the primary nozzle is always ideally expanded for the primary Mach number. This represents very closely actual conditions in a given ejector when operated at different primary Mach numbers. As indicated on the figure the geometric primary nozzle expansion ratio is 13.3; i.e., the primary nozzle is properly expanded for a Mach number of about $M_p = 3.8$. As discussed in Section II.a for higher Mach numbers, the flow adapts itself to a good degree to conditions which a properly expanded nozzle will provide. For Mach numbers lower than 3.8 the overexpanded part of the nozzle becomes increasingly a physical obstruction in the path of the primary as well as the secondary flow, and the analytical values become too optimistic.

The characteristic shown here represents the operating behavior of an ejector with given geometry as closely as the present analysis is able to do.

In Fig. 16, choking conditions ($M_{Ex} = 1$) are indicated as the upper limit for the secondary inlet Mach numbers. This limit i actually too high. According to the discussions in Section II.4, a small t-value (large mixing section contraction) does in reality not allow one to obtain sonic velocity in the mixing section exit. If an attempt is made to increase the secondary Mach number above its limit, which may be actually near $M_{Ex} = 0.6$, shock diffusion in the mixing section increases, leading to an earlier pressure rise in the mixing section. The result is an increased i-value. This can then be cause for immediate choking.

2 BASIC EJECTOR BEHAVIOR

The operational behavior of ejectors is primarily determined by the condition for conservation of momentum. This is borne out by the operating characteristics shown in Figs. 5-8, which have very nearly the shapes of ellipses, reflecting the basic form of the momentum equation. The deviations from the pure elliptic form are due to compressibility and heterogeneity of the operating media. For incompressible, homogeneous operating media (and zero wall friction and diffuser losses) the operating characteristics for the various modes of mixing all become true ellipses.

For a comparison of the mixing modes the study of the relative positions of these ellipses is very helpful. In the following for the three modes of mixing treated in this analysis the momentum equation is written

29

for the incompressible homogeneous case, and the resulting characteristics are plotted.

a. Constant Area Mixing

For incompressible, homogeneous media, disregarding incidental flow losses, one can write Eq (6)

$$\frac{v_p^2}{1+\frac{A_s}{A_p}} + \frac{v_s^2}{1+\frac{A_p}{A_s}} = \frac{v_{EX}^2}{2} + \left[\frac{v_{EX}^2}{2} + \frac{p_{EX}-p_s}{\rho}\right] \tag{58}$$

The expression in brackets is the "total head" of the ejector, which, corresponding to the previously used "ejector pressure ratio", is a constant in the ejector characteristic. With the continuity condition the exit velocity, v_{Ex} can be expressed by the entrance conditions

$$v_{EX} = \frac{v_p \cdot A_p \cdot \rho_p + v_s \cdot A_s \cdot \rho_s}{(A_p + A_s)\rho_{EX}} = \frac{v_p \cdot A_p + v_s \cdot A_s}{A_p + A_s} \tag{59}$$

Upon using H_{tot} and this relation the momentum equation expressed in initial magnitudes becomes

$$v_s^2\left[1-\frac{1}{2\left(\frac{A_p}{A_s}+1\right)}\right] - v_s\frac{v_p\frac{A_p}{A_s}}{\left(\frac{A_p}{A_s}+1\right)} + v_p^2\left[\frac{A_p}{A_s} - \frac{1}{2}\frac{\left(\frac{A_p}{A_s}\right)^2}{\left(\frac{A_p}{A_s}+1\right)}\right] - H_{tot}\left[\frac{A_p}{A_s}+1\right] = 0 \tag{60}$$

This quadratic equation presents an ellipse with its axis turned against the coordinates v_p and v_s by the angle α, where

$$tg\,\alpha = \frac{A_p}{A_s} \tag{61}$$

and with the length ratio of the axis

$$\frac{b}{a} = \frac{\sqrt{2\frac{A_p}{A_s}}}{\frac{A_p}{A_s}+1} \tag{62}$$

<center>62014</center>

It is interesting to note that this relation does not allow a circle as a realistic case of ejector operation. The ellipse given by Eq (60) is plotted in Fig. 17 for $A_p/A_s = 0.2$ and $H_{tot} = 1$, as the larger one of the two ellipses shown in this figure.

b. Constant Pressure Mixing

Equation (6) written for the incompressible homogeneous case without incidental flow losses becomes

$$V_S^2 + V_p^2 \frac{A_p}{A_S} = \left(V_S + V_p \frac{A_p}{A_S} \right) \cdot V_{EX} \tag{63}$$

Constant pressure mixing implies that the ejector "total head" derives solely from the mixing section exit velocity

$$H_{tot} = \frac{V_{EX}^2}{2} \tag{64}$$

With this consideration Eq (63) can be written in the form

$$\frac{\left(V_S - \sqrt{\frac{H_{tot}}{2}} \right)^2}{\left(1 + \frac{A_p}{A_S} \right) \frac{H_{tot}}{2}} + \frac{\left(V_p - \sqrt{\frac{H_{tot}}{2}} \right)^2}{\frac{A_S}{A_p} \left(1 + \frac{A_p}{A_S} \right) \frac{H_{tot}}{2}} = 1 \tag{65}$$

This equation represents an ellipse which has its center at a point shifted in the positive direction of both coordinates by the amount $\sqrt{H_{tot}/2}$ and has as axis ratio

$$\frac{b}{a} = \sqrt{\frac{A_p}{A_S}} \tag{66}$$

For plotting the ellipse Eq (65) is written in the form

$$V_S^2 - V_S \sqrt{2H_{tot}} + V_p \frac{A_p}{A_S} \left(V_p - \sqrt{2H_{tot}} \right) = 0 \tag{67}$$

and is readily solved for v_s.

31

Again, for $A_p/A_s = 0.2$ and $H_{tot} = 1$ the equation is plotted in Fig. 17 as the smaller of the two ellipses.

Before proceeding to the third mode of mixing the typical ejector behavior represented by the two ellipses in Fig. 17 is discussed first.

c. Comparison of Constant Area and
   Constant Pressure Mixing Performance

The solidly drawn portion of the two ellipses in Fig. 17 represent operating conditions which have a meaning for an ejector. Along the line $v_p = v_s$ the two ellipses have a common point. Otherwise, the constant pressure ellipse lies completely inside the constant area ellipse. This means that for the here assumed incompressible, homogeneous ejector media constant pressure mixing is always superior since it requires the lower driver velocity to obtain a certain ejector pressure ratio. This superiority can be postulated from mixing efficiency considerations, as will be shown in Section III.5. The difference in performance between the two mixing cases varies greatly with the secondary velocity, with the greatest difference for $v_s = 0$.

In comparing the two ellipses in Fig. 17, it is interesting to note that for constant pressure mixing the primary velocity is the same for $v_s = v_p$ and $v_s = 0$. This is understandable since for zero secondary flow constant pressure is maintained if the exit cross section is the same as the primary inlet cross section. As in the case of $v_s = v_p$, the point $v_s = 0$ represents simply straight pipe flow. In the latter case, however, the flow is interrupted by a sudden cross section enlargement, followed by an area reduction to that of the original cross section similar to an open jet wind tunnel. If the secondary flow is no longer zero, the exit cross section must be enlarged with larger secondary flow until the constant area case ($v_s = v_p$) is reached. The mechanism of constant pressure mixing consists in accelerating the secondary flow at each location of the mixing section very nearly to the primary velocity before mixing itself occurs, avoiding at the same time impact compression in the primary flow. Such a process fulfills nearly ideally the requirements of an efficient ejector operation (see Section IV). It is obvious that maintaining constant pressure during the mixing process is in reality a sensitive process and not readily attainable, particularly in the supersonic case.

Constant pressure during mixing is not a limiting case since, as will be shown in the next paragraph, the pressure during mixing can also be reduced, constituting, at least theoretically, the most ideal ejector conditions possible.

If we select the portion of the performance curves above the line $v_p = v_s$, where the secondary velocity is higher than the primary one, the roles of the operating media are exchanged. Consistently with this switch, the inlet area ratio becomes 5 instead of 0.2. Then the region above the line $v_s = v_p$ gives a consistent presentation of the behavior of an ejector with an inlet area ratio A_p / A_s larger than one. We find that for this condition the performance difference for the two mixing cases practically disappears.

d. Mixing at a Defined Pressure Distribution

For incompressible, homogeneous operating media and zero incident flow losses Eq (6) can be written in this case, upon utilizing Eq (39b),

$$V_p^2 A_p + V_S^2 A_S - V_{Ex}^2 A_{Ex} = t \cdot \mathcal{T} \left(p_{Ex} - p_S \right) \left(A_p + A_S \right) \frac{1}{\rho} \tag{68}$$

or, somewhat transformed,

$$\frac{\cdot V_p^2}{t \mathcal{T} \left(1 + \frac{A_S}{A_p} \right)} + \frac{V_S^2}{t \mathcal{T} \left(1 + \frac{A_p}{A_S} \right)} = \left[\frac{p_{Ex} - p_S}{\rho} + \frac{V_{Ex}^2}{2} \right] - \frac{V_{Ex}^2}{2} + \frac{V_{Ex}^2}{\mathcal{T}} \tag{69}$$

The expression in brackets constitutes again the "ejector total head". Expressing v_{Ex} by initial magnitudes according to Eq (59), one can transform Eq (69) into

$$V_S^2 \left[1 - \frac{2 - \mathcal{T}}{2t \left(\frac{A_p}{A_S} + 1 \right)} \right] - V_S \frac{V_p \frac{A_p}{A_S} (2 - \mathcal{T})}{t \left(\frac{A_p}{A_S} + 1 \right)} + V_p^2 \left[\frac{A_p}{A_S} - \frac{2 - \mathcal{T}}{2t} \frac{\left(\frac{A_p}{A_S} \right)^2}{\left(\frac{A_p}{A_S} + 1 \right)} \right] - t \cdot \mathcal{T} \left(1 + \frac{A_p}{A_S} \right) H_{tot} = 0 \tag{70}$$

In this form the equation representing a true ellipse can be readily solved, and v_s can be plotted against v_p. (No attempt has been made to derive criteria for shape and position of the resulting ellipse since they appear not to serve any essential purpose in the present discussion.)

The pressure distribution factor i, as contained in τ, occurs as an additional parameter in Eq (70). Its pertinent value cannot be readily estimated. For specific flow conditions it can be derived analytically as it will be shown

further below. At first its influence is shown in a simple parametric form.

In Fig. 18, which contains also the two previously treated mixing cases, Eq (70) is plotted for three t-values and a certain number of i-values. As expected from the definition of the factor i along the constant pressure mixing curve, the influence of i vanishes. Inside this curve the pressure during mixing decreases, and outside it increases.

There is a basic limit to the decrease in pressure during mixing. This becomes immediately obvious for the special operating point where $v_p = v_s$ since this point represents strictly potential flow conditions. For the first two mixing cases the flow is that in a straight pipe; in the third case it represents the flow in a Venturi tube. In all three cases the total pressure must be the same. The Venturi case provides the criterion for the largest pressure drop possible for a given cross section reduction, namely, Bernoulli's criterion for potential flow. For $v_p = v_s$ the factor i follows then under this condition from Eq (68):

$$ i_{po} = 2t \frac{(1-t)}{(1-t^2)} \tag{71} $$

In Fig. 19 the ejector characteristic for the limiting i-value at a mixing section contraction ratio t = 0.3 has been entered. As expected this characteristic meets the t = 1 curve at the $v_p = v_s$ line. Inside this limiting characteristic (shaded area) no ejector operation is possible for the given mixing section contraction ratio.

For i = 0, Eq (70) applies to an increasing mixing cross section area; i.e., t > 1 in the form of a sudden enlargement at the entrance. In Fig. 19 an example is shown for i = 0, t = 2. At the point where the characteristic intersects with the line $v_p = v_s$ the conditions in a so called shock-diffuser are represented.

The present mixing case shows that the ejector performance can be improved against that for constant pressure mixing, at least theoretically, by providing a decrease in pressure during mixing. As expected, the ejector performance will be still more sensitive to incidental flow losses and effects of heterogeneity of the operating media, as was the case with constant pressure mixing, since lowering the pressure implies an increase in flow velocity during mixing and thus an increase in losses associated with flow velocities. It is also obvious, that an increase of velocity augments the danger of choking the mixing section outlet.

To show the influences of the incidental losses the fully implimented ejector characteristics as derived in Section III.1.c. have been applied to the present incompressible case by choosing an ejector pressure ratio of 1.1, which is low enough to be representative for the present case. The mixing section area reduction was chosen as t = 0.7, for which an optimized factor i was determined from Eq (71). Figure 20 shows the results for three different loss conditions. For comparison the corresponding three curves for constant area mixing (t = 1) are also entered.

34

The main result of the plot in Fig. 20 is that it shows the devastating influence of the incidental flow losses on the theoretically optimum ejector performance below a primary to secondary Mach number ratio of about 3 to 4. At the terminal point of the t = 0.7 curves with losses (bending over to higher primary Mach numbers) Mach number one is reached at the mixing section outlet. The comparison shows that, for very high ratios of primary to secondary Mach number, the optimization of the pressure distribution in the mixing section appears to be worthwhile. Since the present thoughts apply to incompressible media, they should be representative for ejector pumps operating with liquids; i.e., proper contouring of the mixing section to minimize the pressure rise during mixing at comparatively low secondary inlet velocities appears to be a desirable design feature.

In the next paragraph it will be demonstrated that for a good performance the thrust augmentor requires an inlet Mach number ratio in the neighborhood of three. For this requirement Fig. 20 indicates that constant area mixing is equal or better than mixing with area reduction and optimized pressure distribution.

e.   Thrust Augmentation

In the basic ejector performance plot of Fig. 17 thrust augmentation can be assigned a definite region. This allows one to determine the importance of the type of mixing for thrust augmentation. The concept of thrust augmentation consists in distributing the kinetic energy of a low mass high speed jet over a large air mass, resulting in a large mass, low speed jet. Thus, a primary requirement for a thrust augmentation ejector is a secondary to primary mass ratio essentially larger than one. For the plot in Fig. 17 this means that the ejector operating point will be above the axis of the inclined ellipse.

Since the secondary velocity can never be higher than the primary velocity, the operating point can never be above the line $v_s = v_p$. As we will see later (Section III.3), wall friction and diffuser losses prevent the operating point to even remotely reach this line. Anticipating results from Section III.3, a realistic inlet velocity ratio v_p/v_s of about 2.5 can be given for the present case. For smaller inlet area ratios, as they are actually common for thrust augmenters, the optimum inlet velocity ratio decreases to about 2.

From the above considerations we see that the operation of thrust augmenters falls into a region where the two types of mixing cause relatively little difference in ejector performance. In addition, the difference between the two types of performance curves becomes less with the reduction of flow losses, in particular, of the diffuser, since the optimum operating point moves to higher mass ratios m_s/m_p. As previously stated, flow losses in general deteriorate the constant pressure mixing performance more than the constant area mixing performance. Thus, no obvious advantage remains for thrust augmentation to be designed specifically for constant pressure mixing.

35

The discussion in Section IV will show that above considerations for the optimum operating regime of thrust augmenters simply reflect requirements which are applicable for the optimization of ejectors in general.

3. THRUST AUGMENTER

a. Derivation of Specific Equations

(1) Operating Conditions

For the thrust augmenter, the diffuser pressure ratio, and thus the diffuser area ratio, must be tailored to the requirement that a maximum of fluid momentum is added to that of the primary flow. In general, the diffuser discharges to ambient, and the diffuser exit pressure is equal to ambient. The total pressure of the secondary medium at the ejector inlet is also ambient if the augmenter is stationary. If the augmenter is moving, the dynamic pressure of the air moving relative to the augmenter is added to the total pressure at the ejector inlet, and an inlet momentum must be considered for the secondary flow.

For the definition of the thrust augmentation one must consider that the primary medium expands in the ejector to a pressure lower than ambient. For the thrust produced without the augmenter the expansion of the primary medium is only to ambient pressure. Thus the definition of thrust augmentation is

$$T_{Aug} = \frac{Th_{Ex} - Th_{in}}{Th_{pr}} \tag{72}$$

Each of the thrust components occurring in this definition is developed in the following in terms of ejector operating data. For each thrust component the general relation applies:

$$Th = A \cdot \rho \cdot v^2 = \gamma \cdot p \cdot M^2 \cdot A \tag{73}$$

with all magnitudes occurring in this relation referred to the pertinent flow cross sections, i.e., to the diffuser exit cross section, the inlet cross section of the air scoop which catches the secondary air, and the exit cross section of the primary air if expanded to ambient pressure from the given plenum pressure.

(2) Exit Thrust

For exit thrust one has (for notations see Fig. 21)

$$Th_{Ex} = P_{Ex} \gamma_{Ex} \cdot M_{Ex-d} \cdot A_{Ex-d} \tag{74}$$

36

From primary assumptions it is $P_{Ex-d} = P_{amb}$. The specific heat ratio γ_{Ex} will be found from Eq (16) after the mass ratio is known from Eq (5). In the following, the diffuser exit Mach number M_{Ex-d} and the diffuser exit area A_{Ex-d} will be expressed in terms of ejector operating conditions. Quite a number of relations must be introduced to accomplish this. These relations will first be derived separately.

As illustrated in the sketch of an I-S diagram in Fig. 21 we can write for the enthalpy change in the diffuser with losses,

$$(\Delta H)_\eta = \frac{V_{Ex}^2}{2} - \frac{V_{Ex-d}^2}{2} \tag{75}$$

It is also

$$(\Delta H)_\eta = c_p T_{Ex-d} - c_p T_{Ex} \tag{76}$$

Considering

$$c_p = \frac{R_{Ex}}{\gamma_{Ex} - 1} \tag{77}$$

we can write

$$V_{Ex-d}^2 = V_{Ex}^2 - 2 \, \frac{\gamma_{Ex} R_{Ex} T_{Ex}}{\gamma_{Ex} - 1} \left[\frac{T_{Ex-d}}{T_{Ex}} - 1 \right] \tag{78}$$

or in terms of Mach numbers

$$M_{Ex-d} = \frac{T_{Ex}}{T_{Ex-d}} \left[M_{Ex}^2 - \frac{2}{\gamma_{Ex} - 1} \left(\frac{T_{Ex-d}}{T_{Ex}} - 1 \right) \right] \tag{79}$$

$$M_{Ex-d} = \frac{T_{Ex}}{T_{Ex-d}} \left[M_{Ex}^2 + \frac{2}{\gamma_{Ex} - 1} \right] - \frac{2}{\gamma_{Ex} - 1} \tag{79a}$$

37

From the definition of the polytropic diffuser efficiency, (Ref. 6)

$$\eta_{pol} = \frac{\ln T_{Ex-is} - \ln T_{Ex}}{\ln T_{Ex-d} - \ln T_{Ex}} \qquad (80)$$

follows

$$\ln \frac{T_{Ex-d}}{T_{Ex}} = \frac{1}{\eta_{pol}} \ln \frac{T_{Ex-is}}{T_{Ex}} \qquad (80a)$$

or

$$\frac{T_{Ex-d}}{T_{Ex}} = \left[\frac{T_{Ex-is}}{T_{Ex}} \right]^{\frac{1}{\eta_{pol}}} \qquad (80b)$$

The diffuser pressure ratio related to this temperature ratio is given by the adiabatic relation

$$\frac{T_{Ex-d}}{T_{Ex}} = \left[\frac{P_{amb}}{P_{EX}} \right]^{\frac{\gamma_{Ex}-1}{\gamma_{Ex}} \frac{1}{\eta_{pol}}} \qquad (81)$$

The pressure ratio in Eq (81) can be written as the product of two pressure ratios:

$$\frac{P_{amb}}{P_{EX}} \cong \frac{P_{amb}}{P_S} \frac{P_S}{P_{EX}}$$

Then Eq (81) reads

$$\frac{T_{Ex-d}}{T_{EX}} = \left[\frac{P_{amb}}{P_S} \frac{P_S}{P_{EX}} \right]^{\frac{\gamma_{Ex}-1}{\gamma_{Ex} \eta_{pol}}} \qquad (81a)$$

The first pressure ratio in Eq (81a) is a function of the inlet conditions. With the augmenter moving with flight Mach number M_{f1}

$$\frac{P_{amb}}{P_s} \cong \frac{(P_s)_0}{P_s} \frac{P_{amb}}{(P_s)_0}$$

The first pressure ratio in this identity is determined by the ejector inlet Mach number M_s, and the second one by the flight Mach number M_{f1}. Assuming isentropic changes of state in each case, we obtain

$$\frac{P_{amb}}{P_s} = \left[\frac{1 + \frac{\gamma_s - 1}{2} M_s^2}{1 + \frac{\gamma_s - 1}{2} M_{f1}^2} \right]^{\frac{\gamma_s}{\gamma_s - 1}} \cdot \tag{82}$$

The second pressure ratio in Eq (81a) is given by Eq (10):

$$\frac{P_{EX}}{P_s} = \frac{B_A}{\gamma_{EX}^2 M_{EX}^2 + 1}$$

Equations (79a), (81a), (82) and (10) determine now the diffuser exit Mach number in terms of ejector operating conditions.

For determining the exit thrust with Eq (74) the diffuser exit area is still needed. It is obtained from continuity,

$$V_{EX} A_{EX} \frac{P_{EX}}{R_{EX} T_{EX}} = V_{EX-d} A_{EX-d} \frac{P_{amb}}{R_{EX} \cdot T_{EX-d}} \tag{83}$$

39

or

$$\frac{A_{Ex-d}}{A_{Ex}} = \frac{v_{EX} \cdot p_{EX} \cdot R_{EX} \cdot T_{Ex-d}}{v_{Ex-d} \cdot P_{amb} \cdot R_{EX} \cdot T_{EX}} \tag{84}$$

or in terms of Mach numbers

$$\frac{A_{Ex-d}}{A_{Ex}} = \frac{M_{Ex} \cdot p_{EX}}{M_{Ex-d} \cdot P_{amb}} \sqrt{\frac{T_{Ex-d}}{T_{EX}}} \tag{85}$$

The temperature ratio in Eq (85) can again be replaced by pressure ratios with the help of Eqs (81a), (82), and (10).

Equations (74) and (85) combined give for the exit thrust

$$Th_{EX} = \gamma_{EX} \cdot M_{Ex-d} \cdot A_{EX} \cdot p_{EX} \cdot M_{EX} \sqrt{\frac{T_{Ex-d}}{T_{EX}}} \tag{86}$$

In this short form we will later enter Th_{Ex} into Eq (72).

(3) Inlet Thrust

The basic relation for the inlet thrust is in accordance with Eq (73)

$$Th_{in} = \dot{A}_{amb} \cdot P_{amb} \cdot M_{fl}^2 \cdot \gamma_{s} \tag{87}$$

The flow cross section A_{amb} required for the secondary mass M_s at flight speed v_{fl} follows from continuity,

$$A_{amb} \cdot v_{fl} \cdot \frac{P_{amb}}{R_s \cdot T_{amb}} = A_s \cdot v_s \frac{p_s}{R_s \cdot T_s} \tag{88}$$

or in terms of Mach numbers,

$$A_{amb} \cdot M_{fl} \cdot \frac{P_{amb}}{\sqrt{T_{amb}}} = A_s \cdot M_s \frac{p_s}{\sqrt{T_s}} \tag{89}$$

40

then

$$A_{amb} = A_s \frac{M_s}{M_{fl}} \frac{p_s}{p_{amb}} \sqrt{\frac{T_{amb}}{T_s}} \qquad (90)$$

The inlet thrust becomes now

$$Th_{in} = M_s \cdot p_s \cdot A_s \cdot \gamma_s \cdot M_{fl} \sqrt{\frac{T_{amb}}{T_s}} \qquad (91)$$

with

$$\frac{T_{amb}}{T_s} = \left[\frac{p_{amb}}{p_s} \right]^{\frac{\gamma_s - 1}{\gamma_s}} \qquad (91a)$$

and p_{amb}/p_s given by Eq (82)

(4) Primary Thrust

We write for the primary thrust with basic Eq (73)

$$Th_{pr} = A_{p\text{-}amb} \cdot p_{amb} \cdot \gamma_p \cdot M_{p\text{-}amb}^2 \qquad (92)$$

From continuity

$$A_{p\text{-}amb} \cdot V_{p\text{-}amb} \cdot \frac{p_{amb}}{R_p \cdot T_{p\text{-}amb}} = A_p \cdot V_p \cdot \frac{p_p}{R_p T_p} \qquad (93)$$

or in terms of Mach numbers

$$A_{p\text{-}amb} \cdot M_{p\text{-}amb} \cdot p_{amb} \frac{1}{\sqrt{T_{amb}}} = A_p \cdot M_p \cdot p_p \frac{1}{\sqrt{T_p}} \qquad (94)$$

$$A_{p\text{-}amb} = \frac{A_p \cdot M_p \cdot p_p}{M_{p\text{-}amb} \cdot p_{amb}} \sqrt{\frac{T_{amb}}{T_p}} \qquad (95)$$

41

We can write for the primary thrust

$$Th_{pr} = A_p \cdot P_p \cdot \gamma_p \cdot M_p \cdot M_{p\text{-}amb} \sqrt{\frac{T_{amb}}{T_p}} \qquad (96)$$

For the primary Mach number without the presence of the thrust augmenter, i.e., for expanding the primary medium from its supply pressure to ambient, we can write, assuming isentropic expansion,

$$M_{p\text{-}amb}^2 = \frac{2}{\gamma_p - 1}\left[\left(\frac{(P_p)_0}{P_{amb}}\right)^{\frac{\gamma_p - 1}{\gamma_p}} - 1\right] \qquad (97)$$

For the pressure ratio in Eq (97) we can write

$$\frac{(P_p)_0}{P_{amb}} = \frac{(P_p)_0}{P_p}\ \frac{P_p}{P_{amb}} \qquad (98)$$

The first pressure ratio is given by the ejector primary Mach number M_p;

$$\frac{(P_p)_0}{P_p} = \left[1 + \frac{\gamma_p - 1}{2} M_p^2\right]^{\frac{\gamma_p}{\gamma_p - 1}} \qquad (98a)$$

The second pressure ratio is given by Eq (82) after considering $p_p = p_s$ according to basic assumptions. With Eqs (97) and (91a) the primary thrust as given by Eq (96) can be determined in terms of ejector operating data.

(5)   Thrust Augmentation Ratio

With Eqs (86) (91), and (96) we can form an expression for the thrust augmentation in short form:

$$T_{Aug} = \frac{A_{EX} \cdot P_{EX} \cdot \gamma_{EX} \cdot M_{EX} \cdot M_{EX\text{-}d}\sqrt{\frac{T_{EX\text{-}d}}{T_{EX}}} - M_s \cdot P_s \cdot A_s \cdot \gamma_s \cdot M_{fl}\sqrt{\frac{T_{amb}}{T_s}}}{A_p \cdot P_p \cdot \gamma_p \cdot M_p \cdot M_{p\text{-}amb}\sqrt{\frac{T_{amb}}{T_p}}} \qquad (99)$$

42

with

$$A_{EX} = A_p + A_s$$

and

$$\frac{p_{EX}}{p_S} = \frac{p_{EX}}{p_p} = \frac{B_A}{\gamma_{EX} M_{EX}^2 + 1}$$

Equation (99) becomes

$$T_{Aug} = \frac{\left(1 + \frac{A_s}{A_p}\right)\frac{B}{(\gamma_{EX} M_{EX}^2 + 1)} \gamma_{EX} \cdot M_{EX} \cdot M_{EX-d} \sqrt{\frac{T_{EX-d}}{T_{EX}}} - M_s \cdot \frac{A_s}{A_p} \cdot \gamma_s \cdot M_{fi} \sqrt{\frac{T_{amb}}{T_S}}}{M_p \cdot \gamma_p \cdot M_{p-amb} \sqrt{\frac{T_{amb}}{T_p}}} \qquad (100)$$

Equation (100) allows to determine the thrust augmentation ratio in a straightforward though lengthy way from the ejector inlet conditions. For this determination the following sequence of equations must be applied

(5) (9) (21) (16) (22) (79a) (81a) (82) (91a) (97) and (98a)

As we will see in the next paragraph the diffuser area ratio can be presented also as a unique function of the ejector inlet conditions. This allows to present the thrust augmentation ratio as a unique function of the diffuser area ratio. This form of presentation allows to readily recognize the potential of thrust augmentation under the influence of various design conditions.

(6) Diffuser Area Ratio

The amount of static pressure recovery in the diffuser of the thrust augmenter is an essential criterion for maximizing the thrust augmentation ratio. For the ejector design this means that the diffuser inlet to exit area ratio appears as an essential geometric condition for maximizing the thrust. To introduce this area ratio into the present analysis the following procedure is applied. The continuity condition written in the form (see Eq (12))

$$m = M \cdot A \cdot p \cdot \sqrt{\gamma} \frac{1}{\sqrt{RT}}$$

allows one to relate entrance to exit area of the diffuser in the following way:

$$\frac{A_{Ex\text{-}amb}}{A_{EX}} = \frac{M_{EX} \cdot p_{EX}}{M_{Ex\text{-}amb} \cdot p_{amb}} \sqrt{\frac{T_{Ex\text{-}amb}}{T_{EX}}} \tag{101}$$

Using Eqs (79) and (81) and applying some transformations, we obtain

$$\frac{A_{Ex\text{-}amb}}{A_{EX}} = \frac{M_{EX}\left[\dfrac{p_{amb}}{p_{EX}}\right]^{\frac{1}{\eta_{pol}} \cdot \frac{\gamma_{EX}-1}{\gamma_{EX}} - 1}}{\sqrt{M_{EX}^2 + \dfrac{2}{\gamma_{EX}-1} - \dfrac{2}{\gamma_{EX}^2-1}\left[\dfrac{p_{amb}}{p_{EX}}\right]^{\frac{1}{\eta_{pol}} \cdot \frac{\gamma_{EX}-1}{\gamma_{EX}}}}} \tag{101a}$$

Considering

$$\frac{p_{amb}}{p_{EX}} = \frac{p_{amb}}{p_S} \frac{\gamma_{EX} \cdot M_{EX}^2 + 1}{B} \tag{102}$$

one can evaluate Eq (101a) in terms of ejector inlet conditions in the same way that the thrust augmentation ratio can be obtained from Eq (100). Thrust augmentation ratio can be presented as a function of the diffuser area ratio.

(7) Mass Ratio

In Eq (100) and associated equations which yield the thrust augmentation ratio, the secondary inlet Mach number M_s is carried as an independent variable. By means of Eqs (44) and (45) the secondary Mach number can be replaced by the mass flow ratio m_p/m_s. This procedure allows one to enter lines of constant mass flow ratios in the performance presentation of the thrust augmenter, as will be shown in the next chapter.

b. Presentation of Results

As indicated before, the thrust augmentation ratio is a strong function of the diffuser area ratio. In particular there is an optimum diffuser area ratio, where the augmentation becomes a maximum. The value of this optimum area ratio changes not only with a change in any of the remaining ejector design parameters but also with the flight speed of the propulsion device employing the thrust augmenter. The individual dependencies of the diffuser area ratio are shown in the Figures 21a-g for air

44

as the operating medium. The first figure, for instance, shows the
strong influence of the inlet area ratio for two diffuser efficiencies.
For the following figures the inlet area ratio has been chosen as 20, repre-
senting a practical layout. Figure 21b shows the extreme importance of a
good diffuser efficiency. Figure 21c indicates that the primary flow Mach
number is of minor importance in optimizing the augmentation, though it
influences to a degree the diffuser area ratio for optimum augmentation.
Figure 21d points out the importance of low wall friction losses upon
considering that a value of $c_f l /(2d)$ = .015 may be achievable in an actual
case. Figure 21e demonstrates the enormous influence of the flight speed.
A few m/sec degrade appreciably the augmentation ratio. The influences of
temperature differences in the operating media are comparatively modest, as
Fig. 21f, shows in terms of the temperature ratio of the operating media.
In Figs 21g and h the mass flow ratio has been entered as an additional
parameter to the diffuser efficiency. These latter two figures allow one
to recognize the appreciable increase in mass flow ratio by changing the
operating media temperature ratio from 1 to 3.

From Eqs. (44) and (45) follows that along a line of constant mass ratio
the secondary inlet Mach number must be also constant for a given primary
Mach number.

4. INCOMPLETE MIXING

The effects of incomplete mixing in an ejector device are not readily
assessable since mixing itself is not a very well defined process. For the
purpose of the analysis, it had been assumed that mixing is completed at
the mixing section exit. This represents desirable conditions. However, it
is not necessarily very detrimental if mixing continues into the subsonic
diffuser. If the unmixed state is of such a nature that the higher velocities
are near the wall, such a condition will actually be beneficial for the dif-
fusion process since it energizes the boundary layer. In an actual ejector
device the primary injection nozzles may be purposely arranged in this way to
benefit the diffusion process. This possibility of trade-offs between mixing
and the diffusion process can substantially reduce detrimental effects of
incomplete mixing at the mixing section outlet.

To obtain an estimate for the influence of incomplete mixing on the
mixing process alone, the pressure rise in a constant area mixing process is
determined and compared with the pressure drop caused by wall friction. The
advantage of this comparison is that wall friction, as shown in Section II.2,
can be given in very simple terms. It is then necessary only to define the
state of incomplete mixing in terms of two different velocities, i.e., by a
single step velocity profile, to determine how the pressure loss, due to the
fact that mixing does not take place, ranks with the pressure loss due to
wall friction.

To make this comparison we simply assume an ejector with constant area
mixing and express in the pertinent Eq (7) the pressure rise during mixing in
terms of the pressure drop due to wall friction as a pure formality, leaving

the wall friction term itself zero in Eq (7). The pressure rise during
mixing reads then

$$P_{EX} - P_S = \left(\Delta p\right)_W$$

or

$$\frac{P_{EX}}{P_S} = \frac{\left(\Delta p\right)_W}{P_S} + 1$$

or with Eq (31)

$$\frac{P_{EX}}{P_S} = C_f \frac{l}{2d} \cdot \gamma_S \cdot M_S^2 + 1$$

Solving Eq (9) with this substitution, we obtain

$$M_P^2 = \frac{1 + \frac{A_S}{A_P}}{\gamma_P} \left[\left(C_f \frac{l}{2d} \gamma_S \cdot M_S^2 + 1 \right) \left(M_{EX}^2 \gamma_{EX} + 1 \right) - 1 - \frac{\gamma_S \cdot M_S^2}{1 + \frac{A_P}{A_S}} \right] \qquad (9f)$$

This equation can be solved only by iteration since the mass ratio must be
known for determining M_{EX} in this equation by means of Eq (22). A sufficient
condition for starting the iteration is $M_p = M_s$ since for the here considered
case of comparing the effects of incomplete mixing with those of wall friction
the two inlet Mach numbers never differ excessively.

As a result of this iterative solution the primary inlet Mach number can
be plotted over the secondary one with the appearance of the wall friction
term c_f $1/(2d)$ as curve parameter. Such a plot is shown in Fig 22. In this
plot we see, for instance, that with a primary Mach number of one and a
secondary Mach number of 0.8 the curve parameter reads about 0.015; i.e., in
a mixing process with the above assumed initial Mach numbers the pressure rise
during mixing is of the order of the pressure drop due to wall friction given
by the parameter value. For a friction coefficient c_f of 0.02 the length to
diameter ratio of the mixing section would have to be 1.5 to obtain above
parameter value.

If we consider the above ejector case as the state of incomplete mixing at
the mixing section exit of an ejector, the implication is that the deficiency
in the pressure rise due to incomplete mixing is of the same magnitude as the
pressure loss due to wall friction if taken into account in the calculations.
In other words, incomplete mixing in this case doubles the pressure loss due
to wall friction alone. This procedure gives some idea of the conditions
under which incomplete mixing will become a major effect. Since mixing con-
tinues in the diffuser, as pointed out before, some of the pressure loss in
the mixing section is recovered in the diffuser. As also mentioned before,
depending on whether the high velocity in the state of incomplete mixing is
near the wall or in the center, the diffuser process itself may gain or lose.

46

SECTION IV

THE OPTIMUM EJECTOR

1. GENERAL CONSIDERATIONS

In the preceding part of the analysis it became obvious that the ejector
performance can, for given thermal properties of the operating media, be
influenced in three ways, by the mixing mode, the inlet area ratio, and the
inlet Mach number ratio. In each case a trade-off between the ejector mass
ratio and the primary Mach number is involved. The analysis made it, however,
not clear how these three ways to influence the ejector performance can be
utilized to arrive at an optimum ejector lay-out. In the following λ will
be shown that the study of the loss mechanism in an ejector provides the
clue for a systematic optimization procedure. Although the considerations
apply to ejector devices in general, the following treatment concentrates on
the optimization of the ejector pump. The optimization of the thrust aug-
menter appeared already in Section III, 3 as an inherent part of the augmenter
performance presentation.

2. EJECTOR LOSS MECHANISM

Five different processes which cause losses in an ejector can be distin-
quished:

> fluid dynamic mixing
> thermodynamic mixing
> shock diffusion
> diffuser pressure recovery
> wall friction

The division into five kinds of losses occurring in an ejector has so
far not appeared in the present analysis, since the basic ejector equations
account for the first three kinds of losses in a summary process. Only the
last two kinds of losses appear in an explicit form. To understand properly
the ejector optimization process it is necessary to look at the influence of
each loss separately, in particular the first three kinds.

Diffuser Pressure Recovery and Wall Friction. As we will see later, the
losses accrued in the subsonic diffuser and due to wall friction are closely
tied to the conditions under which mixing takes place. The outcome of the
optimization can be strongly affected by these losses. However, their basic
cause is independent of the ejector process itself, and for the optimization
they must be simply minimized by making the diffuser and the walls as nearly
perfect as possible. In contrast, the first three loss processes listed
above are in their cause inherently connected to the ejector process and
require a more specific consideration. They are discussed in the following
in the order of their increasing influence on the optimization process.

Thermodynamic Mixing. The thermodynamic mixing losses can be understood
as being caused by an irreversible expansion process, i.e., by a throttling

47

process to which each operating medium is subjected during its expansion to
its partial pressure in the mixing process. These thermodynamic losses do
not directly affect the momentum exchange in the mixing process. This has
already been shown in Section III.1, where a change in the thermal properties
of the operating media hardly changed the primary Mach number necessary to
achieve a given ejector pressure ratio (see Figures 5 and 6). The
exception is the ratio of the specific heats. An increase of this ratio for
the primary medium allows a decrease of its Mach number. The thermal
properties of the operating media affect primarily the ejector mass ratio,
as dictated by the continuity requirements at the inlet to the mixing
section. The influence on the mass ratio translates into a change in the
primary Mach number if the mass ratio is considered a given magnitude in the
optimization process. This indirect influence of the thermal properties on
the ejector performance is then very obvious in its character; a combination
of thermal properties which allows one to lower the ejector mass ratio,
allows on the other hand a lower primary Mach number if the mass ratio is
maintained constant by a proper change of the mixing section inlet areas.
Thus the influence of the thermal properties can be readily predicted and
therefore need not be a part of the optimization process. This leaves only
two loss processes as essential in the present consideration, shock diffusion
and fluid dynamic mixing.

Shock Diffusion. This flow process occurs quite frequently in fluid dynamics
and concerns the pressure rise in a flowing medium due to a sudden enlargement
of its flow cross section, or also in case of a supersonic flow due to a
change of state in the gas, made possible by the inherent instability of
supersonic flows. Shock diffusion of either kind or of both kinds together
occurs in the operating media while undergoing mixing at a rising pressure in
the mixing section. Since shock diffusion is inherently connected with
losses, a pressure rise obtained by shock diffusion is basically undesirable:
i.e., constant pressure mixing is the desirable mixing mode. The pressure
rise to be produced by the ejector should be accomplished after mixing in as
near an isentropic process as possible. As already pointed out, constant
pressure mixing is not a matter of free choice. While it can be readily
achieved in subsonic flows, it is nearly impossible to produce in supersonic
flows due to the flow instabilities inherently present in this case. The
study of the remaining loss process, fluid dynamic mixing, will show that the
optimization of the mixing process itself calls for mixing section inlet con-
ditions which minimize by themselves the pressure rise during mixing, de-
emphasizing the importance of the mixing mode for the optimization.

Fluid Dynamic Mixing. The implications of the mixing of two flows for the
ejector optimization can best be conveyed by a basic consideration of the
mixing efficiency. We assume the simplest case, the mixing of two homo-
geneous, incompressible media at constant pressure and for a mass ratio of
unity. If we also assume zero wall losses and isentropic pressure recovery
of the kinetic energy remaining after mixing, the mixing efficiency is also
the efficiency of an ejector operating under the here assumed conditions.
This extension to a whole ejector system is useful for the definition of the
mixing or ejector efficiency. Various definitions are possible, depending on
the application of the system. Since we are specifically interested in the
ejector pump, we choose the definition which suits best to compare the ejector

pump with other pump types. We relate the isentropic work necessary for the ideal compression of the secondary medium to the actual work expended by the primary medium in the ejector process. We call this ratio "compression efficiency".

The above definition of the efficiency applied to our simple mixing case we can write

$$\eta_{CO} = \frac{v_{EX}^2 - v_S^2}{v_p^2 - v_{EX}^2}$$

The exit velocity v_{Ex} of the mixing process in this relation follows from the momentum law

$$v_{EX} = \frac{v_p + v_S}{2}$$

Introducing this relation in our efficiency equation, we obtain after some simple transformations

$$\eta_{CO} = \frac{1 - \left(\dfrac{2}{\frac{v_p}{v_S} + 1}\right)^2}{\left(\dfrac{2}{1 + \frac{v_S}{v_p}}\right)^2 - 1} \tag{103}$$

The simple point to make here is that the ejector efficiency is basically a function of the mixing section inlet velocity ratio v_s/v_p. The closer this ratio is to one, the higher is the mixing efficiency. This simple rule is decisive for the optimization process. Before going into more details of this process, a differently defined mixing efficiency is derived to show the independence of this rule from the efficiency definition.

We consider a kind of energy "transfer efficiency" of the mixing process for the conditions assumed above, relating the total kinetic energy of the operating media after mixing to the total kinetic energy before mixing with the result

$$\eta_{tr} = \frac{v_{EX}^2}{v_p^2 + v_S^2}$$

Eliminating in the same way as above the exit velocity v_{Ex} from this relation with the help of the momentum law, we arrive after some simple transformations at a relation for the transfer efficiency as a function of the inlet velocity ratio,

$$\eta_{tr} = \frac{1}{2} + \frac{1}{\frac{v_p}{v_S} + \frac{v_S}{v_p}} \tag{104}$$

Again the efficiency increases with the inlet velocity ratio.

In the actual ejector design the requirement for a high inlet velocity ratio can be readily fulfilled by expanding the secondary medium before mixing begins, i.e., by lowering the inlet pressure of the mixing section. In this preexpansion process both media gain in velocity. However, due to the quadratic dependence of the kinetic energy of a flow on its velocity the absolute gain in velocity is higher for the slower medium, i.e., the secondary medium. Thus preexpansion brings the flow velocities of the operating media closer to each other and their ratio increases.

The limitations to preexpansion are obvious. Since the exit pressure of an ejector is a given design magnitude, the pressure recovery in the diffuser of the ejector must be the larger the more preexpansion is applied. For a given diffuser design the absolue flow losses in the diffuser must increase with increasing preexpansion and override eventually gains obtained by a high velocity ratio. To strike the proper balance between these two losses is the most essential part of the optimization process. Since all the other ejector loss processes play their role in this balance, the quantitative determination of the optimum inlet velocity ratio is rather complex and requires the full implementation of the ejector analysis. In the following practical examples for the optimization are calculated. Dealing with compressible media, one conveniently replaces the inlet velocities by inlet Mach numbers without loss in the basic meaning of the above considerations. There is still the question: Which mixing mode is to be chosen for a realistic ejector design in view of the difficulties to accomplish constant pressure mixing? The results of the following examples will give the essential lead in this respect.

3. OPTIMUM INLET MACH NUMBER RATIO

To facilitate the determination of the optimum Mach number ratio the following system of evaluation is employed: For a given total ejector pressure ratio and a given mass ratio the primary Mach number is determined as a function of the secondary Mach number. This is possible only if the inlet area ratio enters as a dependent variable. In anticipation of certain results of the optimization constant area mixing is assumed.

Solving Eq (9) for M_p^2 and Eq (5) for $(A_s/A_p)^2$, one obtains

$$M_p^2 = \frac{1 + \frac{A_p}{A_s}\left[f \cdot \frac{(P_{Ex})_0}{(P_s)_0}\left(1 + \frac{\gamma_s-1}{2}M_s^2\right)^{\frac{\gamma_s}{\gamma_s-1}} + \gamma_s \cdot M_s^2 \cdot C_f\frac{L}{2d} - 1\right]}{\frac{A_p}{A_s}} \cdot \frac{1}{\gamma_p} - \frac{\gamma_s M_s^2}{\frac{A_p}{A_s}\cdot\gamma_p} \tag{105}$$

$$\left(\frac{A_s}{A_p}\right)^2 = \frac{m_s^2}{m_p^2}\frac{\gamma_p \cdot R_s \cdot (T_s)_0}{\gamma_s \cdot R_p \cdot (T_p)_0 \cdot M_s^2\left[2+(\gamma_s-1)M_s^2\right]} \cdot M_p^2\left[2+(\gamma_p-1)M_p^2\right] \tag{106}$$

50

In Eq (105) the total pressure ratio $(p_{Ex})_0/(p_s)_0$ has been introduced with the help of Eq (47), and the relation for an adiabatic change of state.

This allows one to use the total ejector pressure ratio as a parameter in the derivations.

This system of two equations is first solved for the inlet area ratio A_p/A_s. This can be done only in an approximate way since the factor "f" in the first equation is not exactly known. In accordance with previous considerations (Section III.1) we assume for f a value of 1.2. To avoid lengthy expressions the following abbreviations are used:

$$\alpha = f \cdot \alpha_1 + \alpha_2 \tag{107}$$

$$\alpha_1 = \frac{1}{\gamma_p} \frac{(p_{Ex})_0}{(p_s)_0} \left(1 + \frac{\gamma_s - 1}{2} M_s^2\right)^{\frac{\gamma_s}{\gamma_s - 1}} \tag{108}$$

$$\alpha_2 = \frac{1}{\gamma_p} \left[\gamma_s \cdot M_s^2 \cdot c_f \frac{L}{2d} - 1\right] \tag{109}$$

This relation facilitates the iteration process to arrive at an exact f - value. Further abbreviations are

$$b = \frac{\gamma_s}{\gamma_p} \cdot M_s^2 \tag{110}$$

$$c = \frac{2 \cdot \gamma_p \cdot R_s \cdot (T_s)_0}{\left(\frac{m_p}{m_s} M_s\right)^2 \gamma_s \cdot R_p (T_p)_0 \cdot \left(2 + \gamma_s M_s^2 - M_s^2\right)} \tag{111}$$

Eliminating M_p by introducing the first equation into the second one, one obtains an unique relation for the inlet area ratio,

$$\frac{A_s^2}{A_p^2} = c \left[\left(\frac{A_s}{A_p} + 1\right)\alpha - \frac{A_s}{A_p} b\right]\left[2 + \left(\gamma_p - 1\right)\left[\left(\frac{A_s}{A_p} + 1\right)\alpha - \frac{A_s}{A_p} b\right]\right] \tag{112}$$

or, written for its solution, in the form

$$\left(\frac{A_s}{A_p}\right)^2 \cdot A - \frac{A_s}{A_p} \cdot B - c = 0 \tag{112a}$$

where

$$A = 1 - c(\alpha - b)^2 (\gamma_p - 1) \qquad (113)$$

$$B = 2c(\alpha - b)[(\gamma_p - 1)\alpha + 1] \qquad (114)$$

$$C = c \cdot \alpha [2 + \alpha(\gamma_p - 1)] \qquad (115)$$

The equation yields the following standard solution:

$$\frac{A_s}{A_p} = \frac{-B + \sqrt{B^2 - 4AC}}{2A} \qquad (116)$$

Only the positive root sign is applicable in the present case. With the approximated value of the inlet area ratio so found an improved f-value can be determined with the help of Eqs (21), (22), and (47). The iteration is terminated if

$$f_{n+1} = f_n$$

All magnitudes of the ejector problem are then known, and the ejector performance in terms of the required primary Mach number can be plotted as an unique function of the secondary Mach number with the ejector mass ratio as a parameter and the ejector total pressure ratio a given magnitude of the problem. Figure 23 presents such a plot into which the inlet area ratios have been also entered. These inlet area ratios have been obtained in this case independently of the above derivations. They have been plotted in the same way as the total pressure ejector curves in Figures 9 and 10. This method allows the area ratio to appear as a parameter.

In Figures 24(a-d) and 25 a number of optimization examples covering a wide span of performance conditions have been plotted. For clarity's sake the inlet area ratio curves have been omitted in these examples. These optimization plots reveal the following remarkable features.

     (1) The performance maxima are in all cases very pronounced; i.e., it is quite essential to choose the proper secondary Mach number. (This is true even for the case with the perfect diffuser in Figures 24a and 24c. Since mixing is assumed to take place under constant area, shock diffusion occurs, limiting the optimum secondary Mach number.)

     (2) The optimum inlet Mach number ratio, taken in the following as M_p/M_s, is of a comparatively uniform value when one considers the wide spread of the chosen performance requirements, never deviating too far from about 4 to 5 , where the higher value pertains to higher ejector pressure ratios. These prevailing values are quite significant for the choice of the mixing

mode. In Section III we have seen that for an inlet Mach number ratio below about 4 the performance for constant pressure mixing and constant area mixing is no longer significantly different. (See, for instance Figure 13.) Thus, the important conclusion can be drawn in our optimization considerations, that an ejector which is optimized for constant area mixing is fairly near its absolute performance potential with the added feature that the basic assumption of constant area mixing can be realistically fulfilled.

For extremely heterogeneous operating media, such as mercury vapor as driver medium and hydrogen as secondary medium, the optimum inlet Mach number ratios can readily reach values of ten or higher. Since the near equivalence of the ejector performance for constant area and constant pressure mixing shifts in this case also to these higher inlet Mach number ratios, optimizing the performance of extremely heterogeneous ejectors for constant area mixing also yields their near maximum possible performance.

As will be shown in the next paragraph, the optimized performance with constant area mixing can still be improved to some degree by reducing the mixing section exit cross section. The effect of the cross section reduction is that the pressure is lowered during mixing, and, thus, as explained before, shock diffusion losses are reduced.

An optimization problem which has to rely mainly on empirical methods for its solution concerns the flow of the secondary medium around the primary inlet nozzles in the actual ejector. To obtain intense mixing within a short length multiple primary inlet nozzles are quite often employed. The here established optimization requirements call for fairly high secondary inlet Mach numbers. In its flow around the primary nozzles the secondary medium may be subject to essential losses before it enters the mixing section. Thus, a proper compromise and a careful nozzle design must solve this problem. For the subsonic ejector, which includes liquid operating media, constant pressure mixing may be preferable in view of this inlet loss problem.

The here derived optimization requirements allow one also to give the simplified ejector layout presented in Reference 5 a more generalized aspect than originally assumed. This will be discussed in Section VI.

4. MIXING SECTION AREA REDUCTION

Instead of using constant area mixing, the optimum inlet Mach number ratio will now be determined under the more generalized condition of mixing at a defined pressure distribution with the pertinent relations of Section II.4. Equation (112), which yields the inlet area ratio, remains the same as derived for the constant area case, except that two of the coefficients are different:

$$\alpha_1 = \frac{t \, (P_{ex})_0}{\gamma_p (P_s)_0} \left(1 + \frac{\gamma_s - 1}{2} M_s^2 \right)^{\frac{\gamma_s}{\gamma_s - 1}}$$

(108a)

$$\alpha_2 = \frac{t \cdot \tau}{\gamma_p}$$

(109a)

53

Constant area mixing appears now as a special case with t = 1. The only difference is that the wall losses are now referred to the flow conditions at the mixing section exit.

Figure 26 gives an example for the improvement of the performance optimized under constant area mixing by reducing the mixing section exit area. It was assumed that t and i are related as given by the following table

t	=	1.0	0.9	0.8	0.7	0.6
i	=	0	0	0.2	0.6	1.0

These values are very rough estimates. However, the trend they represent, that the pressure distribution in the mixing section becomes less favorable with increasing area reduction of the exit, should be fairly realistic. The above table has been assumed to be applicable equally for all ejector pressure ratios shown. Figure 26 can serve only to show the trends in view of the uncertainty of the specific assumptions for the pressure distributions in the mixing section.

SECTION V

EJECTOR EFFICIENCY

1. "TRANSFER EFFICIENCY"

This efficiency relates the total kinetic energy available at the diffuser exit to the total kinetic energy of the primary and secondary flow entering the mixing section. Available kinetic energy at the diffuser exit means the kinetic energy obtained by expanding the exit flow without loss to the ejector inlet pressure. (Conditions at the end of such expansion are indicated by index "e".) With this consideration the transfer efficiency can be written

$$\eta_{tr} = \frac{(m_p + m_s) v_e^2}{m_p \cdot v_p^2 + m_s \cdot v_s^2} \tag{117}$$

or upon introducing Mach numbers

$$= \frac{(m_p + m_s)(M_e^2)_p \cdot R_e \cdot \gamma_e \cdot T_e}{m_p \cdot M_p^2 \cdot R_p \cdot \gamma_p \cdot T_p + m_s \cdot M_s^2 \cdot R_s \cdot \gamma_s \cdot T_s} \tag{118}$$

or

$$= \frac{\left(\frac{m_p}{m_s} + 1\right)(M_e^2)_p \dfrac{R_e \gamma_e T_e}{R_s \gamma_s T_s}}{\dfrac{m_p}{m_s} M_p^2 \dfrac{R_p \gamma_p T_p}{R_s \gamma_s T_s} + M_s^2} \tag{119}$$

With

$$M_e^2 = \frac{2}{\gamma_e - 1}\left[\left(\frac{(p_{Ex})_0}{p_s}\right)^{\frac{\gamma_e - 1}{\gamma_e}} - 1\right]$$

and the term $(R_e \gamma_e T_e)/(R_s \gamma_s T_s)$ expressed by initial ejector conditions with the help of Eqs (15) to (20), we can write

$$\eta_{tr} = \frac{\left(\frac{m_p}{m_s} + 1\right) M_e^2 \dfrac{T_{Ex}}{(T_{Ex})_0} \cdot P}{\dfrac{m_p}{m_s} \cdot M_p^2 \dfrac{R_p \gamma_p T_p}{R_s \gamma_s T_s} + M_s^2} \tag{120}$$

where P in this equation stands for the entire expression under the root in Eq (20).

Considering

$$M_e^2 \frac{T_e}{(T_{x})_0} = \frac{2}{\gamma_e - 1}\left[1 - \left(\frac{p_s}{(p_{Ex})_0}\right)^{\frac{\gamma_e - 1}{\gamma_e}}\right] \tag{121}$$

55

and

$$\frac{T_p}{T_s} = \frac{(T_p)_0}{(T_s)_0} \cdot \frac{1 + \frac{\gamma_s - 1}{2} M_s^2}{1 + \frac{\gamma_p - 1}{2} M_p^2} \tag{122}$$

one can write the transfer efficiency in terms of initial ejector conditions and the ejector pressure ratio:

$$\eta_{tr} = \frac{\left(\frac{m_p}{m_s} + 1\right) \cdot \frac{2}{\gamma_e - 1} \left[1 - \left(\frac{p_s}{(p_{Ex})_0}\right)^{\frac{\gamma_e - 1}{\gamma_e}}\right] \cdot P}{\frac{m_p}{m_s} \frac{R_p \gamma_p (T_p)_0}{R_s \gamma_s (T_s)_0} M_p^2 \frac{2 + (\gamma_s - 1) M_s^2}{2 + (\gamma_p - 1) M_p^2} + M_s^2} \tag{123}$$

In Fig 27 the transfer efficiency is added to the ejector performance curves already shown in Fig. 16. In Fig. 28 the transfer efficiency is indicated in the performance characteristic for a jet pump which has a layout typically applicable to thrust augmentation. In both these cases one recognizes that the transfer efficiencies reach fairly high values for high secondary Mach numbers.

2. "COMPRESSION EFFICIENCY"

The T-S - diagram in Fig. 29 illustrates the definition of the compression efficiency. The compression work required for the secondary medium is that which brings it adiabatically from the initial total pressure $(p_s)_0$ to the ejector exit total pressure $(p_{Ex})_0$. Thus, for the efficiency for this compression process follows from the T-S - diagram

$$\eta_{co} = \frac{(T_{comp})_0 - (T_s)_0}{(T_p)_0 - (T_{Exp})_0} \cdot \frac{m_s}{m_p} \cdot \frac{c_{p-s}}{c_{p-p}} \tag{124}$$

or

$$= \frac{m_s}{m_p} \cdot \frac{c_{p-s}}{c_{p-p}} \frac{(T_s)_0}{(T_p)_0} \frac{\left(\frac{(T_{comp})_0}{(T_s)_0} - 1\right)}{\left(1 - \frac{(T_{Exp})_0}{(T_p)_0}\right)} \tag{125}$$

56

Considering

$$\frac{(T_{Exp})_0}{(T_p)_0} \equiv \frac{(T_{Exp})_0}{T_p} \frac{T_p}{(T_p)_0}$$

$$= \frac{\left[\frac{(P_{Ex})_0}{P_p}\right]^{\frac{\gamma_p-1}{\gamma_p}}}{1 + \frac{\gamma_p-1}{2} M_p^2} \tag{126}$$

one can write the compression efficiency in terms of the ejector lay-out and magnitudes readily available from the ejector analysis:

$$\eta_{co} = \frac{m_s}{m_p} \frac{c_{p\text{-}s}}{c_{p\text{-}p}} \frac{(T_s)_0}{(T_p)_0} \left[\frac{\left[\frac{(P_{Ex})_0}{(P_s)_0}\right]^{\frac{\gamma_s-1}{\gamma_s}} - 1}{1 - \frac{\left[\frac{(P_{Ex})_0}{P_p}\right]^{\frac{\gamma_p-1}{\gamma_p}}}{\left(1 + \frac{\gamma_p-1}{2} M_p^2\right)}}\right] \tag{127}$$

If the compression efficiency is also to account for the work required to separate the operating media, leaving the ejector in a mixed state, the work necessary for their separation or the equivalent work lost in the mixing process must be added in Eq 124.

The expansion energy lost in the mixing process can be readily derived on the basis of Dalton's law, which requires that each component in the mixing process behaves as if the other component were not present. During mixing each component expands to its partial pressure in the mixture without performing external work; i.e., the expansion work is converted into heat and the expansion process is therefore isothermal. The expansion work converted to heat is then for both components

$$Q_{mix} = p \cdot V_p \cdot \ln \frac{V_p + V_s}{V_p} + p V_s \ln \frac{V_p + V_s}{V_s} \tag{128}$$

$$= p(V_p + V_s)\left[\frac{V_p}{V_p + V_s} \ln \frac{V_p + V_s}{V_p} + \frac{V_s}{V_p + V_s} \ln \frac{V_p + V_s}{V_p}\right] \tag{128a}$$

We introduce the equation of state

$$V = m \frac{R \cdot T}{p}$$

57

Since we want only to find the work lost in the mixing process as the equivalent to the separation work, the temperatures of the media are the same in the present derivation. It is another process, not considered here, to heat and cool, respectively, the media to bring them to their original states in a complete thermodynamic cycle process. Thus, with $T_p = T_s$ we can write for the separation work

$$Q_{mix} = (m_p + m_s) R_{Ex} \cdot (T_{Ex})_0 \underbrace{\left[\frac{Ln\left(1 + \frac{m_s R_s}{m_p R_p}\right)}{1 + \frac{m_s R_s}{m_p R_p}} + \frac{Ln\left(1 + \frac{m_p R_p}{m_s R_s}\right)}{1 + \frac{m_p R_p}{m_s R_s}} \right]}_{\ell} \qquad (129)$$

or, written somewhat differently with the expression in brackets abbreviated by (ℓ),

$$= m_p \cdot R_p \frac{\gamma_p}{\gamma_p - 1} (T_p)_0 \underbrace{\left[\frac{m_p + m_s}{m_p} \cdot \frac{R_{Ex}}{R_s} \frac{R_s}{R_p} \frac{(T_i)_0}{(T_s)_0} \frac{(T_s)_0}{(T_i)_0} \frac{\gamma_p - 1}{\gamma_p} \cdot \ell \right]}_{} \qquad (129a)$$

Considering

$$R_p \frac{\gamma_p}{\gamma_p - 1} = c_{p-p} \qquad (130)$$

and abbreviating now the expression in brackets by L, one can write the compression efficiency with an accounting of the work necessary to separate the operating media in the form of Eq (127) with simply adding L in the denominator:

$$\eta_{co-sep} = \frac{m_s}{m_p} \cdot \frac{c_{p-s}}{c_{p-p}} \frac{(T_s)_0}{(T_p)_0} \frac{\left[\left[\frac{(p_{Ex})_0}{(p_p)_0} \right]^{\frac{\gamma_s - 1}{\gamma_s}} - 1 \right]}{\left[1 - \frac{\left[\frac{(p_{Ex})_0}{p_p} \right]^{\frac{\gamma_p - 1}{\gamma_p}}}{1 + \frac{\gamma_p - 1}{2} M_p^2} \right] + L} \qquad (131)$$

58

The expression represented by L still has to be given in terms of initial ejector conditions. We can do this with the help of Eqs (15a) and (18a). Performing also some simple transformations, we can finally write for this expression

$$L = \frac{(T_s)_0}{(T_p)_0} \frac{\gamma_p - 1}{\gamma_p} \frac{\left(\frac{c_{p \cdot p} \, m_p \, (T_p)_0}{c_{p \cdot s} \, m_s \, (T_s)_0} + 1\right)}{\left(\frac{c_{p \cdot p}}{c_{p \cdot s}} \frac{m_p}{m_s} + 1\right)} \left[\ln\left(1 + \frac{m_s \, R_s}{m_p \, R_p}\right) + \frac{m_s \, R_s}{m_p \, R_p} \ln\left(1 + \frac{m_p \, R_p}{m_s \, R_s}\right) \right] \tag{132}$$

In Fig. 30 the compression efficiency is entered as a parameter curve, and the compression efficiency with accounting for the separation work is entered as single points. The two compression efficiency versions do not differ greatly.

SECTION VI

SIMPLIFIED EJECTOR ANALYSIS

The findings of the preceding section, concerning the existence of a preferred range of inlet Mach number ratios, has an essential impact on the simplified ejector analysis reported in Ref. 5. In this earlier analytical effort the influence of energy conservation was approximated by an estimate of the factor f, which occurs also in the present analysis where it is utilized for solutions by iteration. This simplification allowed one to avoid considerable complexities in the analysis and led to a very simple graphic presentation of the performance potential of the ejector with heterogeneous operating media.

This simplified analysis was, however, only applicable to constant area mixing and therefore considered limited in its application. The use of selective inlet Mach number ratios gives now a unique preference to constant area mixing in the lay-out of ejectors. Since the inlet Mach number ratio occurs typically in the simplified analysis it can be readily used to account for optimization requirements.

The simplified analysis can be derived from Eq (9) of this report by introducing the factor f with the help of Eq (47) and taking it as a constant. The resulting equation can be written in the following form

$$\frac{1}{1+\frac{n}{g}} + g^2 \frac{1}{1+\frac{g}{n}} = \frac{f_{\eta \cdot i} \frac{(P_{ex})_0}{P_s \eta_d} - 1}{M_s^2 \cdot \gamma_s} + \frac{c_f l}{2d} \qquad (133)$$

where

$$n = \frac{m_p}{m_s} \sqrt{\frac{R_p T_p}{R_s T_s}} \qquad (134)$$

$$g = \frac{M_p}{M_s} \sqrt{\frac{\gamma_p}{\gamma_s}} \qquad (135)$$

The magnitudes identified by Eq (134) and Eq (135) represent the coordinates of the simplified ejector lay-out diagram originally given in Fig. 3 of Ref. 5 and repeated here in Fig. 31. The curve parameter in this diagram represents the right side of Eq (133). All terms in the diagram use notations of this report, except for the diffuser pressure recovery factor η_d. Its use to account for diffuser losses contributes to the simplification of the analysis. It has, however, the disadvantage that, in contrast to the polytropic diffuser efficiency, it varies greatly with the diffuser flow conditions. Its numerical relation to other diffuser efficiency definitions are given in Ref. 6, for the adiabatic diffuser efficiency also in Ref. 5. A typically occurring value for ejectors lies near 0.95.

60

The usefulness of the simplified lay-out diagram is based on the fact that the curve parameter P is given by the ejector problem, except for the factor f, which can be readily estimated (see Ref. 5). The secondary Mach number M_s can, as such, be chosen freely. A given P-curve provides the ejector lay-out in terms of the inlet Mach number ratio and the inlet area ratio in dependence of the desired mass ratio. With the free choice of the secondary inlet Mach number different P-values are possible for a given ejector problem. The optimization requirements narrow down this choice considerably, since only a limited range for the inlet Mach number ratio is desirable. This ratio occurs as the principal magnitude in the abcscissa of the diagram and can be readily used to indicate preferred ejector lay-out conditions.

To give a direct numerical demonstration for the preferred range of lay-out conditions performance peaks from Fig. 23 have been transferred to Fig. 31. They appear in this figure as more or less straight lines. They represent the portions of the performance curves which are within 1% of the minimum primary Mach number in Fig. 23. The location for the minimum primary Mach number is also indicated. This plot allows to recognize that near top performance can be achieved within a fairly narrow range of inlet Mach number ratios for all cases.

Not all optimized ejector.designs fall necessarily within the preferred range. Combinations of high ejector pressure ratios with low mass ratios or extreme heterogeneous conditions have their peak performance in Fig. 31 considerably outside the preferred range at higher abscissa values. Since, however, higher abscissa values are associated with a decrease in ejector efficiency they actually do not represent a desirable design range.

In analogy to Eq (133) mixing at a defined pressure distribution yields

$$\frac{1}{1+\frac{n}{g}} + g^2 \cdot \frac{1}{1+\frac{g}{n}} = t \cdot \left[\frac{f_\tau \cdot \frac{(P_{Ex})_0}{P_s \, \eta_d} - \tau}{M_s^2 \cdot \gamma_s} + \frac{c_f l}{2\bar{a}} \right] \tag{133a}$$

where

$$f_\tau = \frac{\gamma_{Ex} \cdot M_{Ex}^2 + \tau}{\left(1 + \frac{\gamma_{Ex}-1}{2} M_{Ex}^2\right)^{\frac{\gamma_{Ex}}{\gamma_{Ex}-1}}} \tag{47a}$$

The right side of Eq (133a) provides again a parameter value for Fig. 31. The dependencies involved are now more complex (see Eq (41)). However, the parameter is again made up of magnitudes essentially given by the ejector problem.

SECTION VII

CONCLUSIONS

In a one-dimensional flow analysis the performance of an ejector, i.e., its pressure ratio and mass flow ratio, can be obtained from the inlet conditions by a straightforward algebraic solution of the governing fluid dynamic and thermodynamic relations (conservation of momentum and energy, and continuity) with no essential difficulties in accounting for compressibility, heterogeneous operating media, wall friction, and diffuser losses. The description of the mixing process amounts in this one-dimensional analysis to the assumption of complete mixing of the primary and secondary media before entering the diffuser and to prescribing the integrated wall forces in the mixing section. Constant area mixing and constant pressure mixing appear as special cases. The resulting performance equations are rather lengthy, but they can be easily handled on a programmable desk calculator.

For determining the performance characteristic of an ejector, in which the primary inlet Mach number is plotted against the secondary inlet Mach number and the ejector pressure ratio appears as a parameter, the analytical problem to find the initial flow conditions for a given ejector performance arises. No explicit solutions for the ejector equations are possible in this case, and an iterative solution must be employed. Fast converging iteration methods have been worked out for this purpose. Performance characteristics of the indicated type are very helpful for studying the effects of the various possible operating conditions, including the mixing modes, on the ejector performance. Findings are given below.

At given inlet conditions, i.e., at a given inlet area ratio, and given primary and secondary inlet Mach number, heterogeneous operating conditions (primary and secondary operating media having different thermodynamic properties) affect the ejector pressure ratio only slightly. Due to thermodynamic mixing losses the influence is degrading. However, an increase of the specific heat ratio of the primary medium over that of the secondary medium brings an improvement of the ejector pressure ratio. The reason is that at a given inlet Mach number the higher specific heat ratio gives the flow a higher momentum. Heterogeneous operating conditions influence the ejector mass flow ratio in correspondence to the change they cause in the flow densities at the ejector inlet. They also lead to choking in a constant area mixing section for a primary Mach number not too far from one.

The influence of the incidental flow losses (wall and diffuser losses) is the reverse of that of the heterogeneous operating conditions. At given ejector inlet conditions they heavily degrade the ejector pressure ratio but hardly affect the mass ratio.

Again, for a given inlet area ratio, constant pressure mixing is, at least analytically (see below), far superior to constant area mixing for very small inlet area ratios (primary over secondary) and very small secondary inlet Mach numbers. Incidental flow losses can strongly reduce this superiority and can even make constant area mixing superior. An important fact is that each mixing mode gives a similar performance if the

62

inlet Mach number ratio (primary to secondary) approaches a value of about 3 to 4, with less difference in performance as this ratio decreases.

Superficially, it appears that the best ejector is obtained with constant pressure mixing, a very low primary to secondary inlet area ratio, and a very low secondary inlet Mach number. However, constant pressure mixing is a highly unrealistic condition for supersonic mixing due to the occurrence of supersonic shocks, and it is even only conditionally applicable for subsonic mixing since shock diffusion due to sudden flow cross section changes cannot be completely avoided in this case.

A lead for a realistic optimization of the ejector performance comes from a study of the ejector loss mechanism. This study provides the inlet Mach number ratio as the governing criterion for the optimization. This ratio establishes the all important balance between a high mixing efficiency and a minimum of losses for the compression process in the ejector. To find the inlet Mach number ratio which gives the best ejector the inlet area ratio of the ejector mixing section is introduced as a variable into the analysis. Then for a given ejector total pressure ratio and a given mass flow ratio the primary inlet Mach number is plotted against the secondary inlet Mach number for a realistic mixing mode. In this way the minimum primary inlet Mach number for a given ejector task can be determined.

Using constant area mixing as the most realistic case, which is not impaired by choking as it can occur with deviations from constant area mixing, gives the interesting result that the optimum inlet Mach number ratio (primary to secondary) falls quite generally into a range of about 4 to 6. This is a range where the mixing mode ceases to be a strong influence on the ejector performance (for extremely heterogeneous operating media this condition is fulfilled also at much higher inlet Mach number ratios). Thus for the highly realistic condition of constant area mixing and an optimum inlet Mach number ratio the ejector performance is near its full capacity. Mixing section area reduction can still bring performance improvements. However, with a tapered mixing section wall forces in the direction of the flow effect the ejector process, and it depends entirely on the pressure distribution along the mixing section whether an area reduction can bring a worthwhile performance improvement. For supersonic mixing conditions it is obvious that compression shocks unfavorably influence the pressure distribution, upon considering that the wall forces should be a minimum for an effective ejector process. Pressure distributions along the mixing section cannot readily be predicted, and only very rough estimates are possible. Only experiments can give the proper answer in this case.

The present ejector analysis has been extended to describe the performance of the thrust augmenter. An explicit solution of the relations allows one to plot the thrust augmentation ratio against the diffuser area ratio, yielding directly the maximum augmentation ratio obtainable under given operating conditions. A number of such plots have been prepared to show the influence of diffuser efficiency, inlet area ratio, wall friction, primary Mach number, temperature ratio of the operating media, and flight speed on the augmentation ratio. An interesting result is that the primary to secondary inlet Mach number ratio associated with the maximum augmentation ratio falls into

63

the range of 3 to 4, as similarly found for the optimized ejector pump. Thus the optimum performance of an ejector device appears to be quite generally connected to the indicated range of inlet Mach number ratios.

The analysis has been used also to determine ejector efficiencies for which various definitions are possible, depending on the ejector application. The formulations are quite lengthy, and, in addition, the concept of an efficiency is only of limited usefulness for the description of ejectors. A "compression efficiency", which allows a direct performance comparison with other pump types, such as mechanical pumps, can, however, be formed.

The present analysis by no means exhausts all aspects of the ejector principle, obviously by the simple fact that it is a one-dimensional analysis. Nonuniformity of the flow outside the mixing section influences, for instance, the diffuser performance, but may also affect choking conditions. Another important aspect which has not been dealt with in this analysis is the occurrence of a phase change during mixing, which is an essential feature of the widely used steam ejector. The analysis has provisions to account in a simplified way for changes of the thermodynamic properties of the operating media during the ejection process as they occur with dissociation or recombination. Condensation can be accounted for in this way as long as the condensation process can be represented as a polytropic change of state, i.e., if the condensation rate is not too high.

The ejector optimization considerations of the present analysis have also an impact on a simplified method for the lay-out of heterogeneous ejectors reported in Ref. 5. In this method a simple diagram allows one to determine the ejector performance under the influence of various operating conditions, in particular, the thermal properties of the operating media. A region can now be readily defined in this diagram where near optimum ejector lay-outs are obtained.
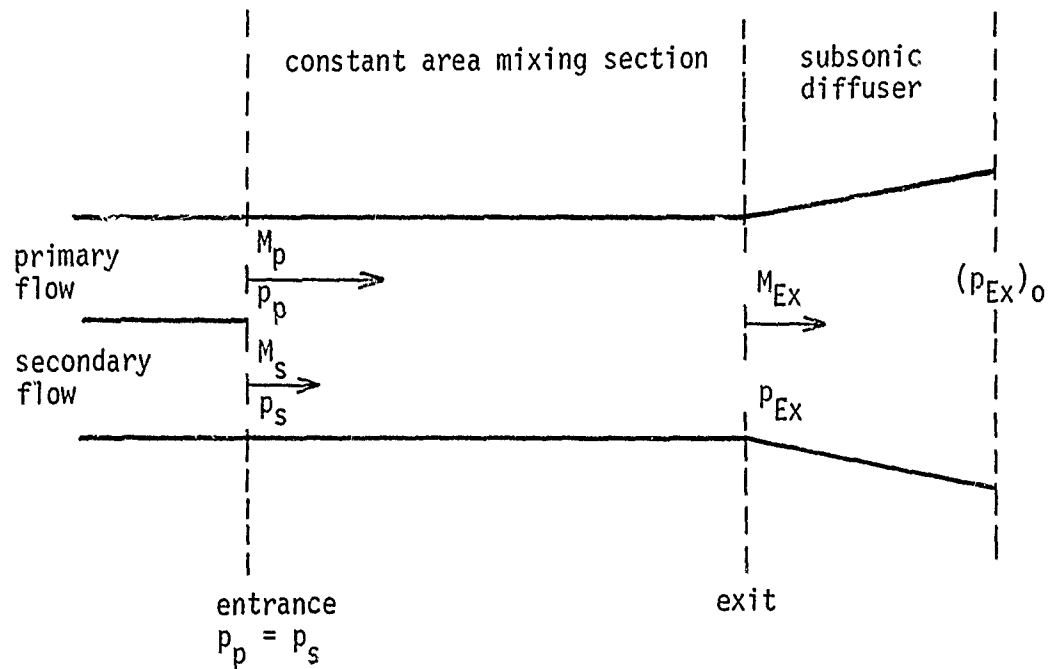
Figure 1. Basic Ejector Flow Scheme for <u>Constant Area Mixing</u>.
(The entrance geometry shown is completely incidental
to the analysis, since only the inlet area ratio enters
the analysis and details of the mixing process are not
considered. For a discussion of the condition $p_p = p_s$
see page 3 of the text.

65
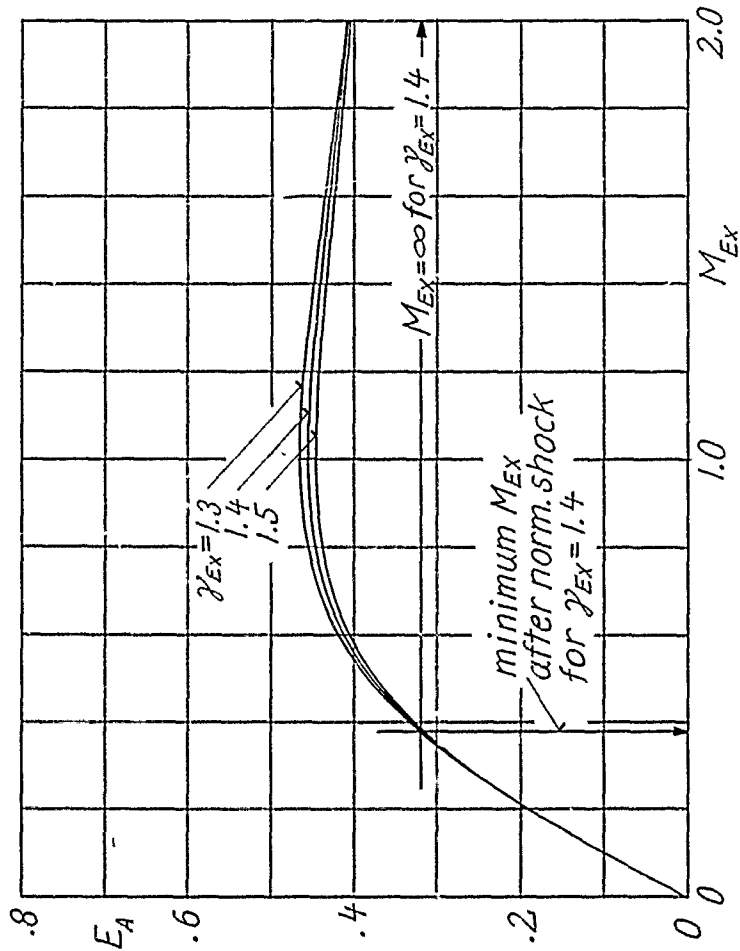
Figure 2. Flow Density Parameter E_A. (This parameter can be
interpreted as a dimensionless flow density in a
given cross section, depending for a given γ_{Ex} solely
on the flow Mach number. It has therefore the property
that a line of constant E_A connects upstream and down-
stream Mach numbers of a normal shock. Its more
general feature is that it allows one to relate the
upstream and downstream flow condition of a mixing
process by means of Eq (21), which gives E_A from the
upstream conditions.)

66

a

| const. pressure mixing section | subsonic diffuser |

M_p p_p

M_s p_s

M_{Ex}, p_{Ex}

$(p_{Ex})_0$

b

| const. pressure mixing section | pseudo-shock diffuser | subsonic diffuser |

M_p p_p

M_s p_s

M_{Ex} p_{Ex}

M_{Ex-sh} p_{Ex-sh}

$(p_{Ex})_0$

entrance
$p_p = p_s$

exit
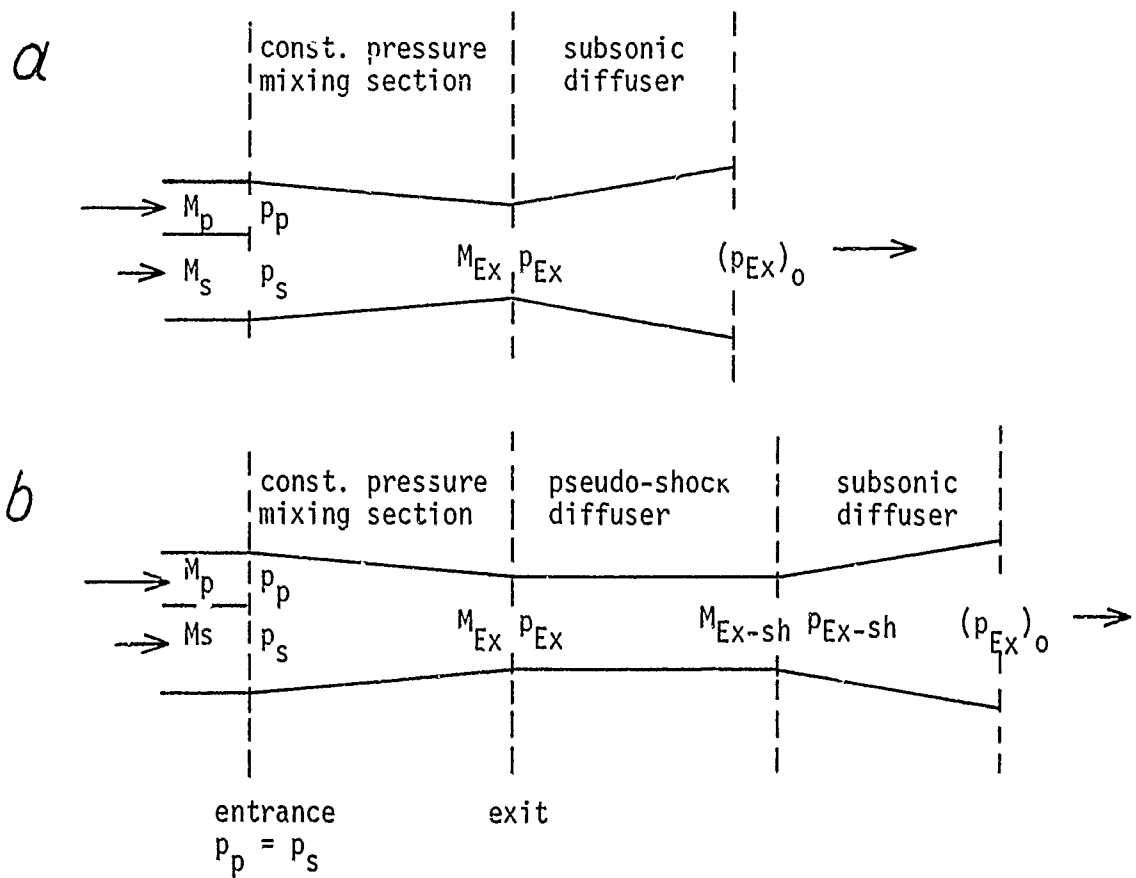
(a) for subsonic M_{Ex}

(b) for supersonic M_{Ex}

Figure 3. Basic Ejector Flow Scheme for <u>Constant Pressure Mixing</u>.
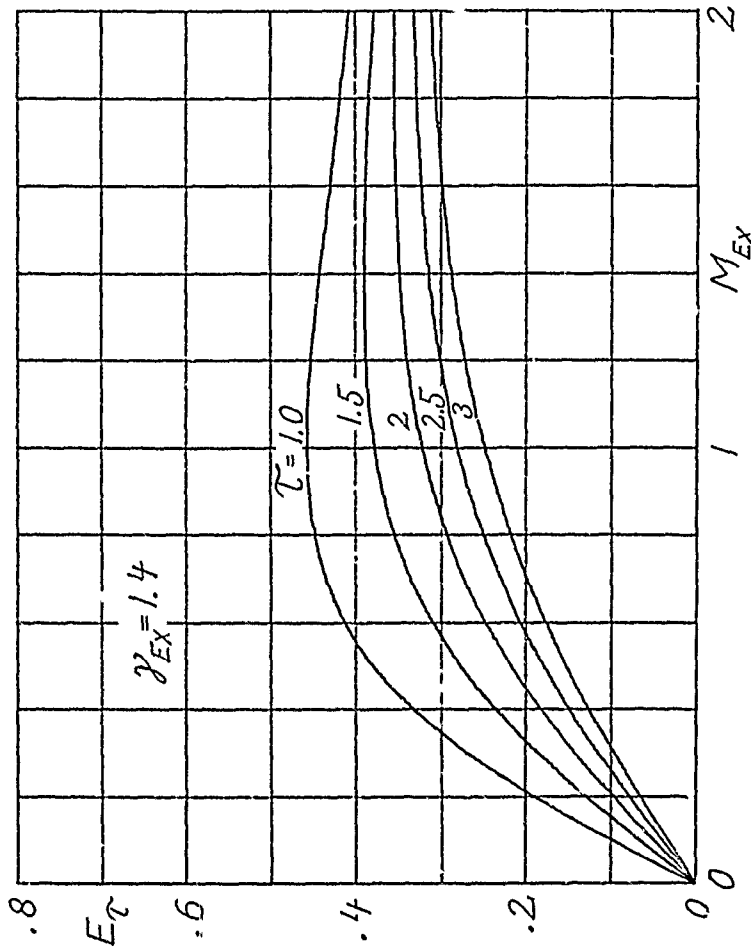
Figure 4. Flow density parameter E_τ. For $\tau = 1.0$ identical with E_A shown in Figure 2 for equal γ_{Ex}. τ - values larger than 1.0 account for wall pressure forces in a nonconstant area mixing section. For $\tau = 1.0$ the wall pressure forces become zero.
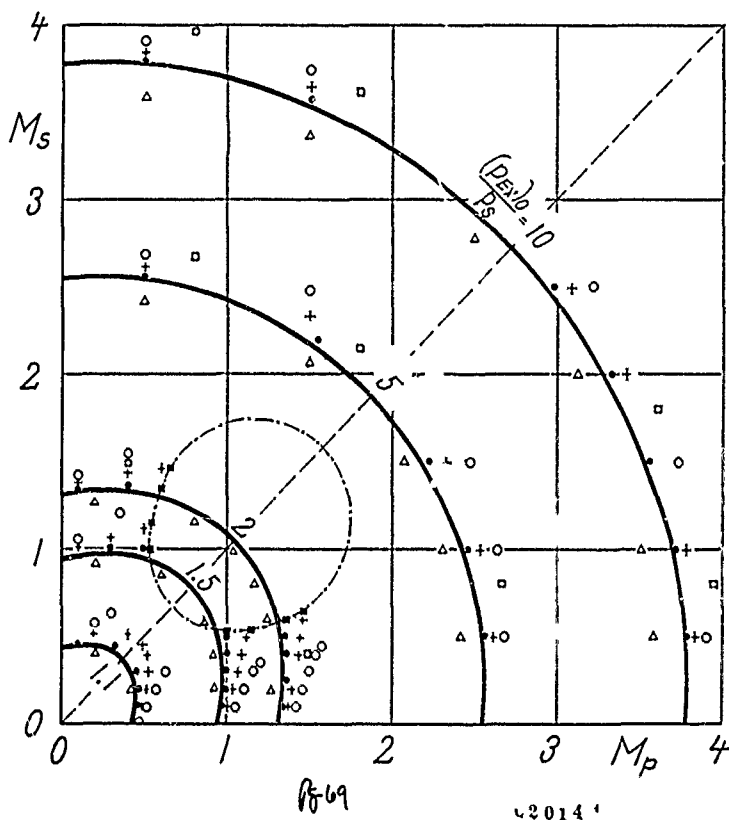
Figure 5. Characteristic Behavior of the Constant Area Mixing Ejector for Inlet Area Ratio A_p/A_s = 1.0. (Showing the influence of incidental flow losses and heterogeneous operating media. The solid lines give the performance for the homogeneous ejector without wall friction and diffuser losses. The marked points give the performance for operating conditions listed in Table I. The plot shows that the influence of the media properties on ejector pressure ratio is almost negligible in contrast to the influence of the incidental flow losses. (For the influence of the media properties and flow losses on the ejector mass ratio, see Figures 7 and 8 and page 23.) The points to the left of the solid curves show that it is advantageous for the driver medium to have a high ratio of specific heats. Points marked (■) indicate sonic speed at the mixing section exit. For operating conditions #3 and #4 choking of mixing section exit occurs inside curve marked (—·—·—).)

TABLE I

EJECTOR OPERATING CONDITIONS FOR FIGS. 5 TO 8, AND 13

NO.		thermodynamic properties					incidental flow losses	
		γ_p	γ_s	R_s/R_p	c_{p-s}/c_{p-p}	$(T_p)_o/(T_s)_o$	η_{pol}	$c_f \frac{\ell}{2d}$
1.	solid line	1.4	1.4	1.0	1.0	1.0	1.0	0
2.	◗	1.4	1.4	1.0	1.0	4.0	1.0	0
3.	+	1.4	1.4	1.0	1.0	4.0	.8	0
4.	0	1.4	1.4	1.0	1.0	4.0	.8	.1
5.	Δ	1.6	1.4	1.0	1.0	1.0	1.0	0
6.	□	1.25	1.48	2.6	2.1	1.2	.85	.05

70
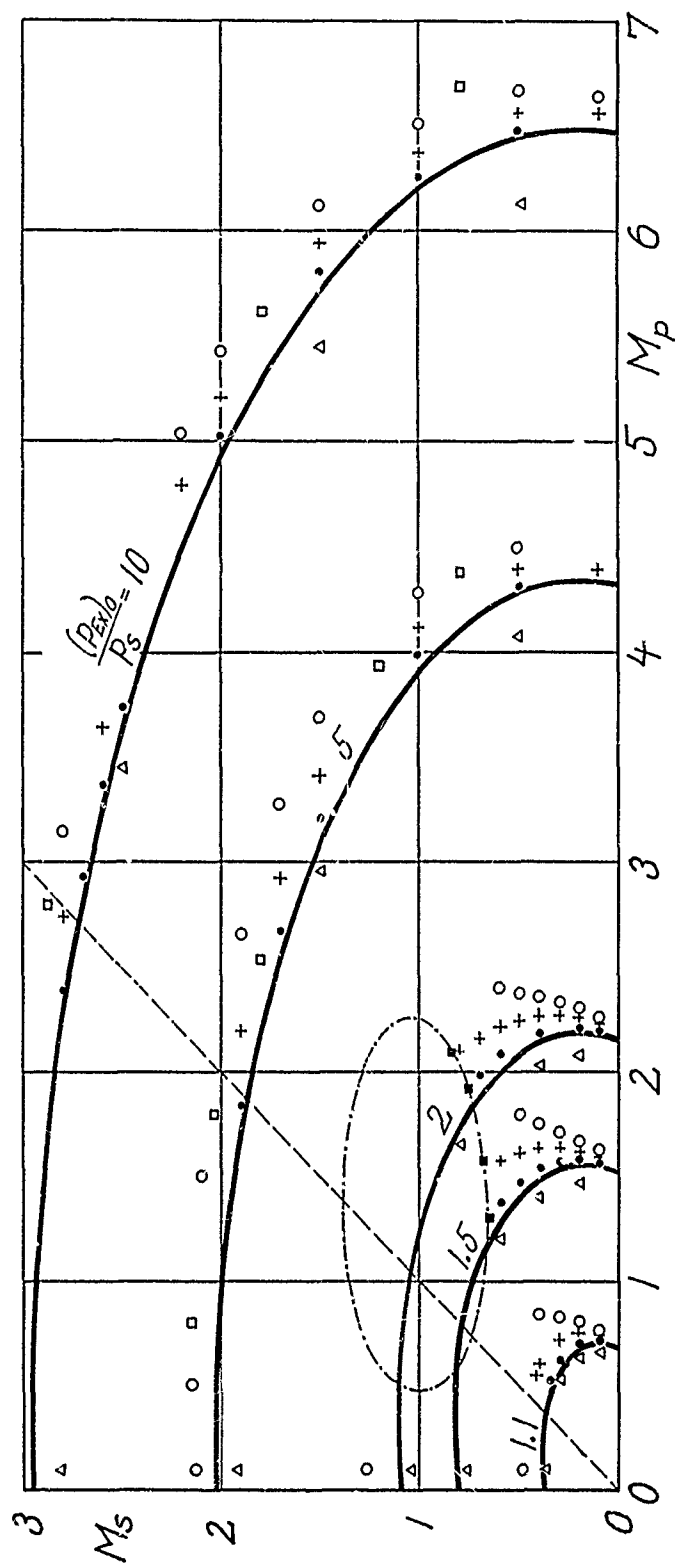
Figure 6. Characteristic Performance of the Constant Area Mixing Ejector for the Inlet Area Ratio $A_p/A_s = 0.2$. (Except for the change of the area ratio from 1.0 to 0.2 all conditions are the same as with the plot in Figure 5.)

71
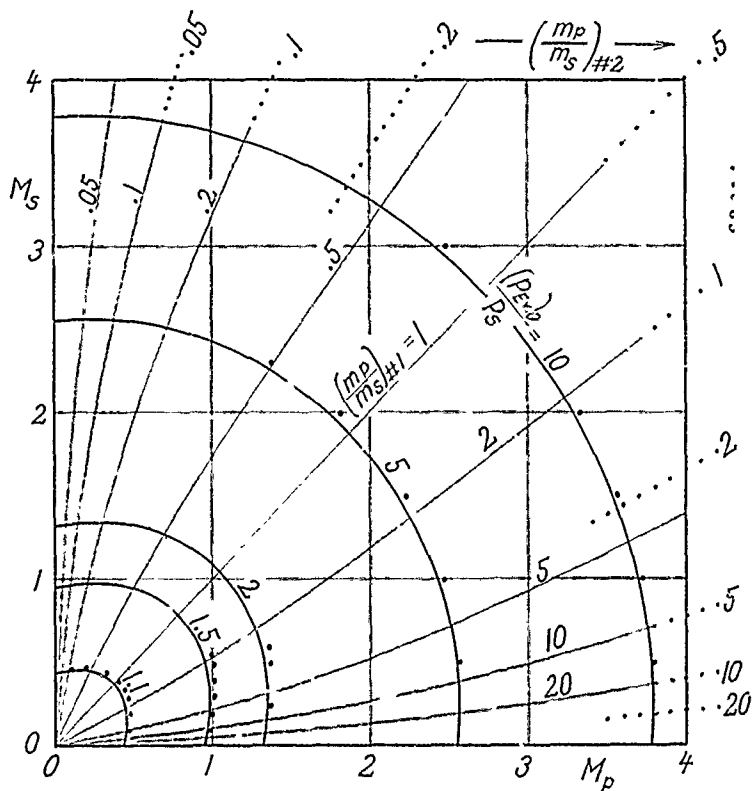
Figure 7. Primary to Secondary Mass Ratio m_p/m_s Together With the Ejector Pressure Ratio $(p_{Ex})_0/p_s$ for <u>Constant Area Mixing</u> (same as in Figure 5) for Operating Conditons #1 and #2 (see Table I) at an Inlet Area Ratio $A_p/A_s = 1.0$.

#1 solid lines
#2 dotted lines
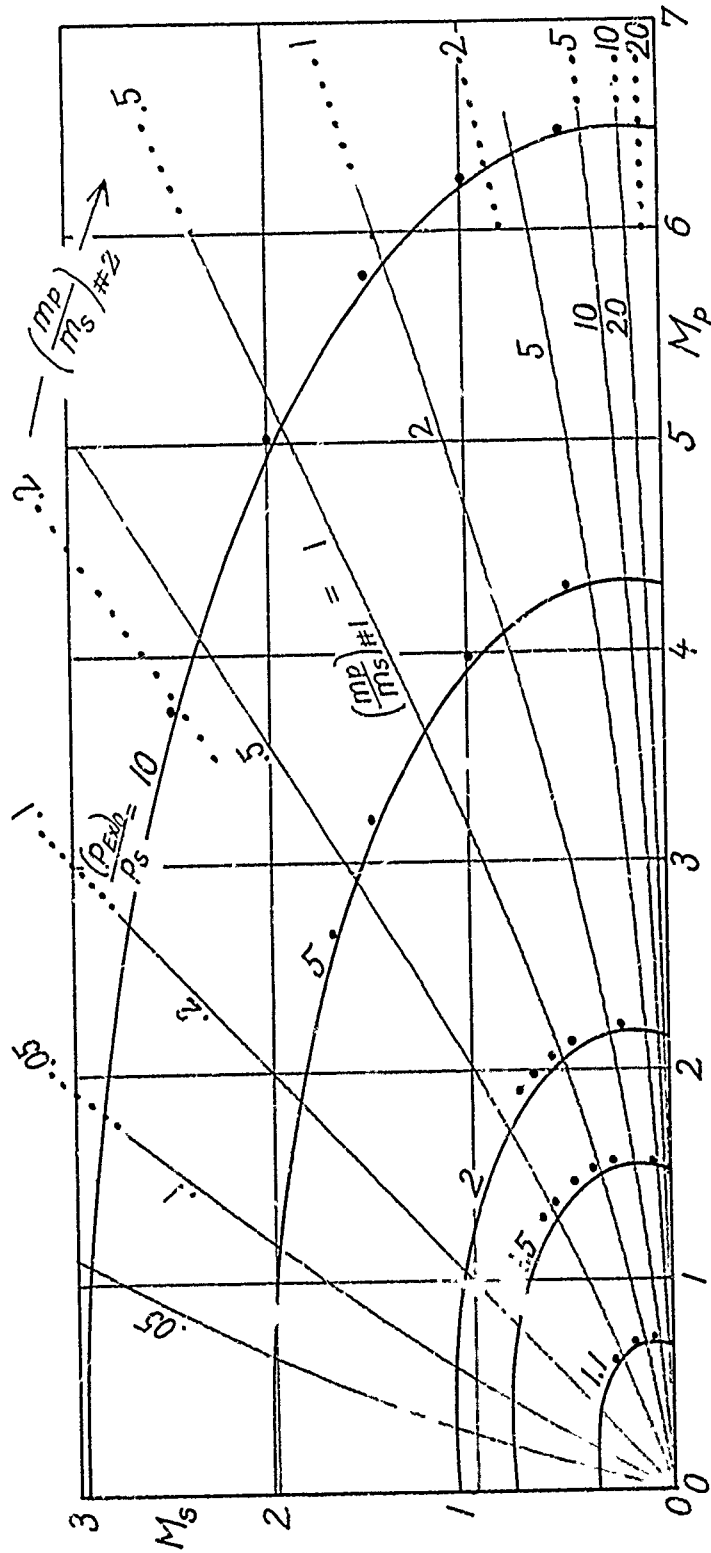
Figure 8. Primary to Secondary Mass Ratio m_p/m_s Together With the Ejector Pressure Ratios $(p_{Ex})_3/p_s$ for Constant Area Mixing (same as in Figure 6) for Operating Conditions #1 and #2 (see Table I) at an Inlet Area Ratio A_p/A_s = 0.2.
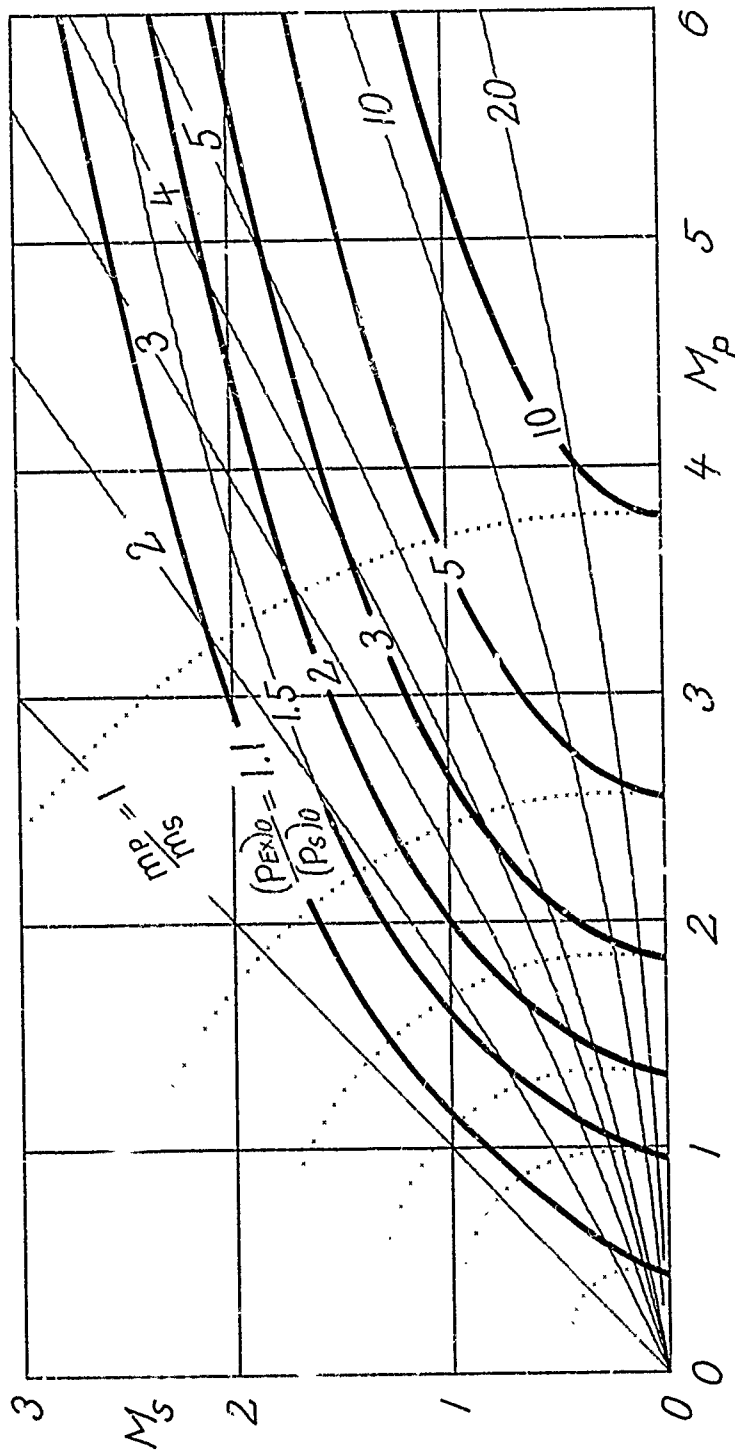
Figure 5. "Total Ejector Pressure Ratio" Together With Mass Ratios for Constant Area Mixing at an Inlet Area Ratio $A_p/A_s = 1.0$. (Curves marked (.........) are the ejector pressure ratio $(p_{Ex})_o/p_s$ curves also shown in Figures 5 and 7. This plot shows that a mass ratio line can intersect a total ejector pressure ratio line twice, indicating that for a given total ejector pressure ratio the mass ratio can be minimized.)
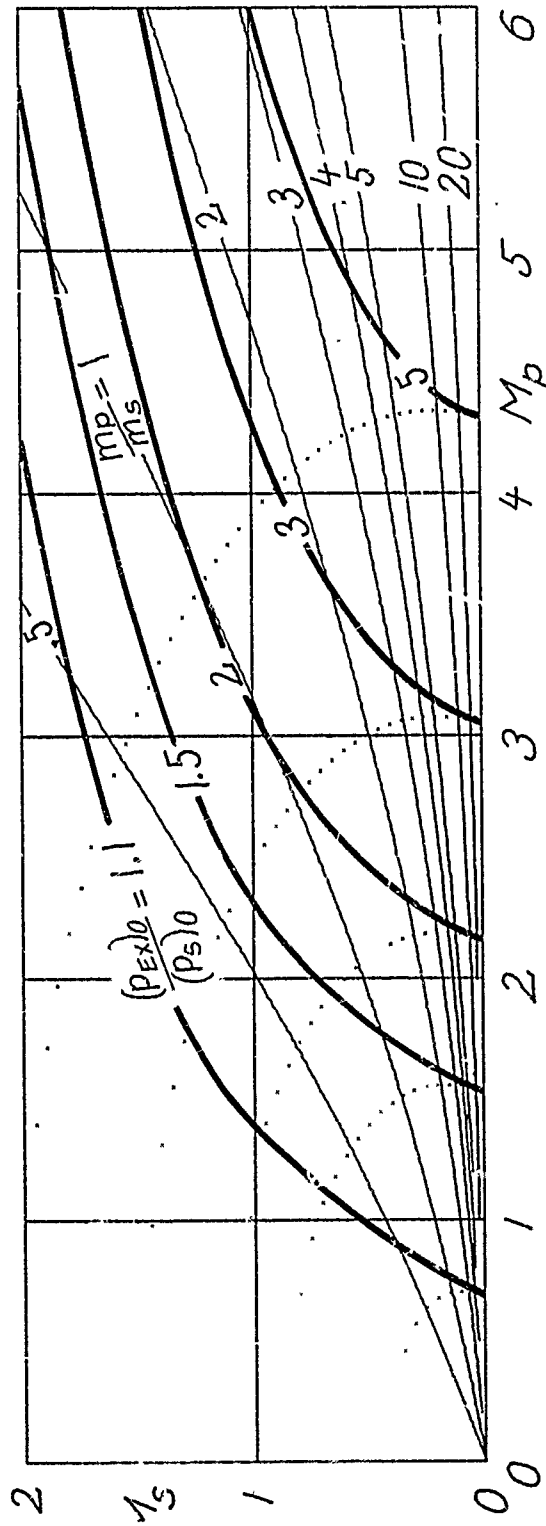
Figure 10. "Total Ejector Pressure Ratios" Together With Mass Ratios for Constant Area Mixing at an Inlet Area Ratio $A_p/A_s = 0.2$. (The curves marked (-...-) are the ejector pressure ratios $(p_{Ex})_o/p_s$. They are identical to the curves shown in Figure 6. Otherwise the remark given in Figure 9 applies.)
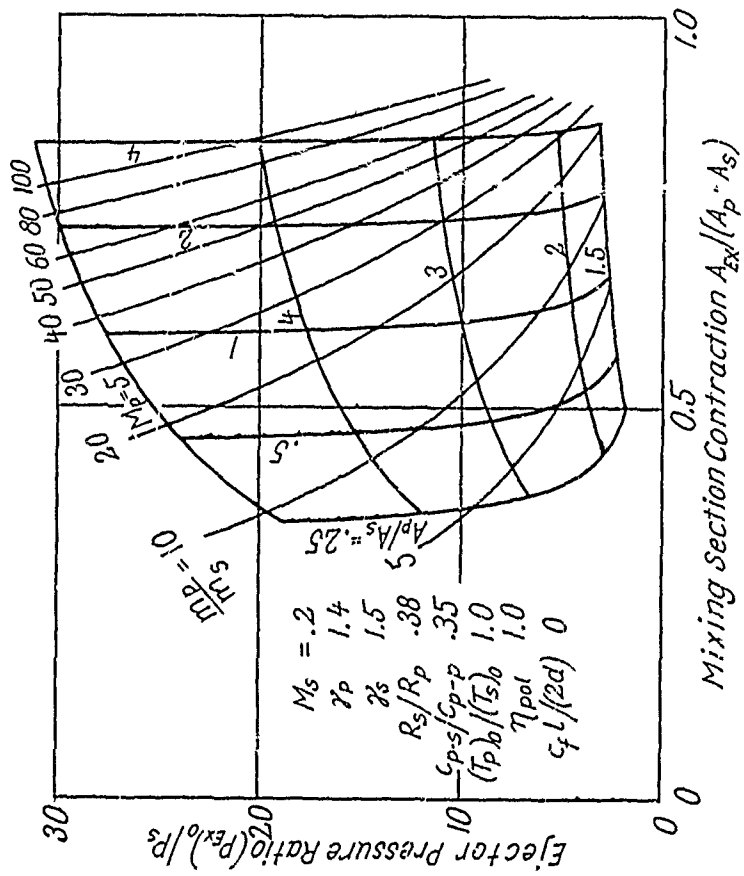
Figure 11. Example of the Relation Between the Ejector Pressure Ratio and the Mixing Section Contraction Ratio for Constant Pressure Mixing at a Given Secondary Inlet Mach Number $M_S = 0.2$.

76
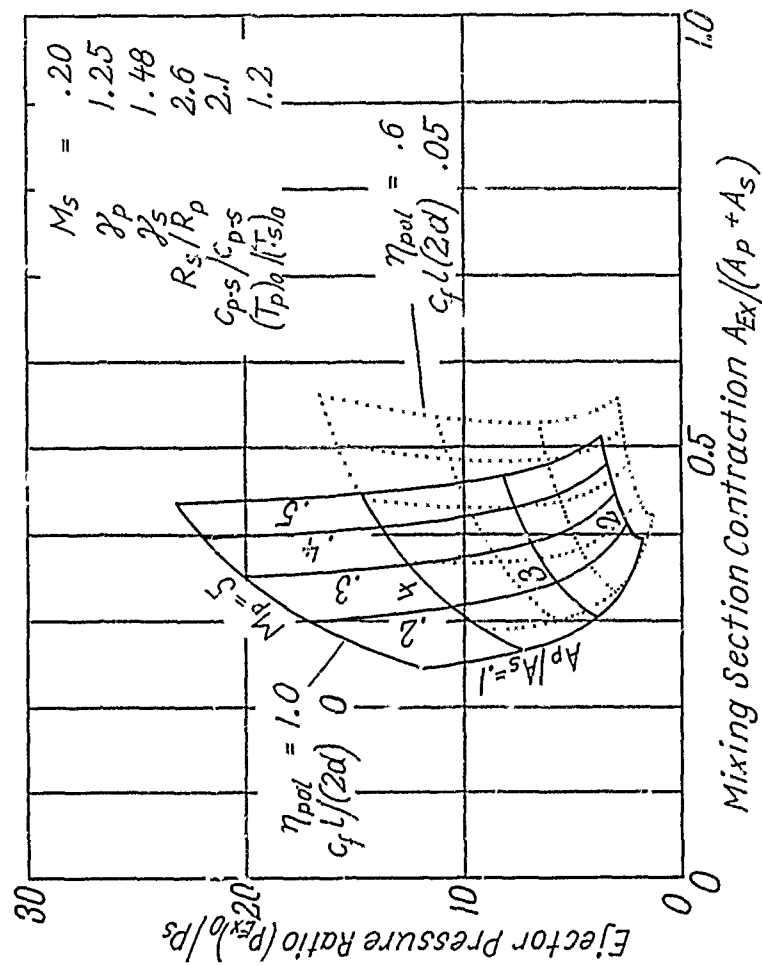
Figure 11a. Example for the Influence of the Incidental Losses (Wall Friction and Diffuser) on the Ejector Performance and the Required Mixing Section Contraction. (The solid line diagram converts to the one given by the dotted lines if the incidental losses are changed from zero to the indicated values.)

77
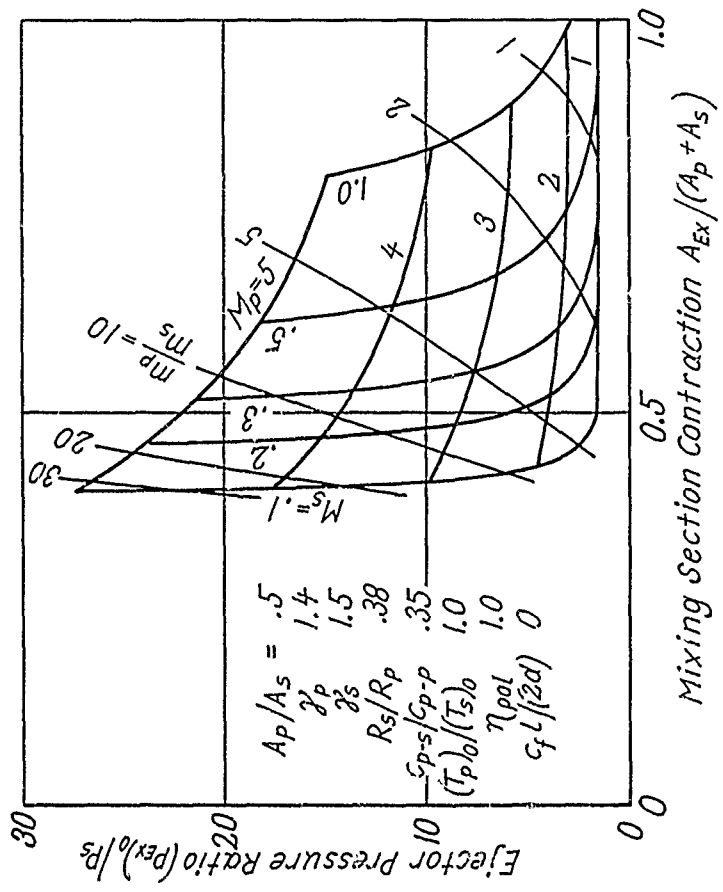
Figure 12. Example of the Relation Between the Ejector Pressure Ratio and the Mixing Section Contraction Ratio for <u>Constant Pressure Mixing</u> at a Given Area Inlet Ratio A_p/A_s = 0.5.
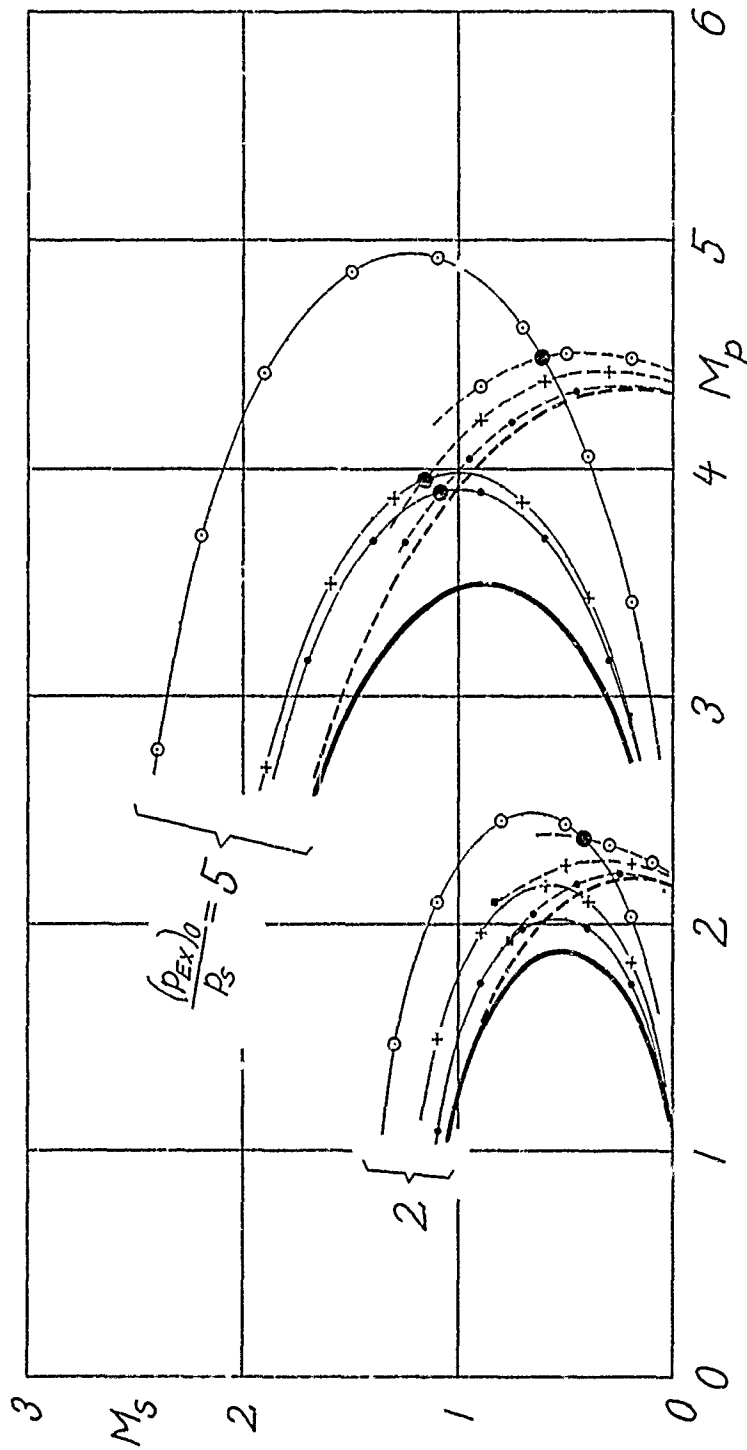
Figure 13. Characteristic Performance of Constant Pressure Mixing Ejector for Inlet Area Ratio $A_p/A_s = 0.2$. (The heavy solid lines give the performance for the homogeneous ejector without wall friction and diffuser losses. The marked points give the performance for operating conditions listed in Table I. For comparison portions of the performance curves for constant area mixing (— — — —) are entered. The crossover points of corresponding curves are marked by (⊙). The comparison indicates that heterogeneity and incidental losses have a much stronger influence with constant pressure mixing than with constant area mixing. The mixing section contraction ratio $A_{Ex}/(A_p + A_s)$ necessary for constant pressure mixing increases strongly with increasing secondary Mach number as can be seen from Figure 12 along a line of constant ejector pressure ratio. The performance curves therefore do not reflect the behavior of an ejector with a given geometry. This is shown in Figures 16 and 19.
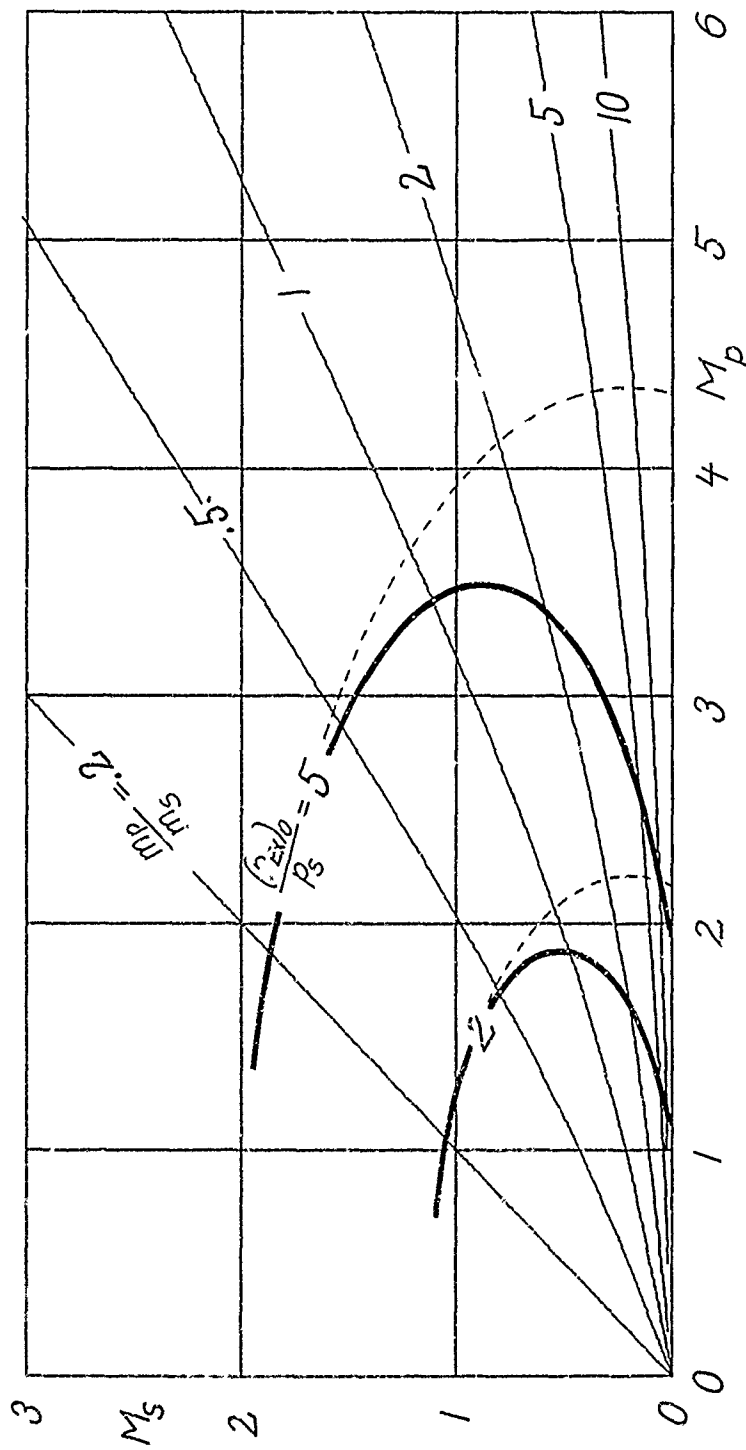
Figure 14. Mass Ratios for Pressure Ratio Curves Shown in Figure 13. (The mass ratio curves are identical with the ones for constant area mixing shown in Figure 8, operating condition #1; ----- constant area mixing)
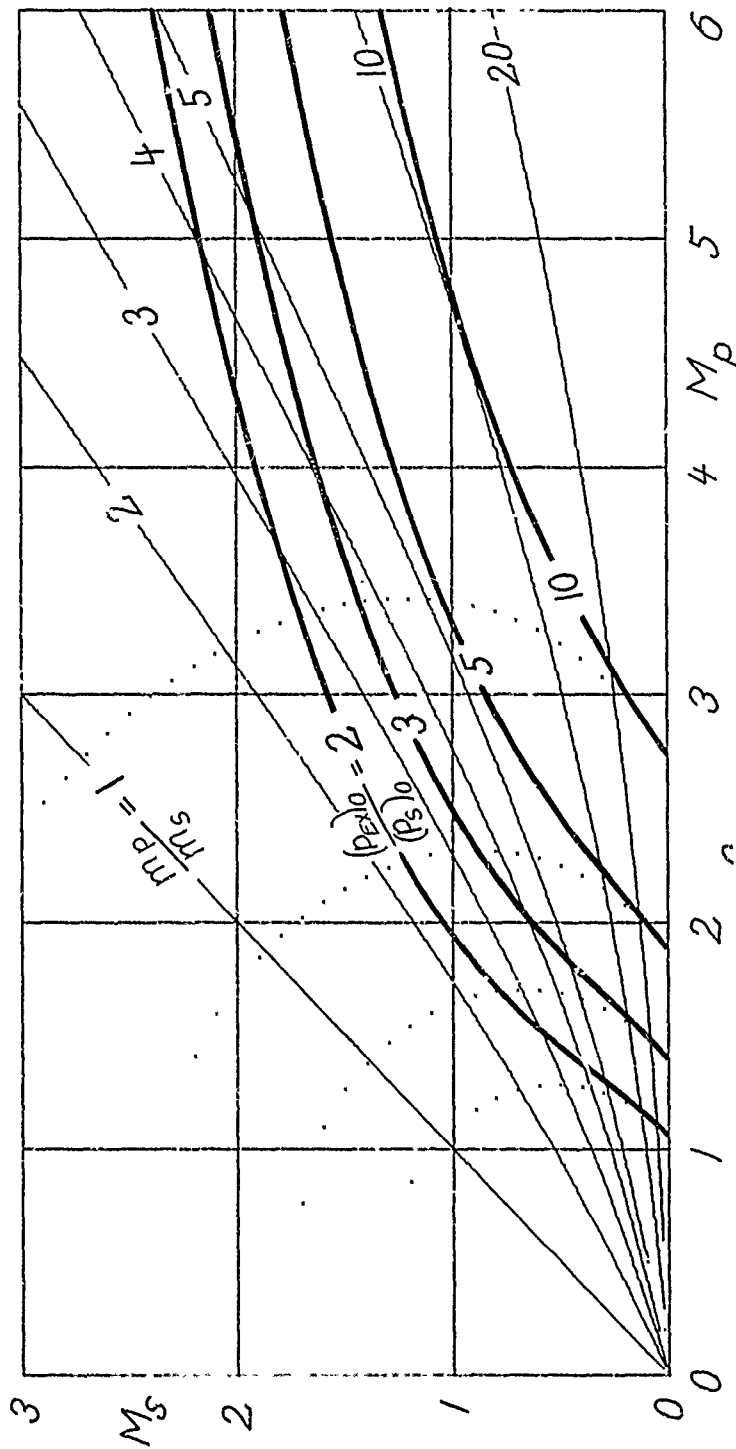
Figure 15. Total Ejector Pressure Ratio $(p_{Ex})_o/(p_s)_o$ for the Homogeneous Ejector Without Incidental Losses at Constant Pressure Mixing for an Inlet Area Ratio $A_p/A_s = 1.0$ Together with the Mass Ratio Curves, which are Identical with Those Shown in Figure 7. (Also entered is the ejector pressure ratio $(p_{Ex})_o/p_s$ marked by (........).

81

1	$(A_p/A_s)_{geo}$	.11
2	γ_p	1.26
3	γ_s	1.48
4	R_s/R_p	2.60
5	c_{p-s}/c_{p-p}	2.10
6	$(T_p)_o/(T_s)_o$	1.20
7	η_{pol}	.60
8	$c_f l/(2d)$	.05
9	β	1.00
10	t	.30
11	i	.60
12	$(A_p)_{geo}/A^*$	13.30

$A^* = $ primary nozzle throat area
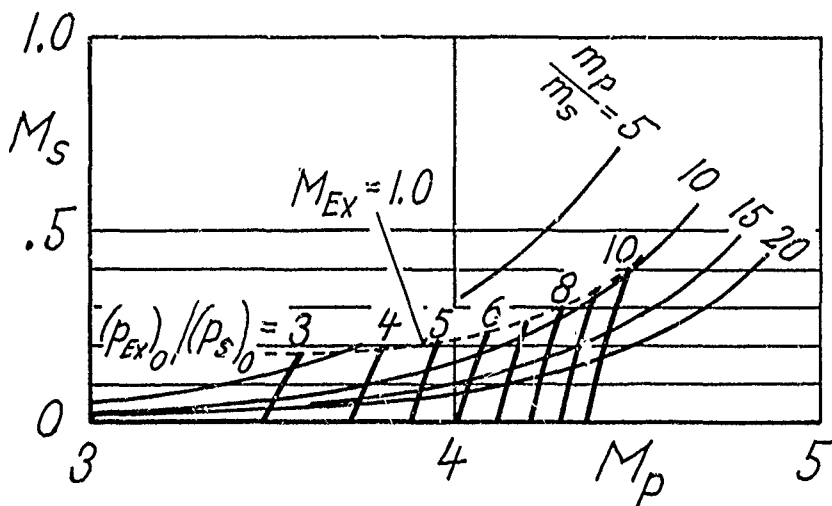
Figure 16. Example of a Performance Characteristic of an Ejector With a Mixing Section Contraction of $t = 0.3$ and a Pressure Distribution Factor $i = 0.6$. (Plotted are the total ejector pressure ratio and the mass ratio for the condition that the ejector geometry is fixed except for the injection nozzle of the primary flow, which is assumed to be always properly expanded, i.e., the inlet area ratio changes with M_p. This condition approaches fairly closely that for a completely fixed geometry (see page 3 of the text).
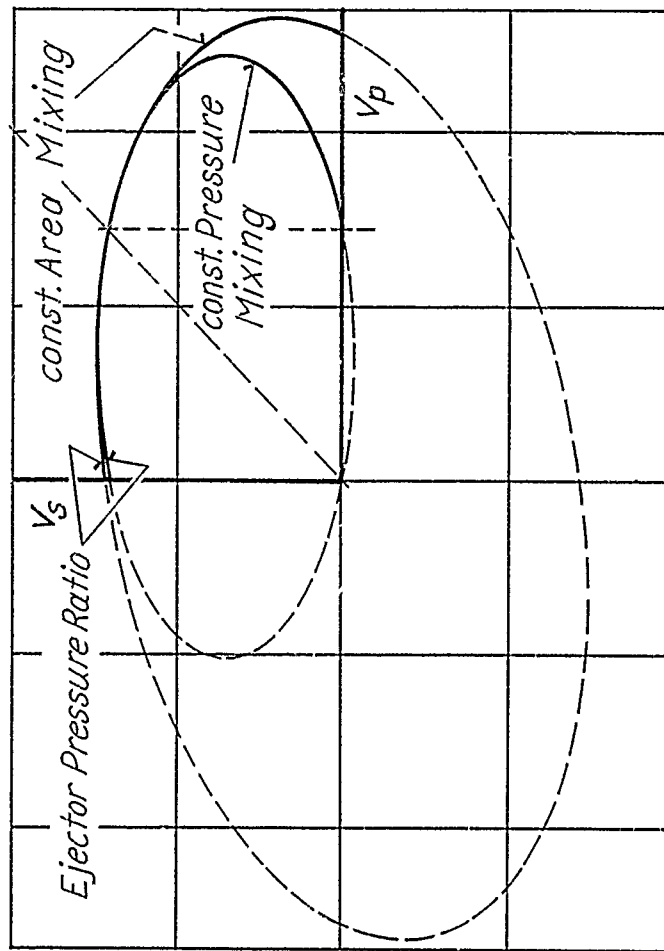
Figure 17. Basic Comparison of the Ejector Performance for Constant Area and Constant Pressure Mixing. (Shown is the case for the ejector with homogeneous, noncompressible operating media. In this basic case the performance curves appear as true ellipses, as indicated by the dashed part of the curves. Since heterogeneous conditions, which comprise also compressibility, have no crucial influence on the performance curves (ejector pressure ratio curves) as shown in Figures 5, 6, 7, 8, and 13, the curves shown are typical in general for ejectors. They allow one to recognize the apparent advantage of constant pressure mixing with decreasing secondary flow velocities. Whether constant pressure mixing can actually be established in all cases is a problem of the detailed flow conditions, particularly for supersonic flows. The excentricity of the ellipses shown is mainly a function of the inlet area ratio. For the case shown the inlet area ratio A_p/A_s is 0.2. Lower values of this ratio stretch out the ellipses in such a way that the point, which is common to the curves at $v_p = v_s$, maintains its position.)
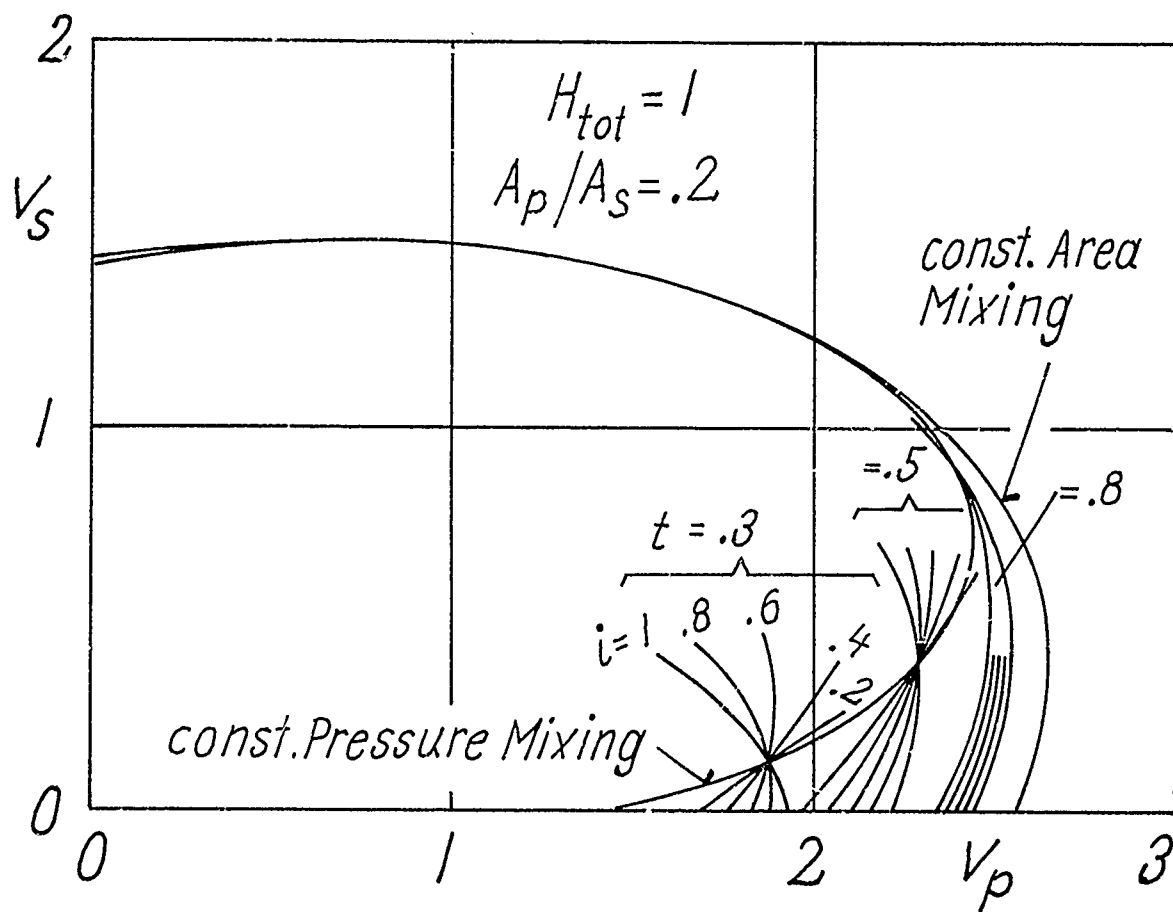
Figure 18. Basic Performance Characteristic for Ejectors With Fixed Mixing Section Area Ratio $t = A_{Ex}/(A_p + A_s)$ and Certain Pressure Distribution Factors i. (The performance curves for constant area and constant pressure mixing, shown already in Figure 17, are also entered. All performance curves for a given value of t must cross at one point on the constant pressure mixing curve, since at this point the pressure distribution influence must disappear. In the region inside the constant pressure mixing curve the pressure drops during mixing; outside, it increases. Since the pressure during mixing cannot be reduced arbitrarily only a limited region exists inside the constant pressure mixing curve where ejector operations are possible. These limitations are demonstrated in the next Figure 19.)
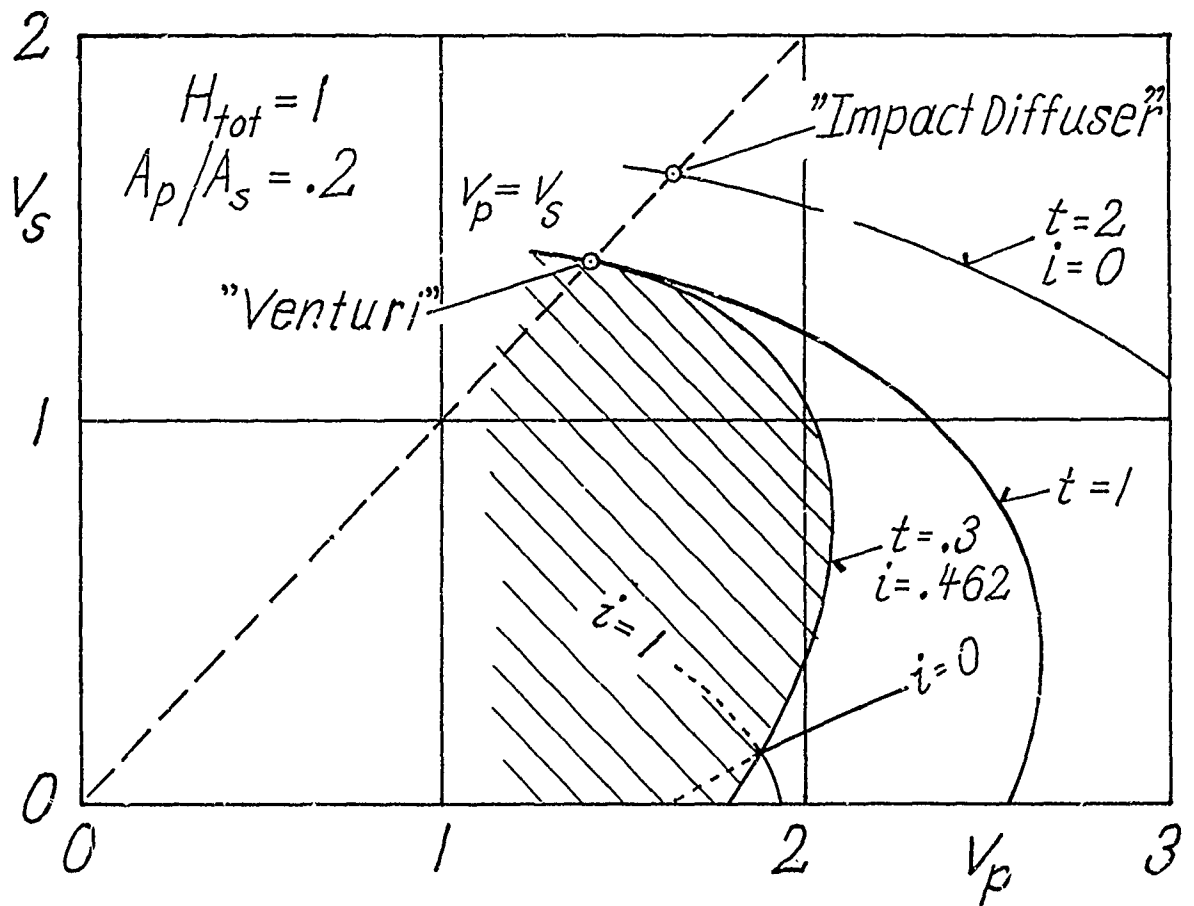
Figure 19. Limiting Regions for the Ejector Operation With Given Mixing Section Area Reduction t. (For a given t-value only such a minimum i-value is possible which makes a constant t-curve meet the constant area mixing curve at the point $v_p = v_s$. At this point potential flow conditions exist for all mixing section area reductions since no mixing losses are present if primary and secondary flow have the same velocity. This also means that the total head of the flow must be the same for all area reductions. The flow conditions are simply those in a Venturi pipe becoming a straight pipe for t = 1. The potential flow requirements allow one to determine the minimum i-value admissible for a given t-value. Inside the resulting limit curves (shaded area) no ejector operation is possible. The curve t = 2, i = 0 is an example for the use of the pressure distribution factor i to describe the flow conditions in a sudden enlargement. At the point $v_p = v_s$ the curve presents the conditions for the so-called "impact diffuser", which consists of a sudden enlargement in a flow duct.)
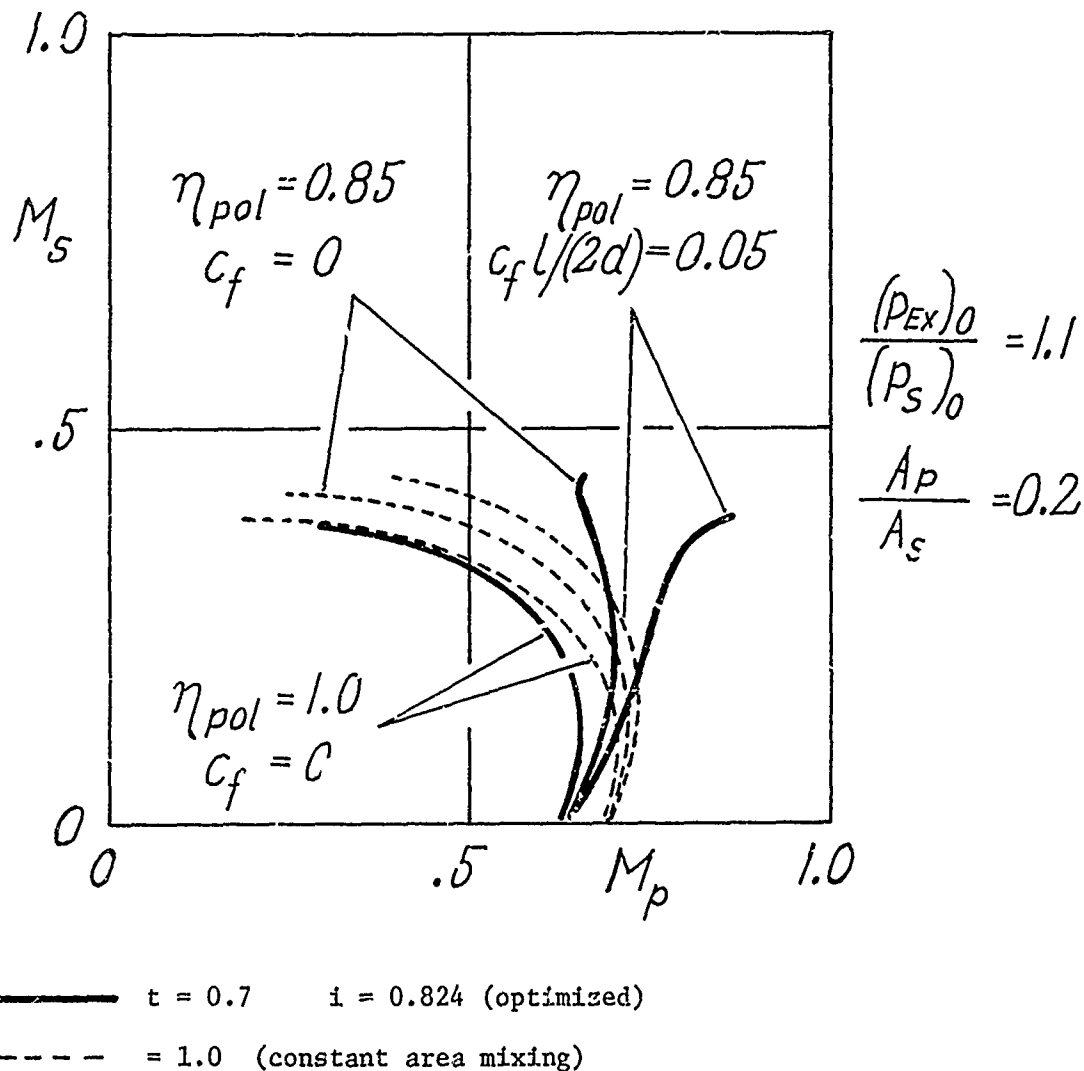
Figure 20. Influence of Wall Friction and Diffuser Losses on the Idealized Ejector Performance Shown in Figure 19. (The curves are obtained from the fully implemented analysis to allow inclusion of losses. The chosen ejector pressure ratio is sufficiently low to be representative for the incompressible case. For mixing section area reduction t = 0.7 the performance is increasingly reduced by the losses with increasing secondary Mach number. By comparison the influence remains small for constant area mixing (t = 1). The incompressible case is representative for thrust augmentation. Since thrust augmentation employs fairly high secondary velocities area reduction is not advantageous in this case. For the area reduction influence on the performance of high pressure ratio ejectors see Figure 26.)
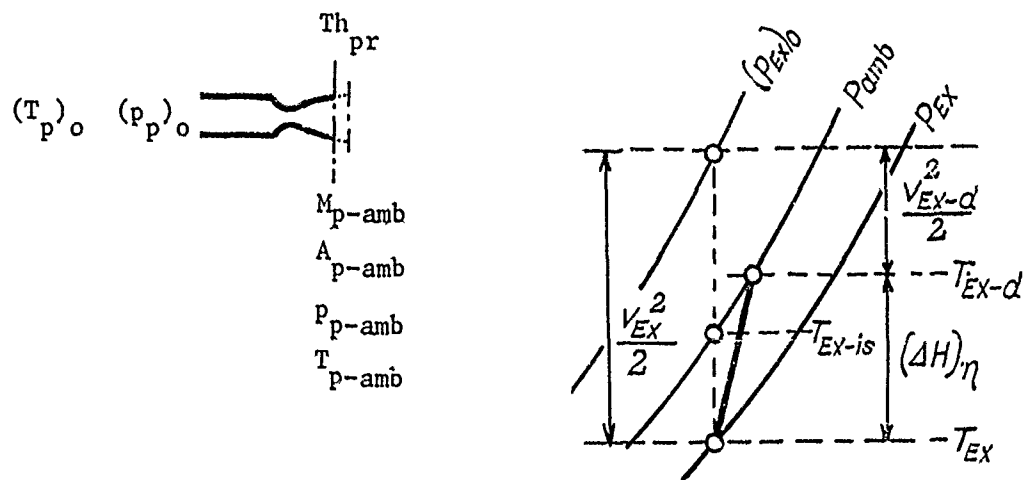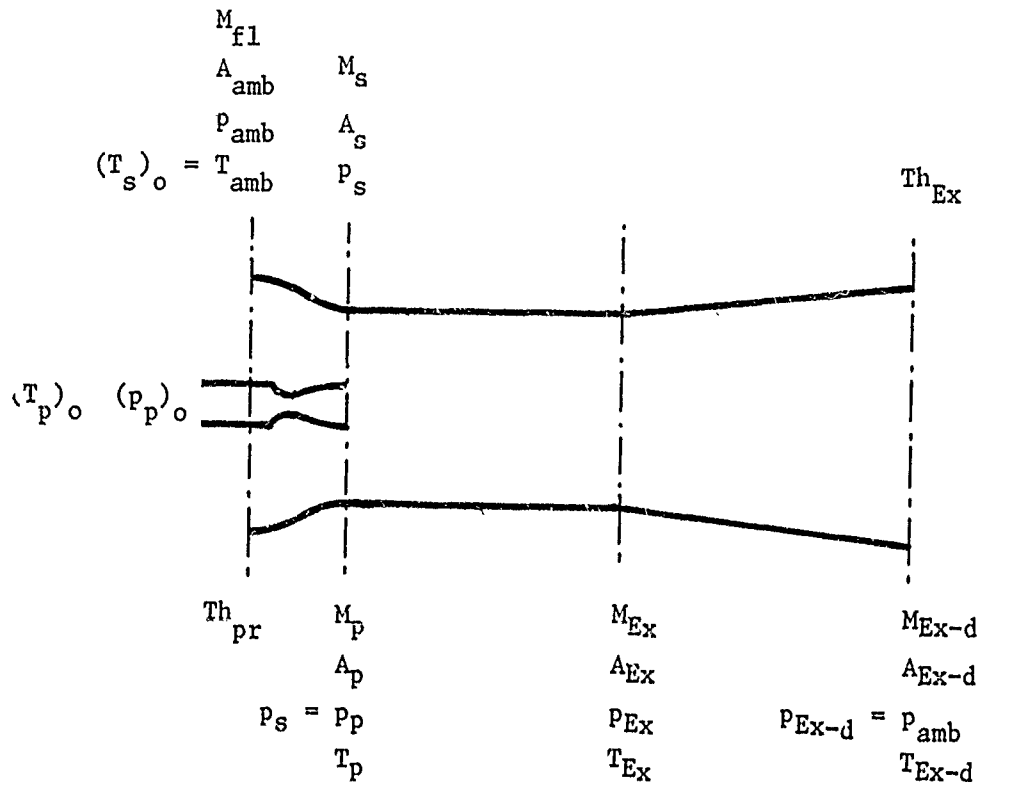
Figure 21. Notations for the Thrust Augmenter.
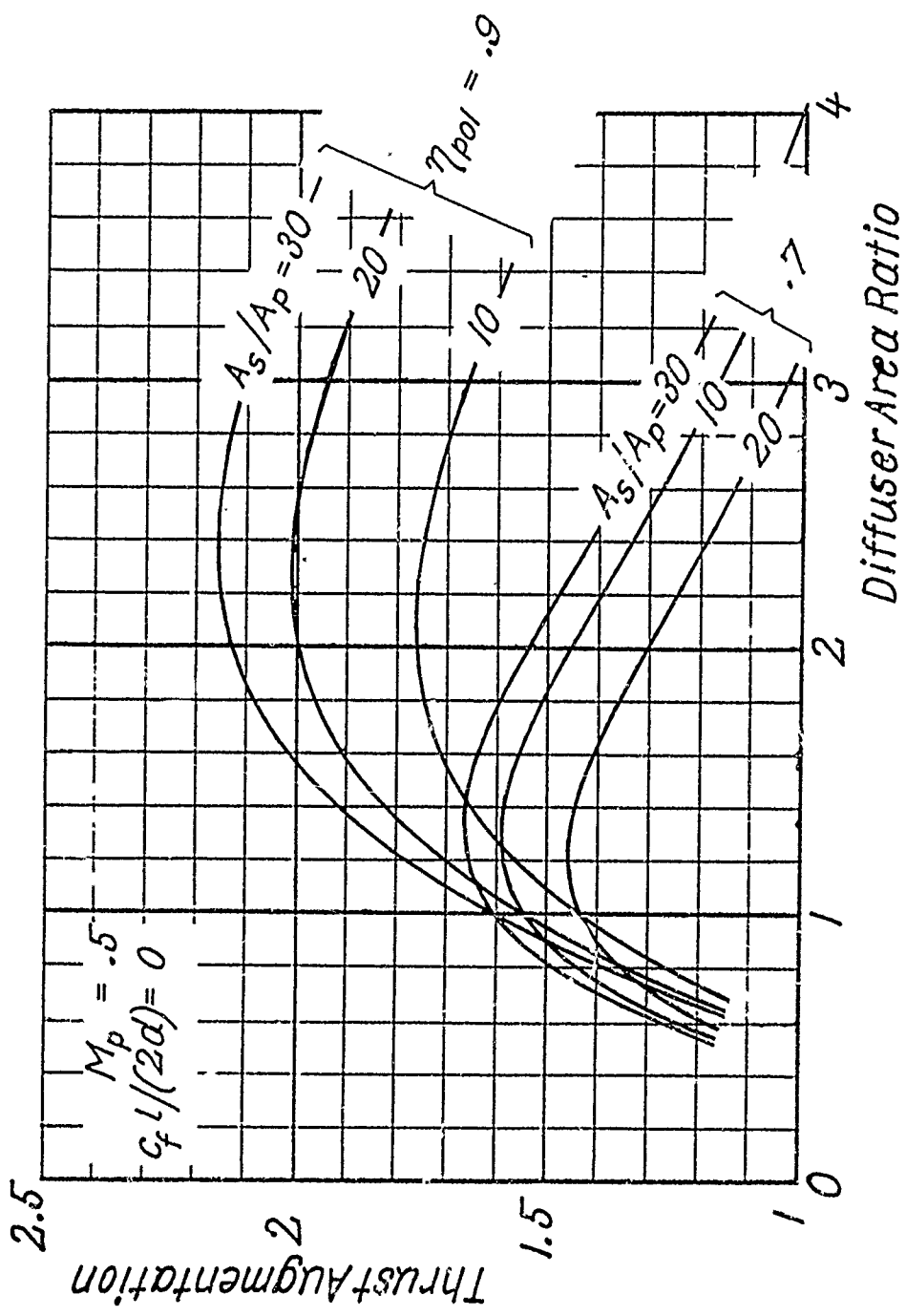
a. Inlet Area Ratio

Figure 21a to 21f. Thrust Augmentation as Function of Various Design Parameters.

The graph shows Thrust Augmentation (vertical axis, ranging from 1 to 2.5) versus Diffuser Area Ratio (horizontal axis, ranging from 0 to 4). Parameters shown: $A_s/A_p = 20$, $M_p = .5$, $c_f \, l/(2d) = 0$. Curves labeled $\eta_{pol} = .9$, $.85$, $.8$, $.75$, $.7$.
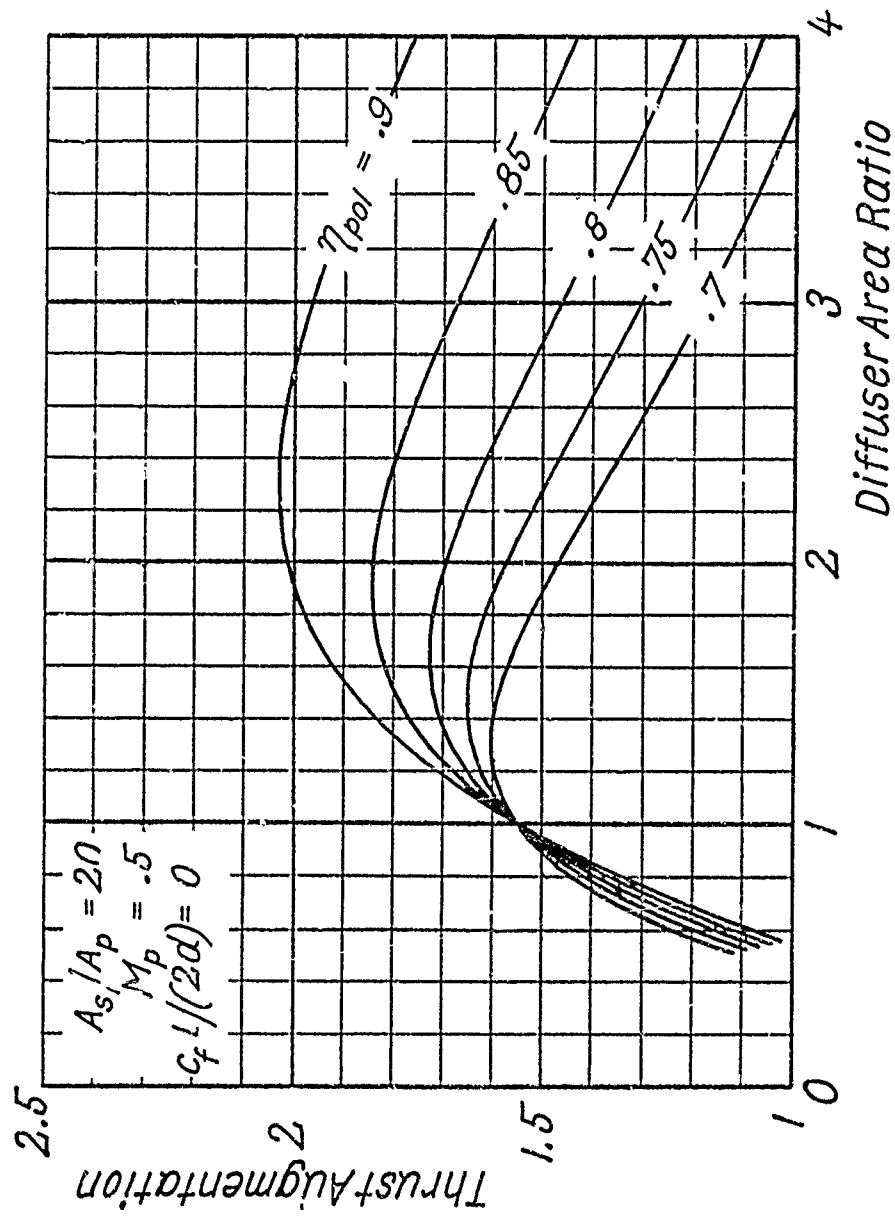
b. Diffuser Efficiency

Figure 21a to 21f. (Continued)
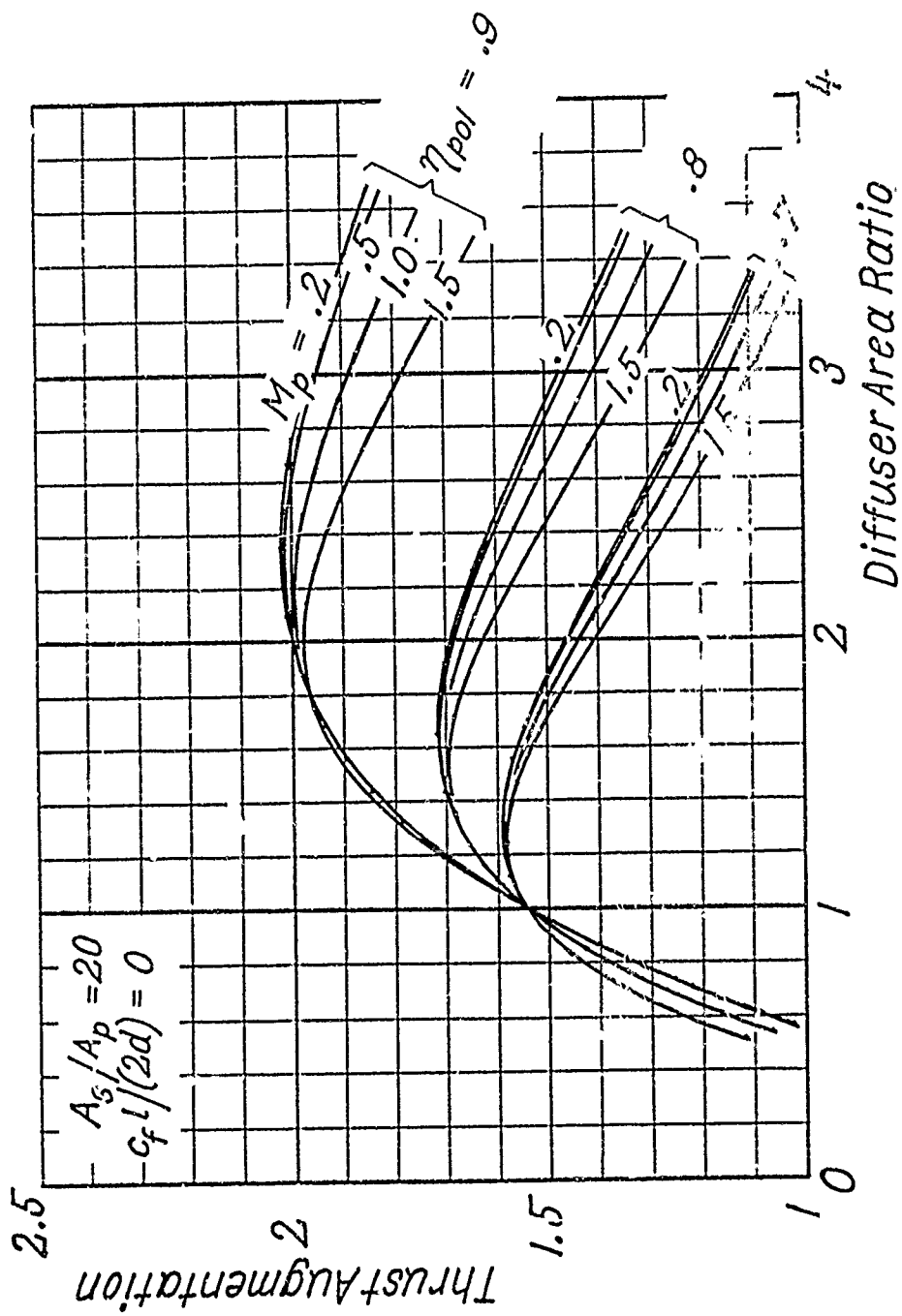
c. Primary Inlet Mach Number

Figure 21a to 21f. (Continued)

90
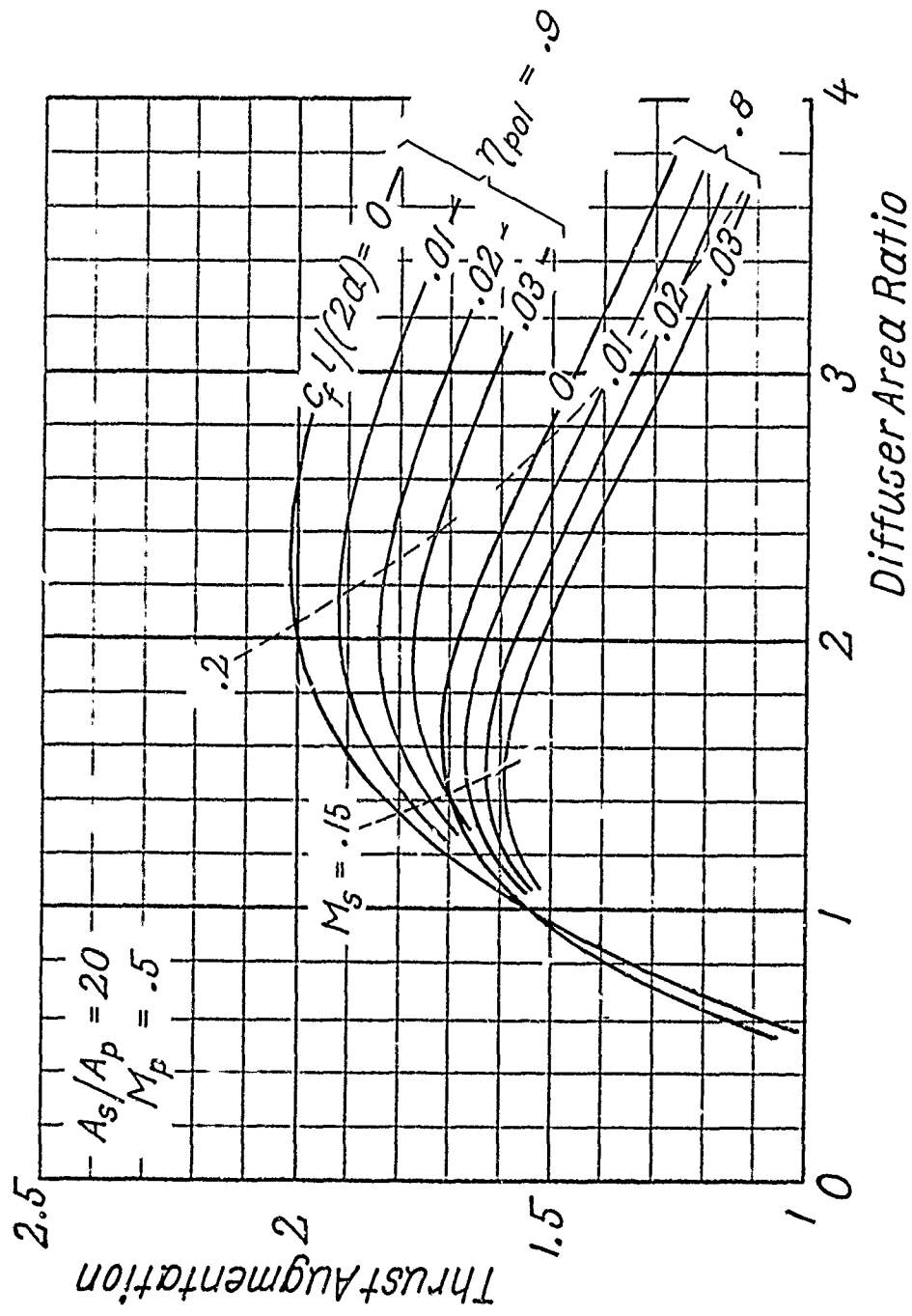
d. Wall Friction Loss

Figure 21a to 21f. (Continued)

The graph axes and labels:

- Vertical axis (left): Thrust Augmentation, ranging from 1.0 to 2.5
- Horizontal axis (bottom): Diffuser Area Ratio, ranging from 0 to 4

Annotations on graph:
$A_s/A_p = 20$
$M_p = .5$
$M_s = .15$
$c_f \, l/(2d) = 0$
$.01$
$.02$
$.03$
$\eta_{pol} = .9$
$.8$
$.2$

91
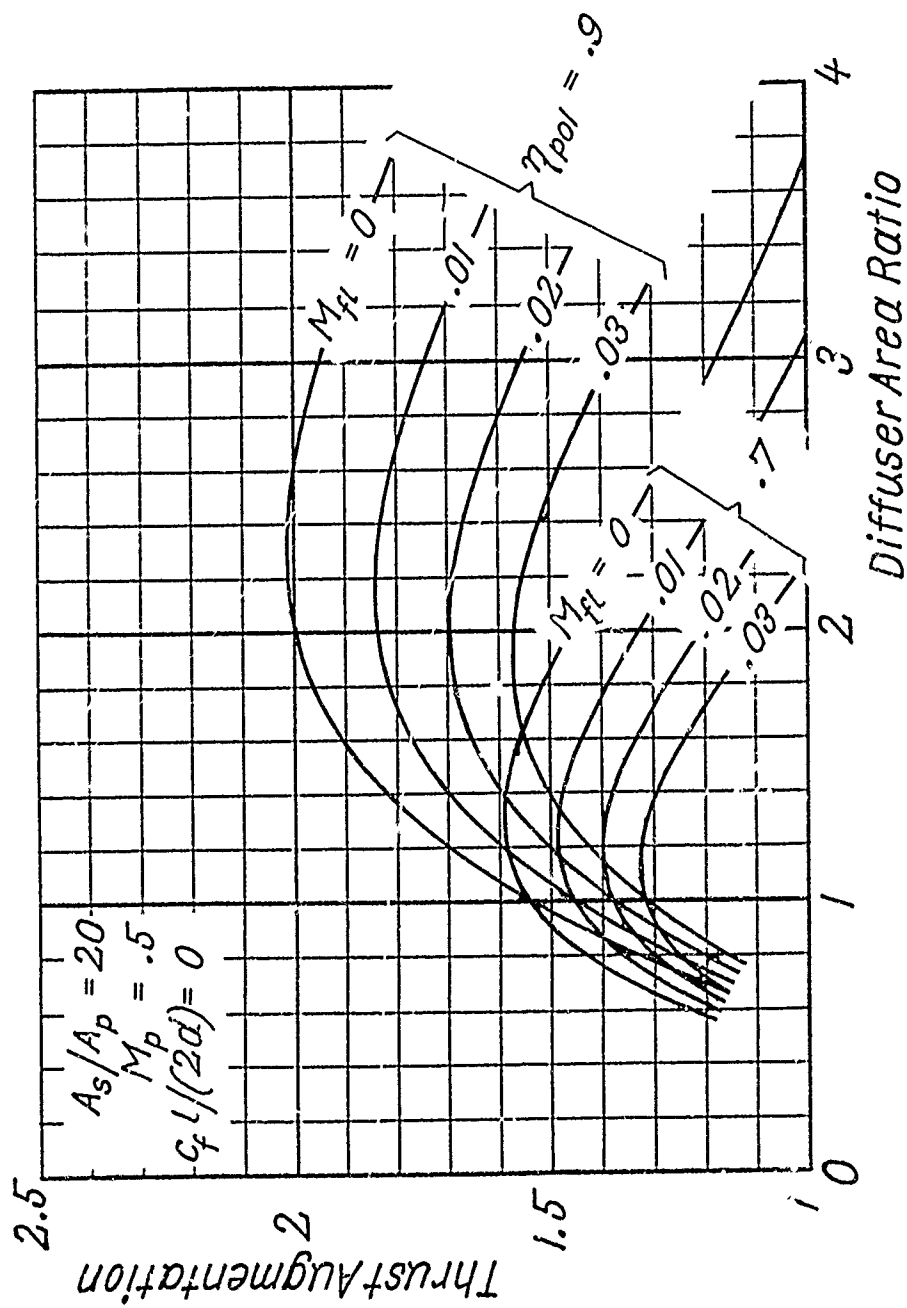
e. Flight Mach Number

Figure 21a to 21f. (Continued)
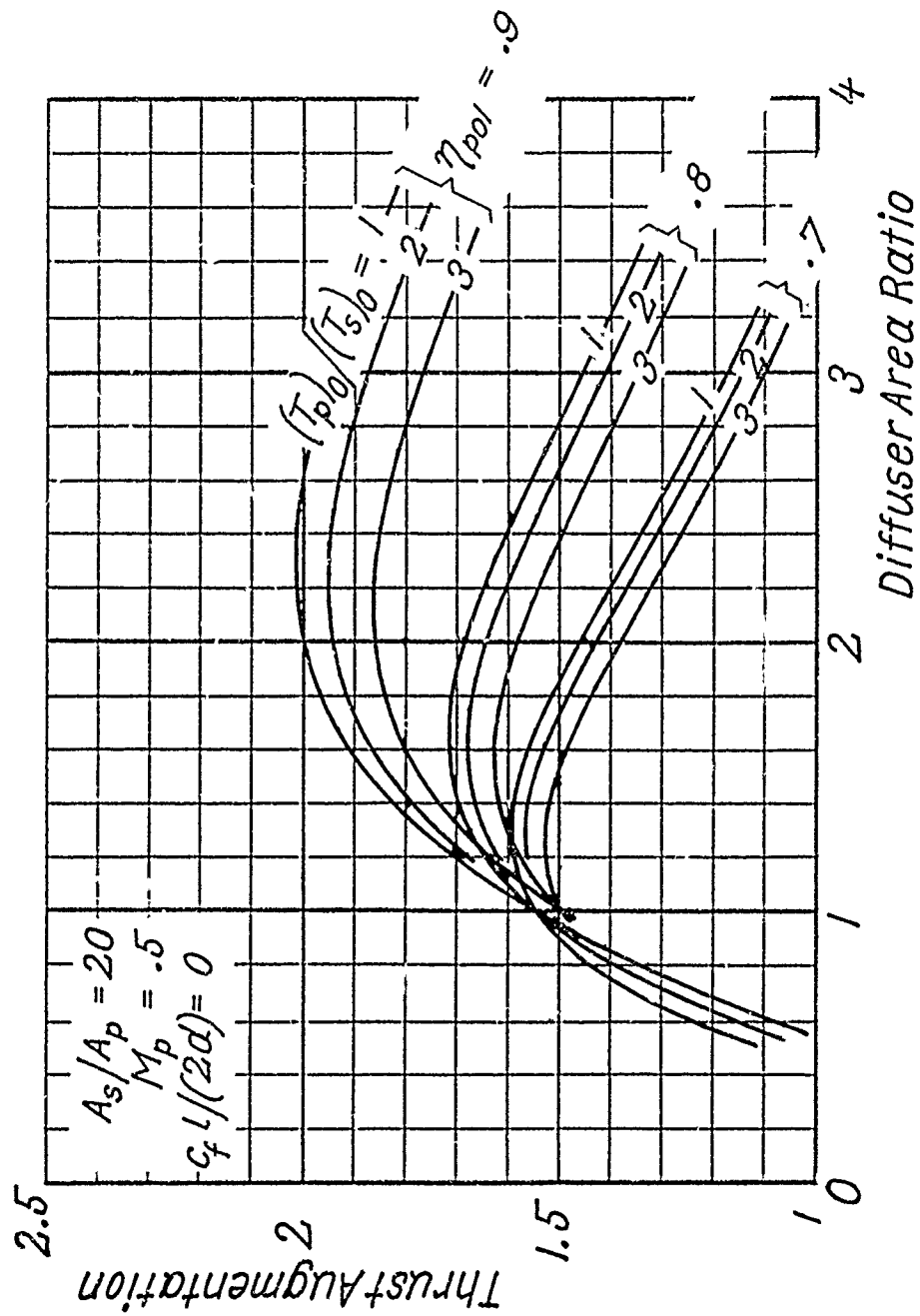
f. Primary to Secondary Flow Temperature Ratio

Figure 21a to 21f. (Continued)
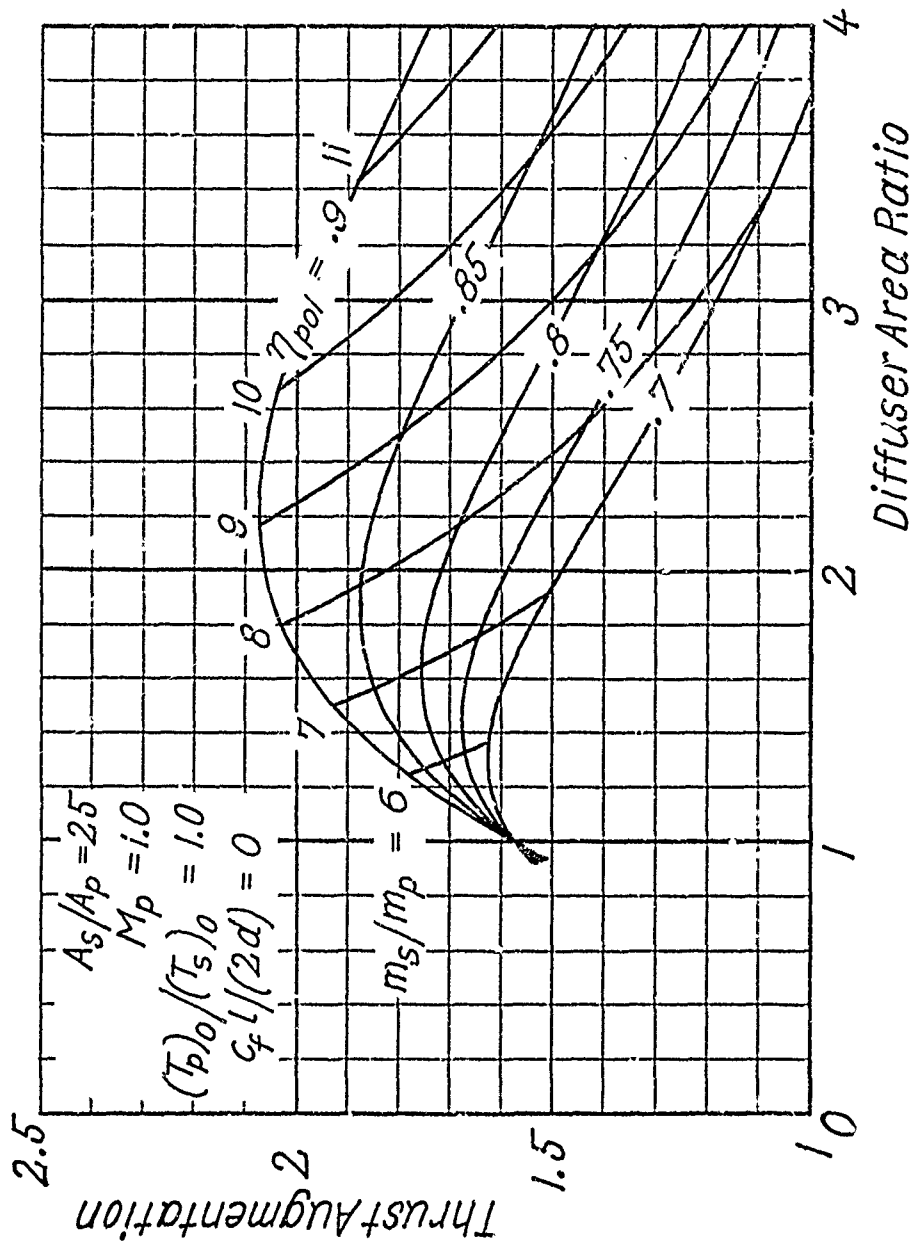
Figure 21g. Mass Ratios for Thrust Augmenter With Primary to Secondary Flow
Temperature of 1. (Along a constant mass ratio curve the secondary
inlet Mach number is also constant; e. g. for mass ratio 7 the
secondary inlet Mach number is 0.305.)

94
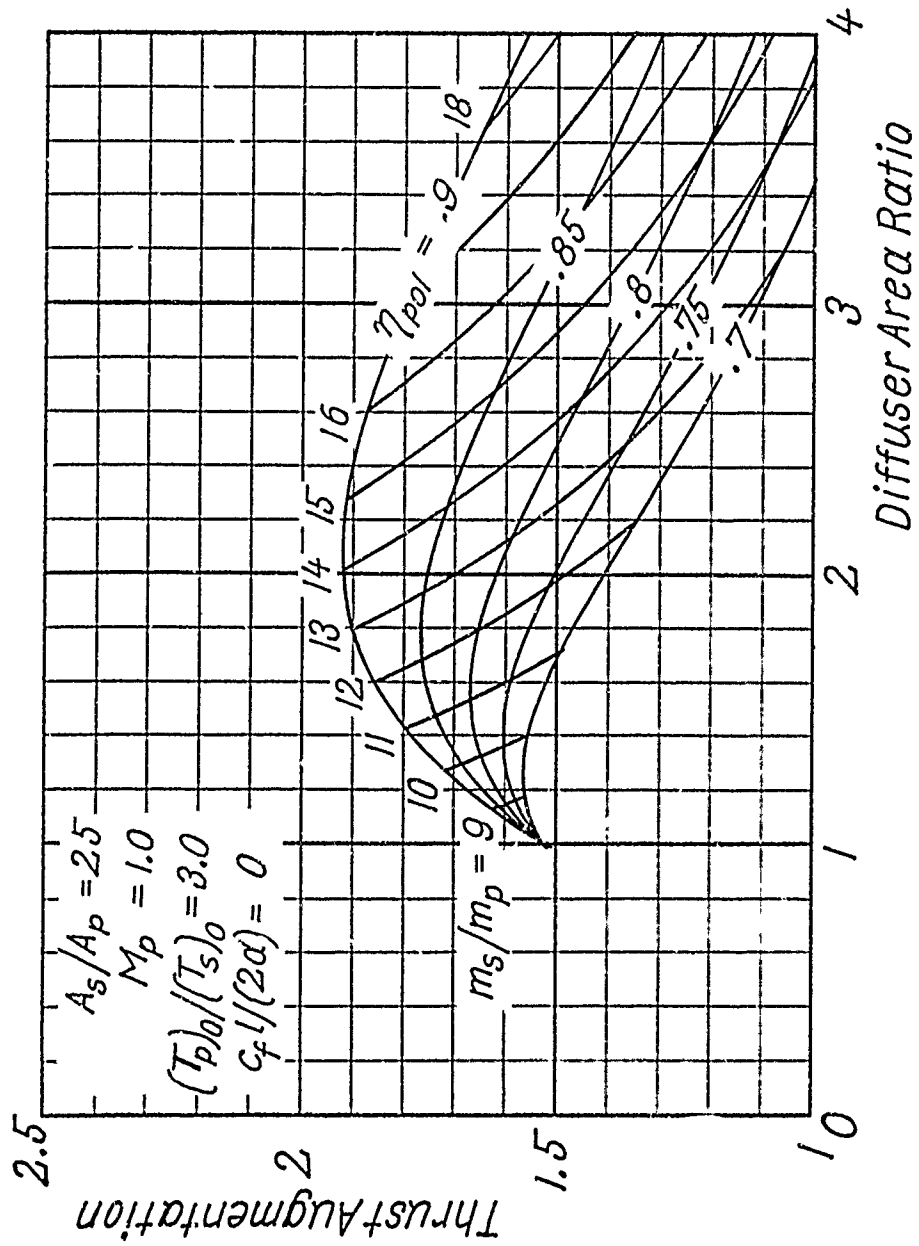
Figure 21h. Mass Ratios for Thrust Augmenter With Primary to Secondary Flow Temperature Ratio of 3.
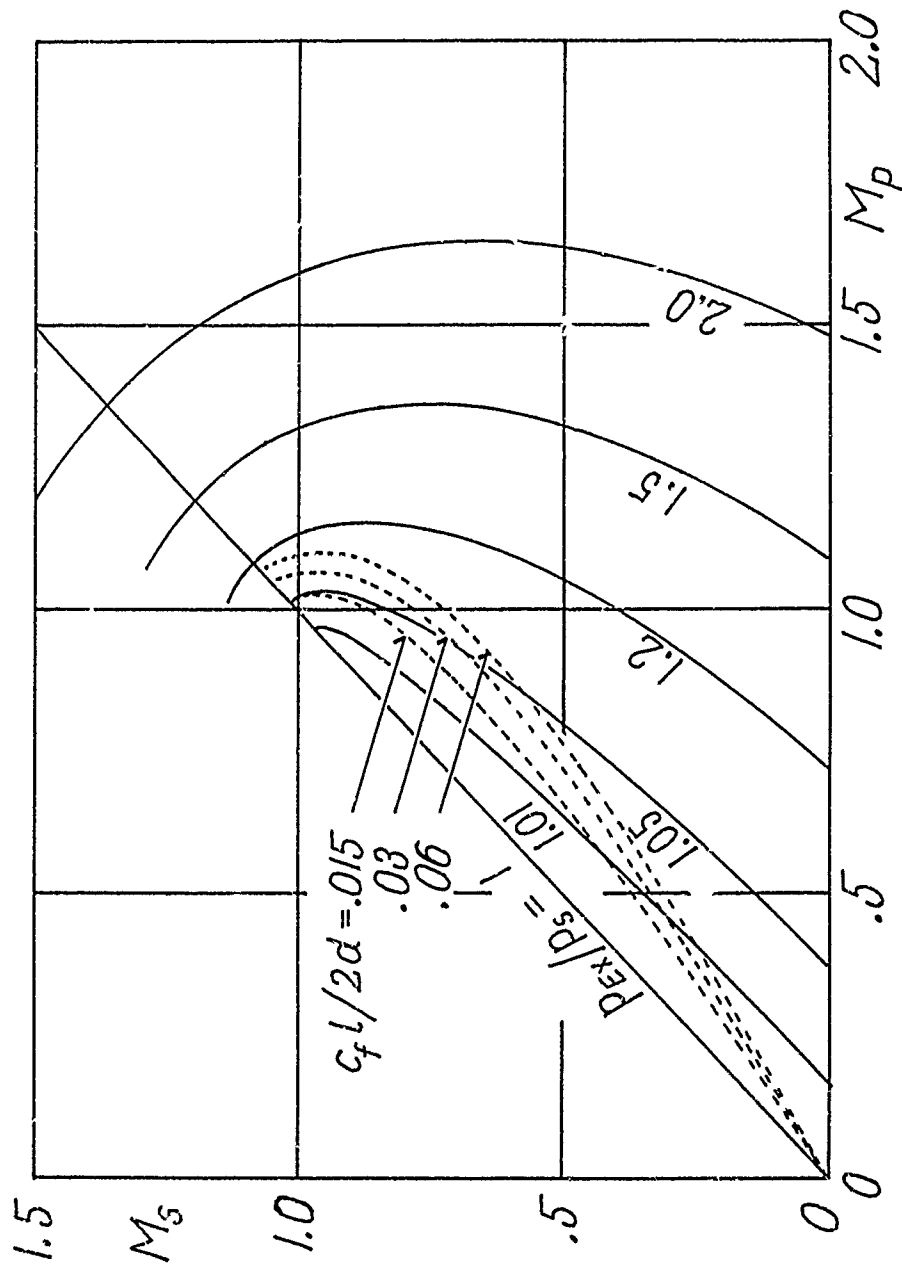
Figure 22. Effect of Incomplete Mixing on the Ejector Pressure Ratio Expressed in Terms of Effects of Wall Friction. (If one represents the state of incomplete mixing by a single step profile with M_p and M_s being the high and low Mach number in this profile, the diagram gives the wall friction condition under which the pressure drop caused by the wall friction is the same as the one caused by the unmixed state, assuming constant area mixing.)
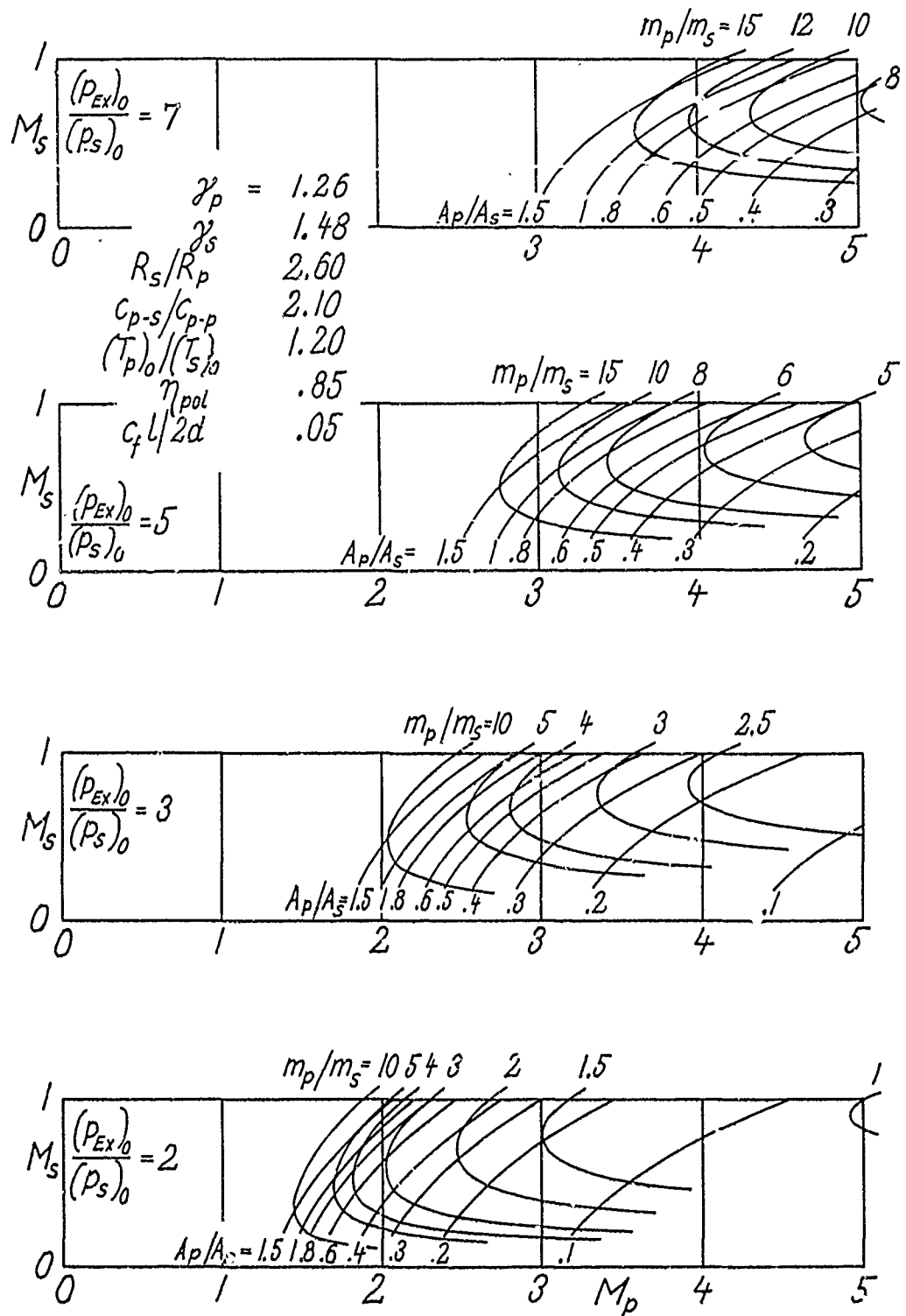
Figure 23. Performance Optimization for Constant Area Mixing for Four
Different Total Ejector Pressure Ratio .
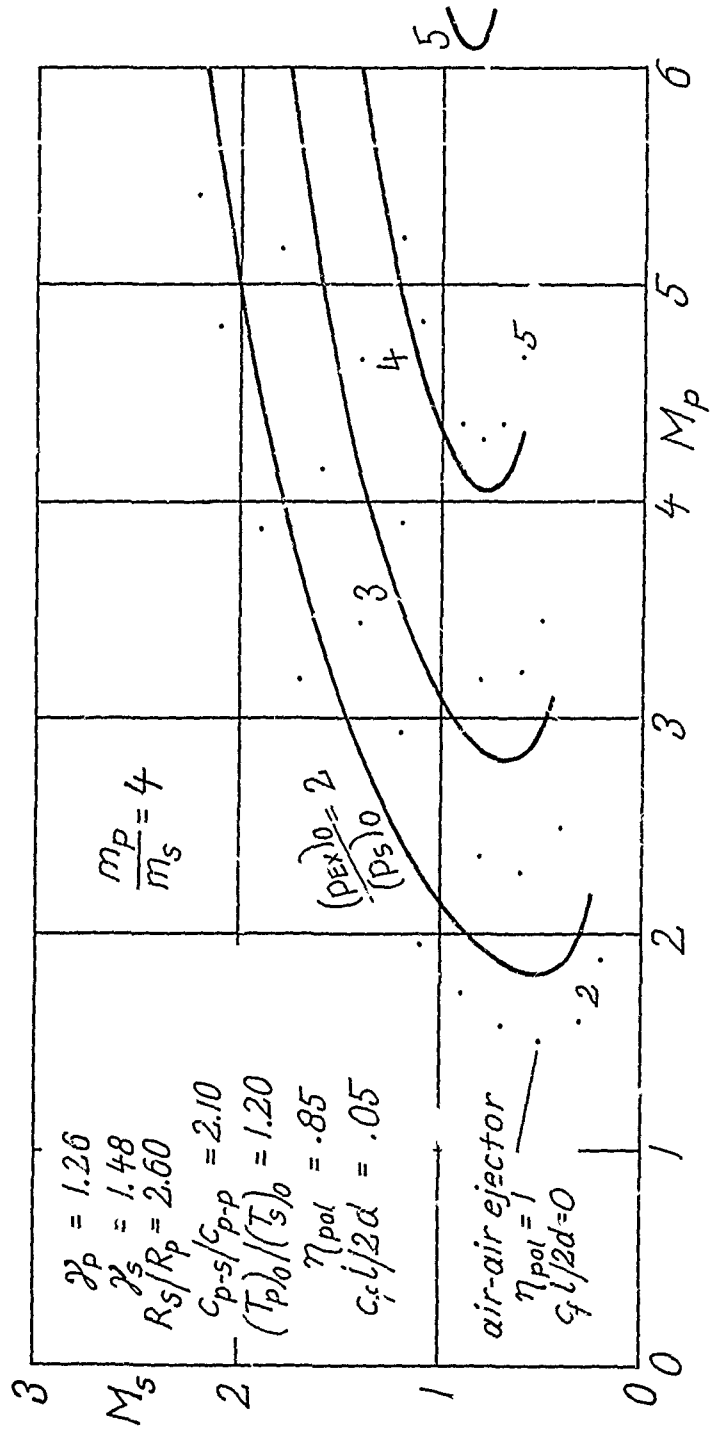
Figure 24a. Performance Optimization for Constant Area Mixing at Given Total Ejector Pressure Ratios for Four (a-d) Different Mass Flow Ratios. (The operating conditions are the same as in Figure 23 except for the air ejector as indicated in (a) and (c).)

98
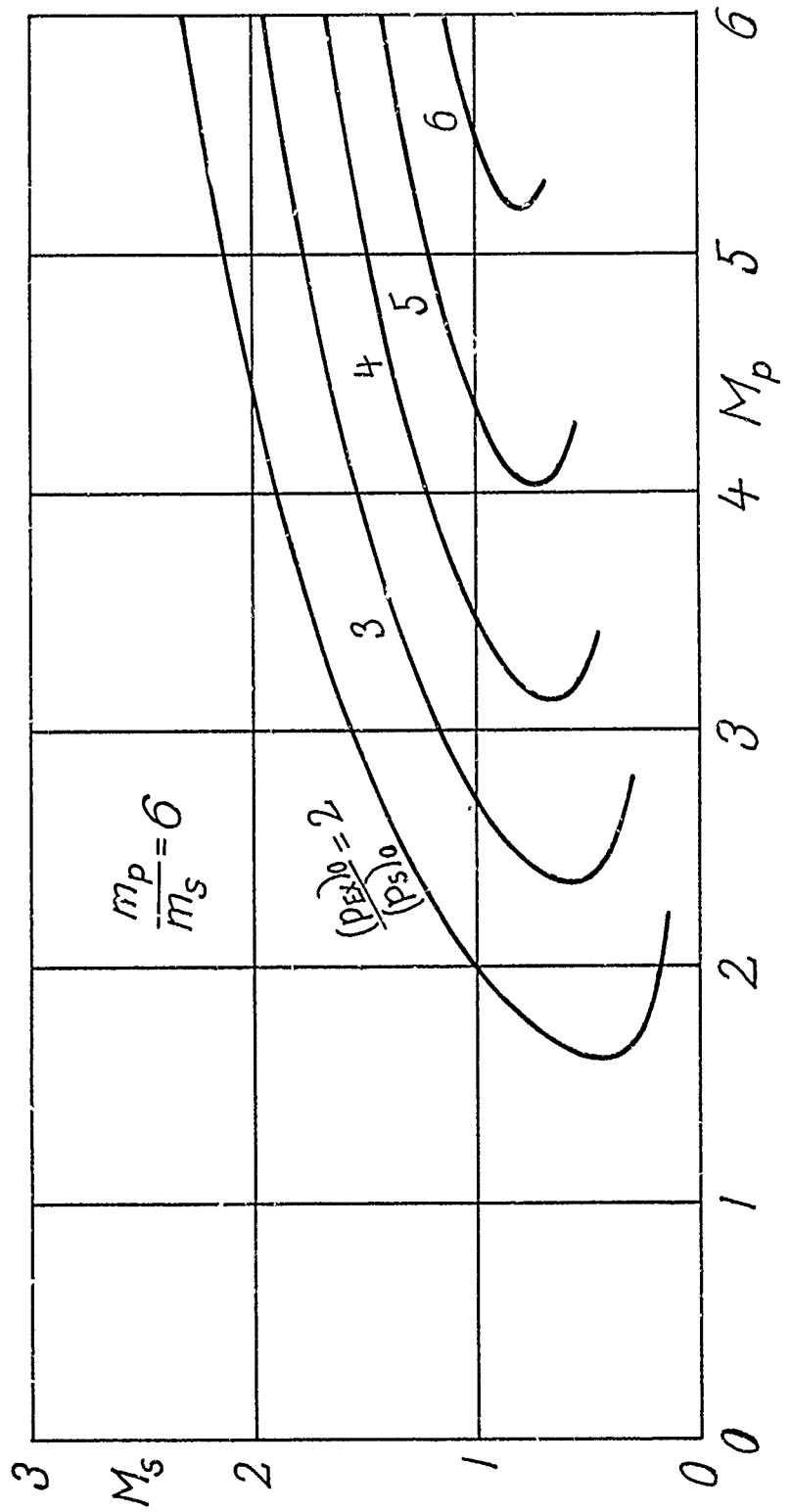
Figure 24b.   (Mass Flow Ratio 6)

99
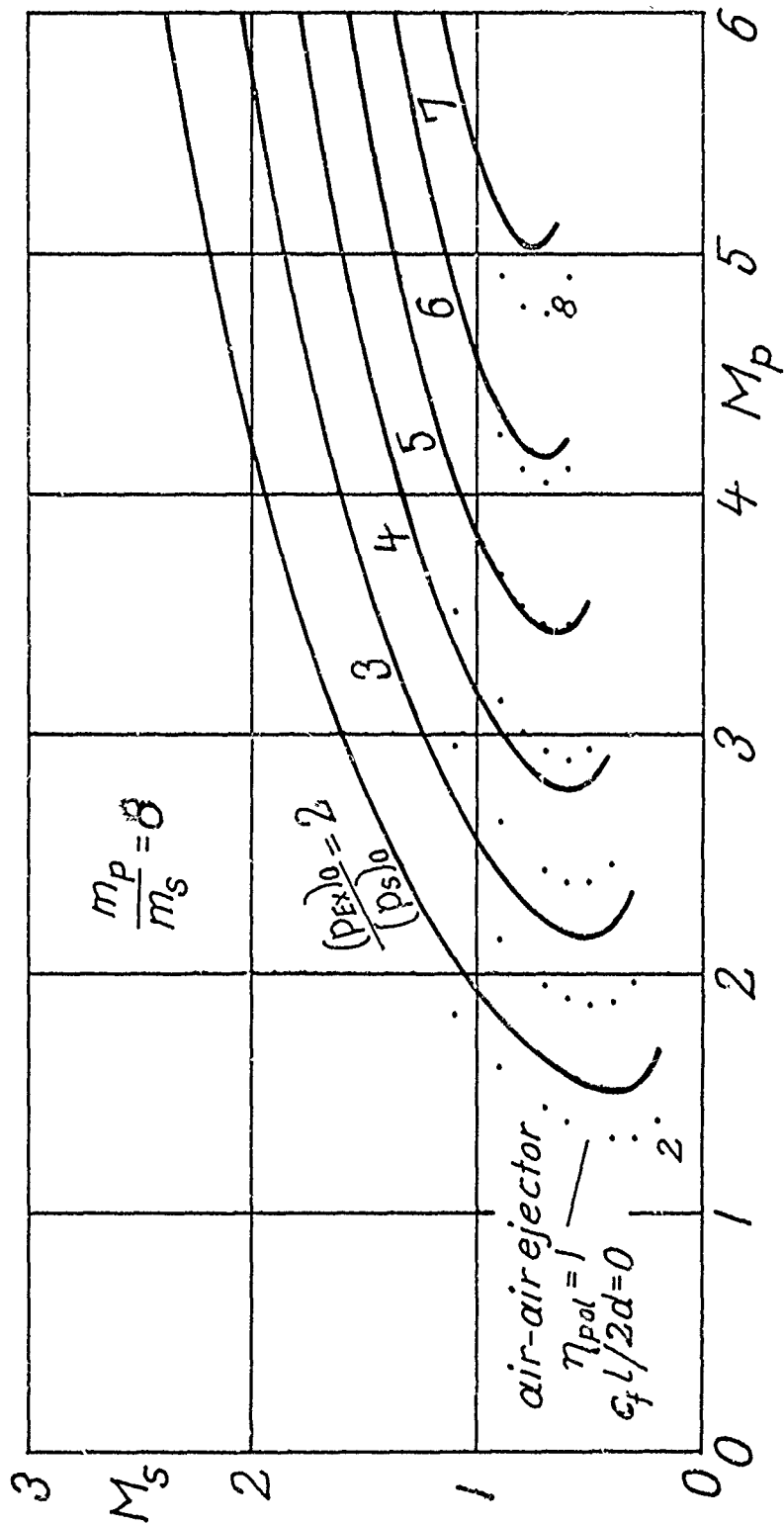
Figure 24c. (Mass Flow Ratio 8)

100
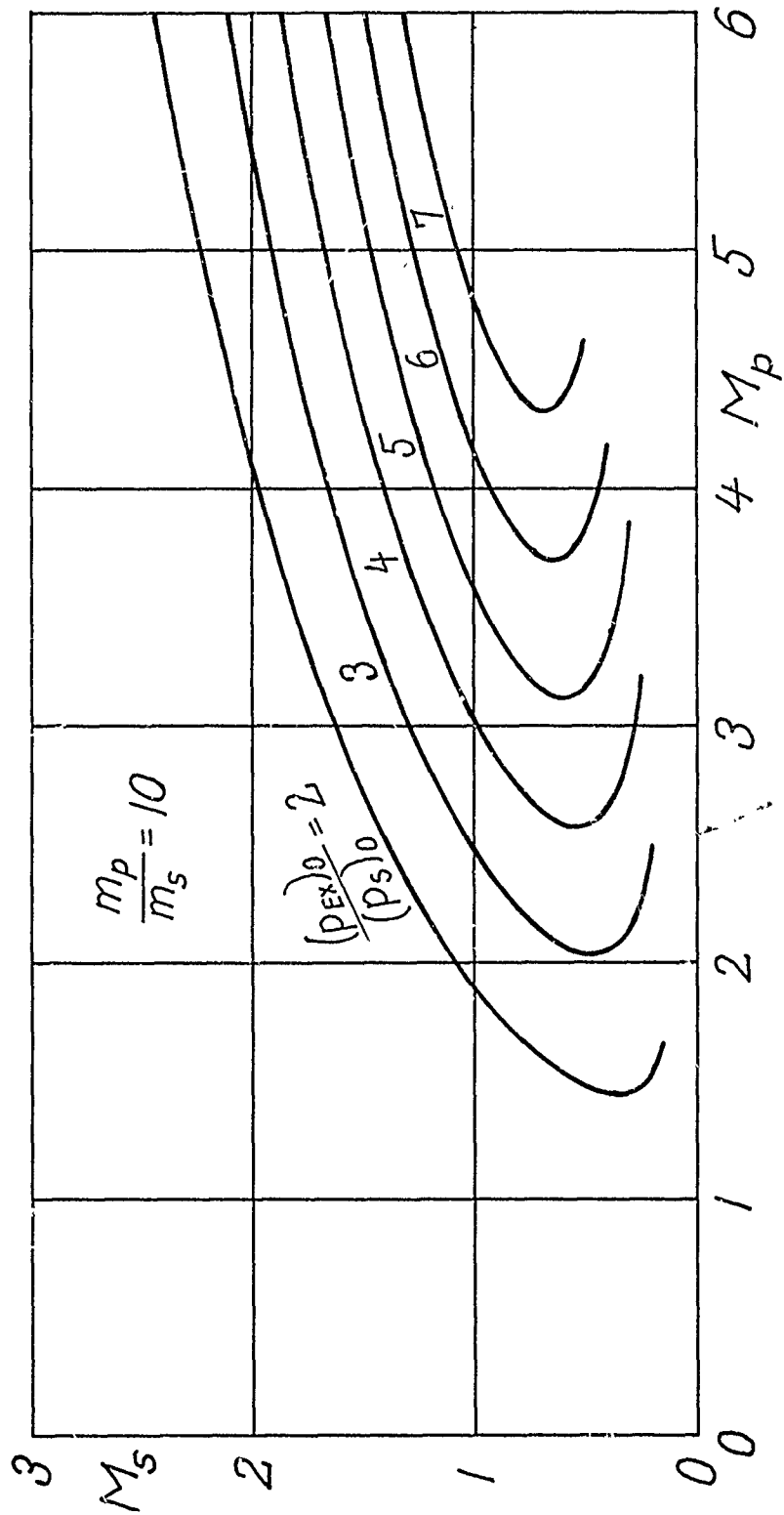
Figure 24d. (Mass Flow Ratio 10)
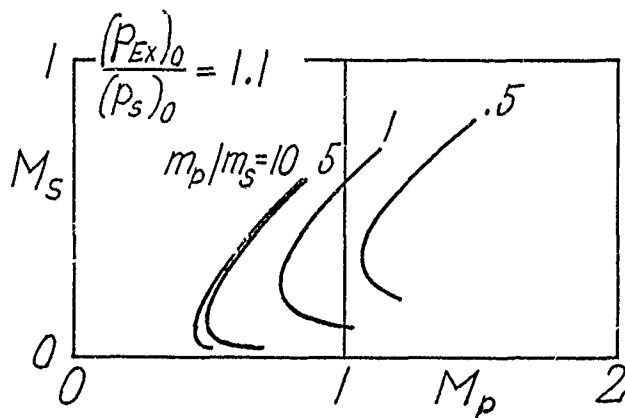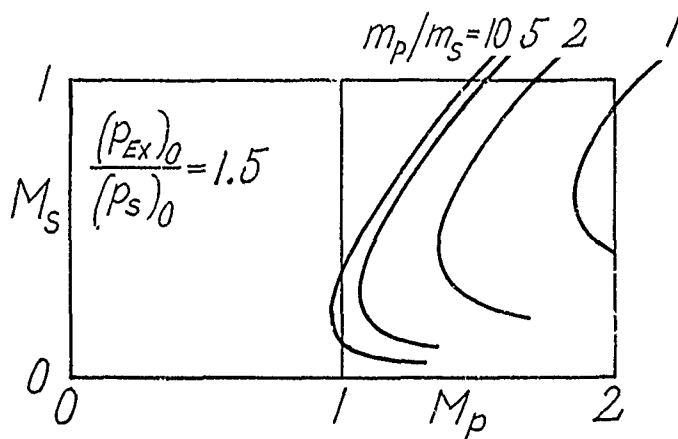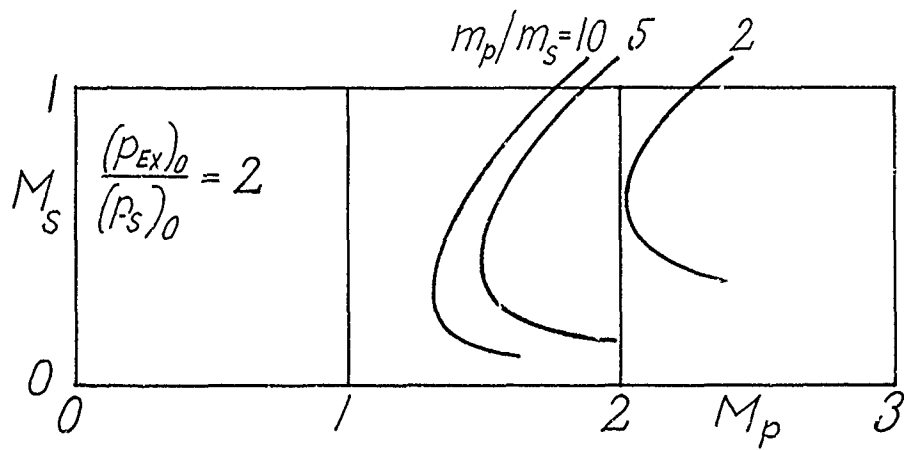
Figure 25. Performance Optimization for Constant Area Mixing and Low Total Ejector Pressure Ratios.

102
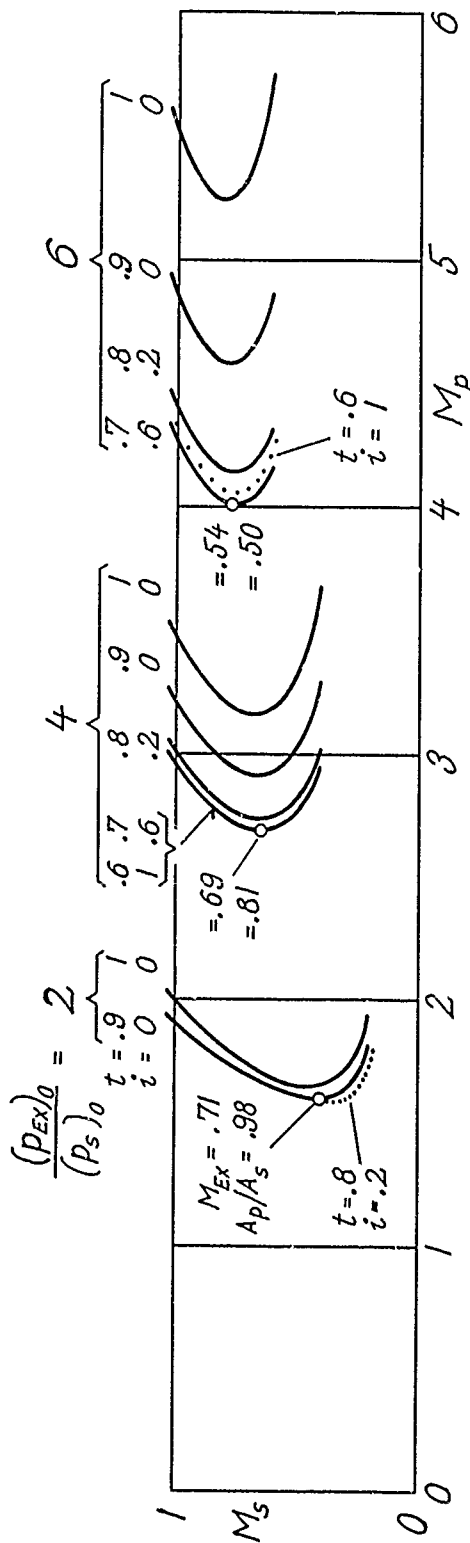
Figure 26. Example for the Improvement of the Optimized Performance for Constant Area Mixing By Reducing the Mixing Section Exit Area Against the Inlet Area. (The indicated area reductions (t) and associated pressure distribution factors (i) are estimates for achievable values.)

103

|		
1	$(A_p/A_s)_{geo}$	.11
2	γ_p	1.26
3	γ_s	1.48
4	R_s/R_p	2.60
5	c_{p-s}/c_{p-p}	2.10
6	$(T_p)_o/(T_s)_o$	1.20
7	η_{pol}	.60
8	$c_f l/(2d)$	.05
9	β	1.00
10	t	.30
11	i	.60
12	$(A_p)_{geo}/A^*$	13.30
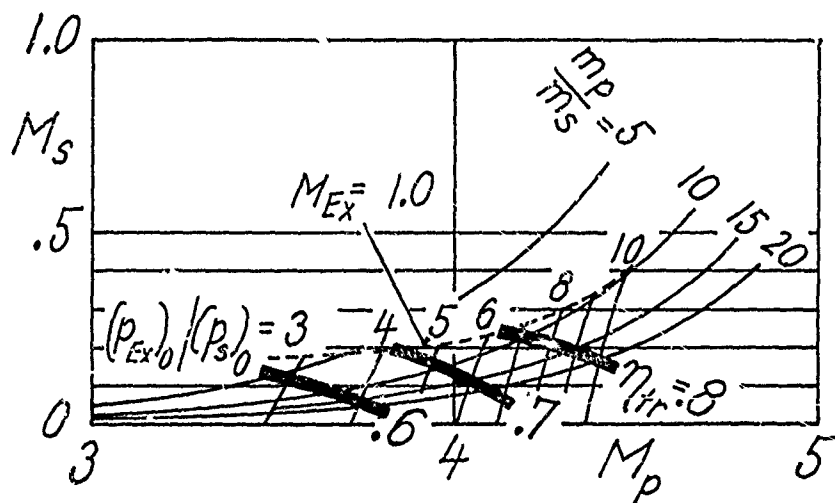
Figure 27. Ejector Performance Characteristic Shown in Figure 16 With Ejector "Transfer Efficiency" Added.

104

Air-Air Ejector (const. area mixing)
$A_S/A_P = 25$
$\eta_{pol} = .85$
$c_f\, l/2d = .05$
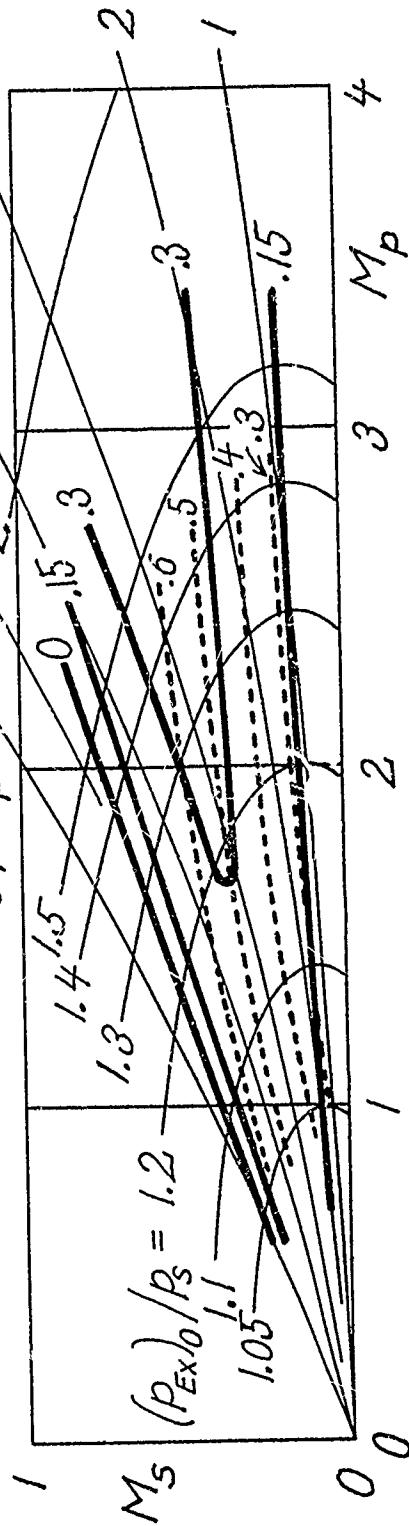
Figure 28. Ejector Performance Characteristic for an Ejector Lay-Out Typical for Thrust Augmentation. (Ejector "Transfer Efficiency" (– – – –) and ejector "compression efficiency" (———) are entered in the characteristic.)

105
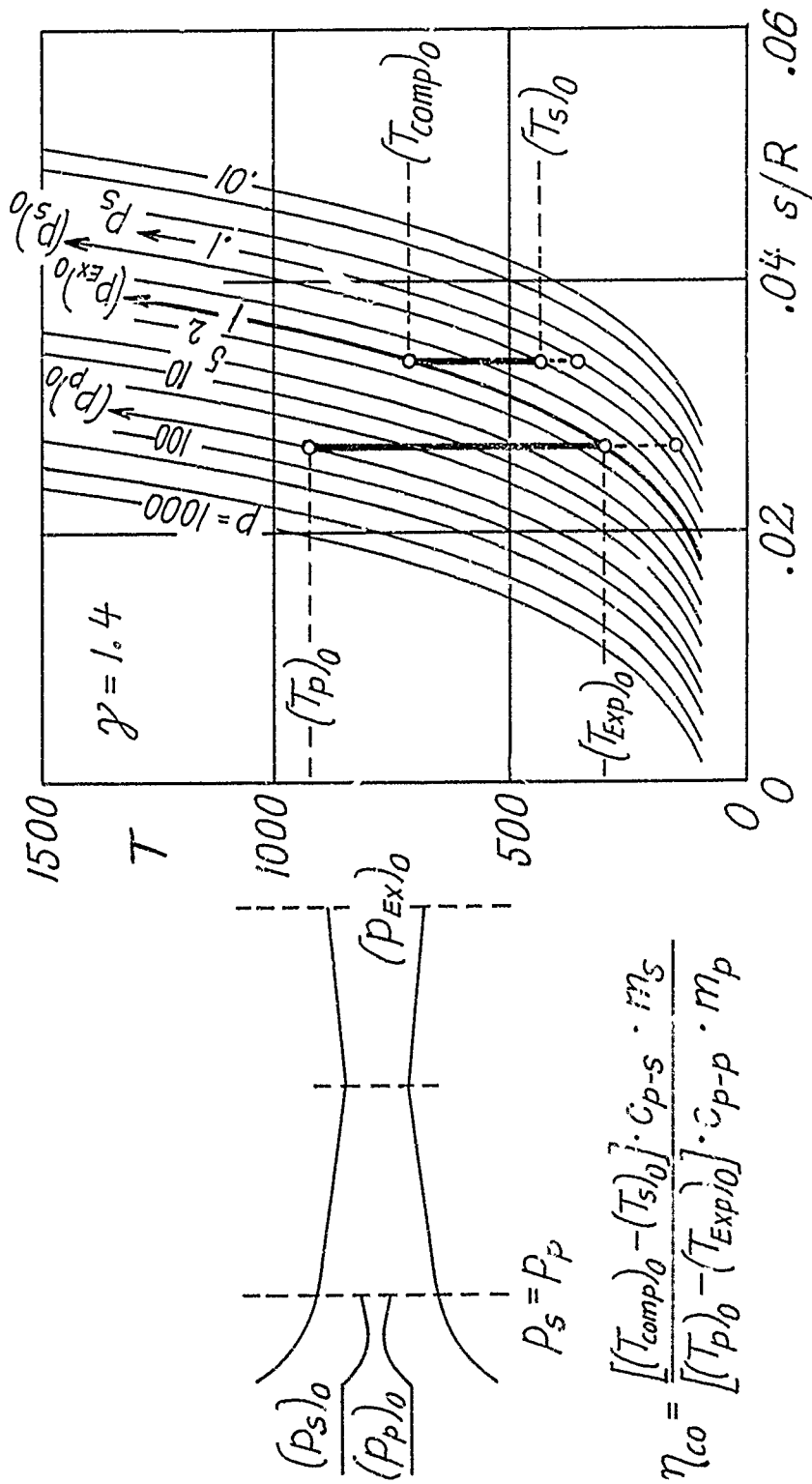
Figure 29. TS-Diagram Illustrating the Formation of the Ejector Compression Efficiency (by relating the adiabatic compression work required to bring the secondary medium to the desired total pressure $(p_{Ex})_0$ to the expansion work provided by the primary medium by expanding it adiabatically from its supply pressure $(p_p)_0$ to $(p_{Ex})_0$. This efficiency definition applies in the same way to a turbine-compressor system with the specific requirement that the total pressures at the exit of the turbine and compressor are equal.)

| 1	$(A_p/A_s)_{geo}$	.11
2	γ_p	1.26
3	γ_s	1.48
4	R_s/R_p	2.60
5	c_{p-s}/c_{p-p}	2.10
6	$(T_p)_o/(T_s)_o$	1.20
7	η_{pol}	.60
8	$c_f l/(2d)$	.05
9	β	1.00
10	t	.30
11	i	.60
12	$(A_p)_{geo}/A^*$	13.30
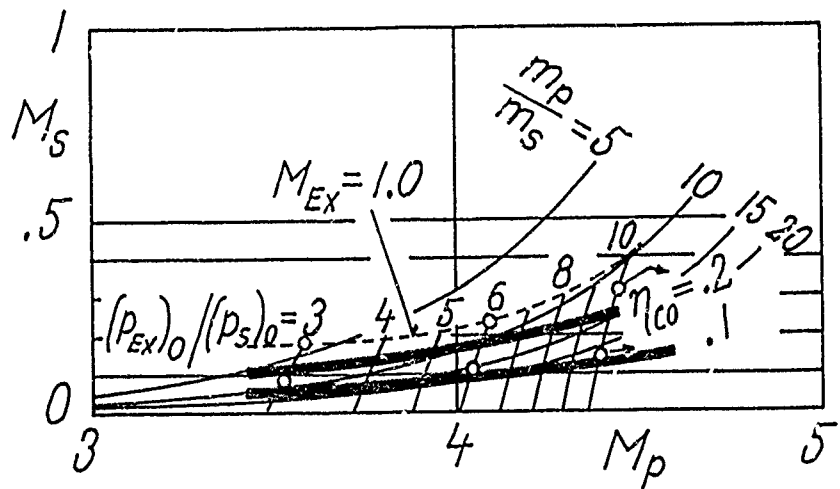
Figure 30. Ejector Performance Characteristic, Shown in Figure 16, With the Ejector Compression Efficiency Added. (Points marked Q include separation work.)
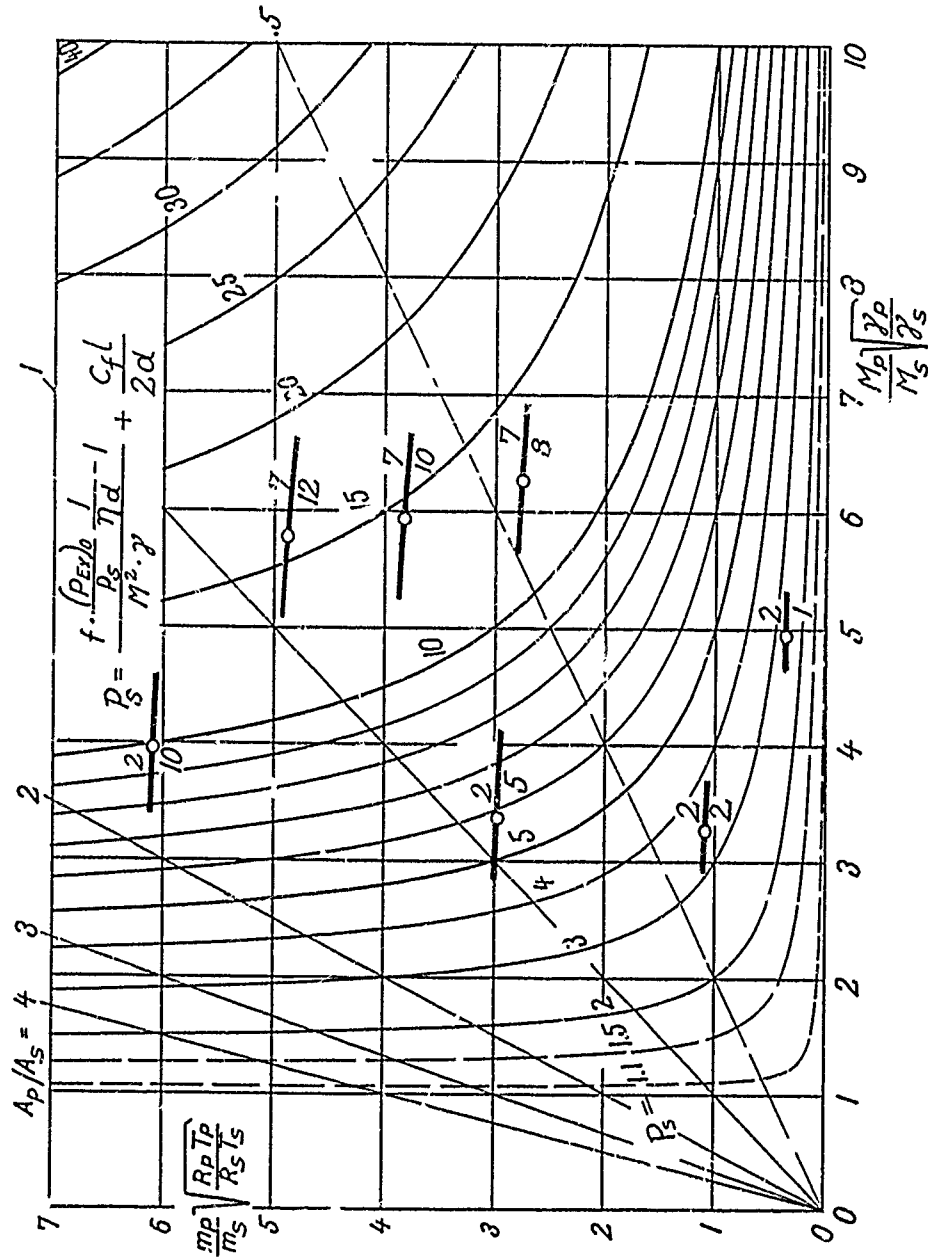
Figure 31. Simplified Ejector Lay-Out Diagram from Ref. 5 with Optimum Ejector Conditions Indicated. (The short lines represent performance peaks (within 1% of the minimum primary inlet Mach number) from Fig. 23. The top number on each line gives the ejector total pressure ratio the bottom number the mass ratio. The circle indicates the performance curve apex.)

REFERENCES

1. Fluegel, G., "Berechnung von Strahlapparaten", VDI Forschungsheft, No. 395, Berlin, Germany, 1939; also Zeitschrift VDI, Vol. 83, pp. 1065-1069, 1939.

2. Keenan, J. H., Neumann, E. P. and Lustwerk, F., "An Investigation of Ejector Design by Analysis and Experiment", Journal of Applied Mechanics, Vol. 17, No. 3,   pp 299-309, September 1950.

3. Fabri, J. and Paulon, J., "Theory and Experiments on Supersonic Air-to Air Ejectors", NACA TM 1410, 1958.

4. Chow, W. L. and Addy, A. L., "Interaction Between Primary and Secondary Streams of Supersonic Ejector Systems and Their Performance Characteristics", AIAA Journal, Vol. 2, No. 4, pp 686-695, April 1964.

5. Hasinger, S., "Simplified Lay-out of Supersonic, Heterogeneous Ejectors", Aerospace Research Laboratories, Wright-Patterson AFB, Technical Report ARL 73-0149, November 1973.

6. Croco, L., "One-Dimensional Treatment of Steady Gas Dynamics", Fundamentals of Gas Dynamics, edited by H. W. Emmons, Princeton University Press, Princeton, N.Y., Vol. III, pp 146 and 279, 1958.

LIST OF SYMBOLS

m	mass flow rate
v	flow velocity
ρ	mass density
A	flow cross section
a	sonic speed
γ	ratio of specific heats
R	gas constant
T	abs static temperature
p	static pressure
M	Mach number
c_f	pipe friction coefficient
l/d	length-diameter ratio of mixing section
t	flow cross section area reduction of mixing chamber (Eq 35)
i	pressure distribution parameter (Eq 37)
η_{pol}	polytropic compression efficiency
f	factor for iteration process (Eq 47)
c_p	specific heat at constant pressure

Indices

p	refers to primary ejector medium
s	refers to secondary ejector medium
Ex	refers to mixing section exit
$(\ )_o$	indicates stagnation condition

For further explanation of symbols see Figures 1, 3, and 21.